ULTRASENSITIVE DETECTION OF PATHOGENS IN REAL-TIME. POTENTIOMETRIC BIOSENSORS BASED ON SINGLE-WALLED CARBON NANOTUBES AND APTAMERS

Gustavo Adolfo Zelada Guillén

Dipòsit Legal: T. 1713-2011

UNIVERSITAT ROVIRA I VIRGILI
ULTRASENSITIVE DETECTION OF PATHOGENS IN REAL-TIME. POTENTIOMETRIC BIOSENSORS BASED ON SINGLE-WALLED CARBON NANOTUBES AND APTAMERS
Gustavo Adolfo Zelada Guillen
DL:T. 1713-2011

ULTRASENSITIVE DETECTION OF PATHOGENS IN REAL-TIME. POTENTIOMETRIC BIOSENSORS BASED ON SINGLE-WALLED CARBON NANOTUBES AND APTAMERS

PhD Thesis by
Gustavo Adolfo Zelada-Guillén

Universitat Rovira i Virgili
Tarragona, Spain

Gustavo Adolfo Zelada Guillén

ULTRASENSITIVE DETECTION OF PATHOGENS IN REAL-TIME. POTENTIOMETRIC BIOSENSORS BASED ON SINGLE-WALLED CARBON NANOTUBES AND APTAMERS

PhD Thesis

Supervised by Dr. Jordi Riu Rusell

And Prof. Francesc Xavier Rius Ferrús

Departament de Química Analítica i Química Orgànica

UNIVERSITAT ROVIRA I VIRGILI

TARRAGONA, SPAIN

2011

UNIVERSITAT
ROVIRA I VIRGILI
DEPARTAMENT DE QUÍMICA ANALÍTICA I
QUÍMICA ORGÀNICA

Campus Sescelades
Carrer Marcel·lí Domingo s/n
43007 Tarragona
Tel. +34 977 55 97 69
Fax +34 977 55 84 46
e-mail: secqaqo@urv.cat

Dr. JORDI RIU RUSELL, and Prof. FRANCESC XAVIER RIUS FERRÚS, Associate Professor and Professor at the Department of Analytical Chemistry and Organic Chemistry at the Universitat Rovira i Virgili

CERTIFY THAT:

The PhD Thesis entitled "ULTRASENSITIVE DETECTION OF PATHOGENS IN REAL-TIME. POTENTIOMETRIC BIOSENSORS BASED ON SINGLE-WALLED CARBON NANOTUBES AND APTAMERS" defended by GUSTAVO ADOLFO ZELADA GUILLÉN in order to achieve the Degree of Doctor, has been carried out under our supervision, at the Department of Analytical Chemistry and Organic Chemistry at the Universitat Rovira i Virgili.

Tarragona, October 27th, 2011

Dr. Jordi Riu Rusell

Prof. Francesc Xavier Rius Ferrús

This PhD Thesis has been possible thanks to the direct and indirect contribution of many people in different ways. That's why I would like to acknowledge to all the people that has touched my life in a positive way during this stage.

First, I would like to express my genuine gratitude to Prof. F. Xavier Rius and Dr. Jordi Riu for their invaluable help, advice and continuous support throughout this period of my life. I would thank them for trusting me when this graduate study position was offered to me four years ago. Their exceptional support during the drafting and editing stages of the writing process was priceless, without their hints and suggestions we probably could not have finished this Thesis on time.

I would also like to thank to Prof. H. Ulrich Göringer and Dr. Moritz Niemann from Darmstadt University of Technology for their invaluable suggestions, guidance, scientific and technical support in the development and assessment of the biosensors reported in ***Chapter 7***, as well as during the writing process of the article related to it. Additionally, special thanks go to Prof. Göringer for accepting to be part of the evaluation committee. To Ailis Tweed-Kent from Harvard University for her unconditional support, scientific discussions and the great teamwork displayed during the last part of this project in the design and development of the blood-buffering system used in ***Chapter 7***, for her advice during the writing stage of the respective article and of course, for the energy contributed to the lab during her stay in TGN. To Suryakant V. Bhosale from URV for his huge effort, curiosity and passion shown throughout his stay in the research group in order to develop and assess the biosensors for *E. coli* detection reported in ***Chapter 6***, as well as for the evening leisure activities carried out during the past years. To José Luis Sebastián-Ávila from IBEC for his great effort, enthusiasm and scientific contributions during the development and assessment of the biosensors for *S. aureus* detection reported in ***Chapter 5***. And to Ali Düzgün from URV, for his technical and scientific guidance during the early stages of this Thesis when the biosensor reported in ***Chapter 4*** was developed, but also for eventually sharing with me the Turkish culinary delights. My best wishes to all of you in your careers.

I would additionally thank to Prof. Rosa Puchades from Polytechnic University of Valencia, Dr. María Isabel Pividori from Autonomous University of Barcelona, Dr. José Manuel Costa and Dr. Jorge Ruiz Encinar from University of Oviedo, Dr. Pascal Blondeau and Dr. Santiago Macho from URV for accepting to be part of the evaluation committee and for their time offered during this last step in my doctoral studies.

Quiero también agradecer especialmente a Santiago Macho por todo el apoyo incondicional ofrecido durante toda la Tesis y sobre todo, en la etapa final de escritura de la misma, sin su apoyo no habría sido posible completar esta Tesis en el tiempo adecuado. También agradezco a Teresa Codera y a Santiago Moreno de la URV por todas las facilidades y apoyo logístico constante a lo largo de este tiempo. A Mercè Moncusí, Mariana Stefanova, Núria Canela, Cristina Peñalver, Ramón Guerrero y Rosa Ras del SRCiT de la URV por todos los consejos y la ayuda científica y técnica aportada. A la Prof. Carmen Claver, al Dr. Josep M. Montornès y Jordi Sanahujes del CTQC así como a Diana Campo del CTTI de la Fundación URV sin cuyo apoyo ofrecido de cara al cierre temporal de la Universidad no habría sido posible completar en tiempo las últimas etapas de escritura y corrección de esta Tesis.

También quiero agradecer al resto de los compañeros y profesores del Grupo de Quimiometría, Cualimetría y Nanosensores de la URV y de otros Departamentos, por el apoyo ofrecido en todo momento y por hacer de la estancia en este laboratorio algo agradable. Especialmente agradezco a Idoia Martí cuyo entusiasmo y alegría siempre han resultado contagiosos; a Rafa Hernández Malo por su energía, buen humor y disposición a apoyar a todos en todo momento; a Enrique Parra quien siempre estuvo dispuesto a echar una mano cuando se necesitaba; a Carolina Di Anibal por su constante apoyo y compañerismo demostrados durante todo este tiempo; a las nuevas adquisiciones del laboratorio, Jonathan Sabaté, Sabrina Küpper, Marta Novell y Tomàs Guinovart, por toda la energía renovada, entusiasmo, alegría y buen humor que trajeron al laboratorio con su llegada; a Ricard Boqué por las discusiones académicas del bus y por el entusiasmo constante demostrado; a Pascal Blondeau por las interesantes discusiones académicas sostenidas durante este tiempo y por su incondicional apoyo ofrecido en todo momento; a Jaume Capdevila por su apoyo y los momentos compartidos en las semanas de la ciencia; a Eulalia Ortiz, Olga Magriñà,

Avelina Lacueva y Zoe Magí sin cuyo apoyo no habría sido posible completar esta etapa; y a la Prof. Aurora Ruiz y Xavi Rius Jr. por recibirme con los brazos abiertos en mi llegada a Tarragona y por todo el apoyo recibido. También agradezco a los antiguos miembros del Grupo, Vanessa del Río por su entusiasmo, alegría, apoyo incondicional y por los ratos amenos vividos fuera del laboratorio; y a Nicolás Spegazzini por su gran apoyo durante mis primeros momentos en Tarragona así como también por las interesantes discusiones científicas llevadas a cabo. A todos les deseo el mejor de los éxitos profesionales.

Quiero dar un agradecimiento muy especial a Aitor Gual, a Cyril Godard y a Miriam Díaz de la URV por todos sus consejos, discusiones científicas y no-científicas, por las interesantes tertulias vespertinas sostenidas a lo largo de este tiempo y por supuesto, por las agradables sesiones Croustianas y de mojitos. También un agradecimiento a Carlos Rosales de la URV por los divertidos momentos vividos y por su papel como pieza clave en la cadena de suministro de productos alimenticios transatlánticos. Les deseo todo el éxito en su trayectoria académica y en todo aquello que emprendan en un futuro.

Gracias también a la peña asturiano-aragonesa de la UPS, Ricardo Rodríguez, Fany Piedra y Noel Nebra por los buenos momentos vividos y la calidez mostrada en el tiempo de conocerlos, and of course also to the canadian section represented by Eric Derrah for the nice moments shared at both sides of the Pyrenees as well as for the canadian delights contributed, a todos ustedes, éxito a donde sea que sigan la carrera profesional. También al nuevo fichaje estrella de los Pumas, Susanna Porcel del IQ-UNAM, por los gratos momentos compartidos, te deseo mucho éxito en tu nueva asignación. Y a Bea Lastra y Ana Escribano por los divertidos momentos culinarios compartidos. Thanks as well to Marius Gheorghita from Swinburne University of Technology for all those good moments downtown and the delicious foodstuff brought from hometown. A special thank to Boaz Vilozny and Paolo Actis from UC Santa Cruz, Manuel A. Palacios and Maël Manesse from Tufts University, Andre A. Adams from US Naval Research Lab, Aaron Rowe from UC Santa Barbara, João Borges from Universidade do Porto, Samuel Chigome from Rhodes University, Carlos A. Polanco from University of Virginia, Adam K. Wanekaya from Missouri State University, Thomas

Theriault from Roche, Xi Wang from UC at Irvine, Yan-Jun Liu from Institut Curie and Golnaz Borghei from University of Cambridge for the very nice moments shared as well as the interesting scientific and non-scientific discussions and their academic and professional recommendations. I also thank to Joseph C. Liao from Stanford University for his kind suggestions and scientific discussions.

Je voudrais également remercier au Marie Claude Chatelain et Raphaël Arches pour m'acueillir avec les bras ouverts à Toulouse, pour vos conseils et votre contribution du materiel scientifique. J'espère qu'on se verra prochainement!.

Gracias también a la Prof. Luz Elena Vera-Ávila, a la Mtra. Rosario Covarrubias, a la Mtra. Carmen Sansón y al Prof. Alan Queré de la FQ-UNAM por haberme brindado durante mi período de licenciatura las herramientas necesarias para poder sacar adelante un proyecto como éste.

Agradezco muy especialmente a los Bellver González, Mario, Mario Jr. y Eren, por su amistad y apoyo incondicional, por los momentos vividos en Tarragona y por las divertidas sesiones de tiempo libre compartidas.

También agradezco con mucho cariño a la familia ESBO Jaime, María Cristina, Jaime jr., Fabiola, Laura y la abuela Esther por todo el apoyo brindado de corazón a lo largo de este tiempo y por recibirme siempre con los brazos abiertos.

A mis tíos Nelson, Jaime, Ovidio, Edgardo, Nancy, Carmen, a mi Abuela Lupe y mi abuelo Carlos (D.E.P.), mi padrino Oscar, mis hermanos y mis padres, también de todo corazón les doy las gracias por todo el apoyo otorgado, pues sin las herramientas que me han brindado no habría podido sortear con éxito ésta etapa de mi vida.

Y por último, un agradecimiento de todo corazón a Martha por estar siempre conmigo y apoyarme incondicionalmente en todo, especialmente cuando más lo he necesitado. Muchas gracias por todo!...

Acknowledgements/Agradecimientos

This project has been possible thanks to the generous support of the following grants:

Doctoral fellowship of the FI-DGR program. Funded by the *Comissionat per a Universitats i Recerca del Departament d'Innovació, Universitats i Empresa de la Generalitat de Catalunya* and the *European Social Fund*.

Doctoral fellowship associated to a Research Project. Funded by the *Subprograma de Formación de Personal Investigador, Ministerio de Ciencia e Innovación*, *Gobierno de España*.

Research project 'Miniaturized potentiometric sensors for the fast, sensitive and selective point-of-care detection of pneumonia-causing pathogens'. Funded by the *Ministerio de Ciencia e Innovación*, *Gobierno de España*, Ref. CTQ2010-18717, Jan 2011 – Dec 2013.

Research project 'New field effect transistors and selective electrodes based on carbon nanotubes for bioanalysis: determination of ions, biomolecules and bacteria'. Funded by the *Ministerio de Ciencia e Innovación*, *Gobierno de España*, Ref. CTQ2007-67570/BQU, Oct 2007 – Sep 2010.

Research project 'Development of new sensors based on carbon nanotubes for the determination of choline and related compounds. Their miniaturisation and scaling down to the nanometric range'. Funded by the *Universitat Rovira i Virgili*, Ref. 2007URV/ICIQ-03, Nov 2007 – Nov 2010.

Contents

Abbreviations

^{13}C-NMR	Carbon-13 nuclear magnetic resonance
^{1}H-NMR	Proton nuclear magnetic resonance
A	Adenine
Ab	Antibody
AnTat X	Antwerp Trypanozoon antigen type X
BSA	Bovine serum albumin
C	Cytosine
CATT	Card agglutination test for Trypanosomiasis
CECT	Colección Española de Cultivos Tipo
CFU	Colony-forming units
CNT	Carbon nanotubes
CTAB	Cetyltrimethylammonium bromide
DCTA	trans-1,2-Cyclohexanediaminetetraacetic acid
DI	Deionized (e.g. DI water)
DMR	Diagnostic magnetic resonance
DNA	Deoxyribonucleic acid
EAP	Extracellular adherence protein
EDC	N-(3-dimethylaminopropyl)-N′-ethylcarbodiimide hydrochloride
EDTA	Ethylenediaminetetraacetic acid
ELISA	Enzyme-Linked Immunosorbent Assay
ELONA	Enzyme-Linked Oligonucleotide Assay
EMF	Electromotive force
ESEM	Environmental scanning electron microscope
ETat X	Edinburgh Trypanozoon antigen type X
EtOH	Ethanol

ETD	Everhart-Thornley detector
FT-IR	Fourier transform infrared spectroscopy
G	Guanine
GC	Gas chromatography
GFP	Green fluorescent protein
HP	Human plasminogen
HPLC	High performance liquid chromatography
HSA	Human serum albumin
Ig	Immunoglobulin
IgX	Immunoglobulin X
ILRAD	International Laboratory for Research on Animal Diseases
ILTat X	ILRAD Trypanozoon antigen type X
LAPS	Light addressable potentiometric sensors
LB	Lysogeny broth (Luria-Bertani medium)
LDA	Linear discrimination analysis
LF	Lateral flow
LiTat X	Lille Trypanozoon antigen type X
LOD	Limit of detection
mAb	Monoclonal antibody
MALDI	Matrix-assisted laser desorption/ionization
MB	Methylene blue
MeOH	Methanol
MES	2-(N-morpholino) ethanesulfonic acid
Min	Minute
MIP	Molecularly imprinted polymer
MiTat X	Molteno Institute Trypanozoon antigen type X
MG	Methylene green
MOSFET	Metal-oxide-semiconductor field-effect transistor
MRS	deMan, Rogosa and Sharpe
MSA	Mannitol Salt Agar (Chapman medium)
MWCNT	Multi-walled carbon nanotube
NHS	N-hydroxysuccinimide

NMR	Nuclear magnetic resonance
pAb	Polyclonal antibody
PAGE	Polyacrylamide gel electrophoresis
PBS	Phosphate buffer solution
PCR	Polymerase chain reaction
PFU	Plaque-forming unit
PNA	Peptide nucleic acid
PQQGDH	Pyrroquinoline quinone glucose dehydrogenase
PSA	Prostate-specific antigen
Pyr	Pyrenil
QCM	Quartz-crystal microbalance
RNA	Ribonucleic acid
RoTat X	Rode Trypanozoon antigen type X
RP	Reverse phase
SAM	Self-assembled monolayer
SD	Standard deviation
SD_{noise}	Standard deviation of the noise
SDS	Sodium dodecyl sulfate
SEM	Scanning electron microscope
SPR	Surface plasmon resonance
ST	*Salmonella enterica* serovar Typhi
SWCNT	Single-walled carbon nanotube
T	Thymine
TEM	Transmission electron microscope
TOF	Time-of-flight mass spectrometer
TSA	Tryptic soy agar
TSB	Tryptic soy broth
U	Uracil
UV-Vis	Ultraviolet-Visible spectrophotometer
VAT	Variant antigen type
VSG	Variable surface glycoprotein
XLD	Xylose-lysine-deoxycholate agar

Chapter 1

Introduction

1.1. State of the art in analytical methods for pathogen and disease-related proteins detection

The purpose of section ***1.1*** is to give a chronological overview of the current analytical methods for protein (subsection ***1.1.1***) and pathogen detection (subsection ***1.1.2***). A special remark is made on those biosensing platforms based on nanostructured components, which display outstanding characteristics in limits of detection or time of analysis. Additionally, a comparison between past and current techniques is discussed in order to give an appropriate perspective of the methods available. A constantly increasing number of articles are published in peer-reviewed journals related to the field of analytical methods for pathogen and protein detection. Therefore, the bibliographic revision in this section was mainly limited to the most relevant analytical techniques aimed for the direct detection of bacteria, disease-related proteins and molecular biomarkers for other pathogens such as viruses or parasites. The term 'direct' stands for those methods that use sensors –therefore establishing a direct contact between the target in the sample and the recognition layer of the sensor– and do not need significant pre-processing steps. However, some analytical methods that do not make use of sensors but represent an important breakthrough in pathogen or protein detection at very low concentrations are also included in this section. As an example, state of the art analytical techniques related to the detection of clinically relevant proteins involved in infectious and non-infectious diseases at extremely low concentrations, as in prion-related diseases or cancer, are discussed. In the relevant cases, a brief description of the advantages and limitations of the techniques is also included.

1.1.1. Methods for the detection of disease-related proteins

Protein detection methods can be classified into four major groups: a) electrophoretic separations; b) techniques based on the measurement of variations in surface properties due to molecular recognition events between a molecular receptor and its target (e.g. surface plasmon resonance, surface-enhanced raman spectroscopy and others); c) mass spectrometry-based techniques; and d) immunoassay-based

methods, in which an antigen-antibody interaction is detected by electrochemically active labels, luminescence, fluorescence or radioactivity.[1] Among this latter type of techniques, the methods most commonly used in diagnostics rely on western-blot assays, immunoblotting techniques, immunoprecipitation, immunofluorescence and immunosorbent assays.[1–3] These methods are widely used in research as well. All of them are characterized by different advantages: in general they are highly sensitive and specific. On the other hand they are labor-intensive, time-consuming and require highly trained technical staff. In many cases expensive equipment is needed, which makes them unsuitable for high-throughput protein detection or point-of-care diagnostics applications. In 1971, one of the immuno-assay based techniques, the enzyme-linked immunosorbent assay (ELISA), was developed by Engvall and Perlmann.[4] The technique represents one of the most important revolutions in protein detection in the past decades and has been adapted for the detection of a large number of target proteins. The technique represents the preferred tool in both, clinical diagnostics and protein research protocols.[5] ELISA assays have the advantage of being completely customizable towards different targets, they are affordable and can achieve very low detection limits. However, the assay also requires highly qualified personnel and special equipment and the reproducibility of antibodies is not always guaranteed. Furthermore, an accurate quantification of the analyte is not possible and false negative results can be obtained if the target protein is not extracted from the matrix effectively.[6]

Nanostructured materials, assigned mainly to group (b) in the classification made above, are ideal for biosensor applications in protein detection.[7] Nanomaterials possess extraordinary optical, electronic and catalytic properties, which allow the design of simplified detection platforms at lower detection limits within shorter assay times than traditional detection techniques.[8] Very interesting approaches on the development of detection platforms based on quantum-dots (QD), nanoparticles (NP), nanotubes, nanorods, nanowires and nanosheets that make use of their optical, electrical, magnetic or catalytic properties have recently been explored in protein detection at very low concentrations either for diagnosis of infectious diseases or in proteomic research.[9,10] In this context, electrochemical immunoassays coupled with

the recent advances in nanobiotechnology and nanoparticles offer new alternatives for clinical diagnostic procedures. Nanoparticles are being used for the electrochemical detection of proteins at fM to pM concentration levels taking advantage of their versatility and electrochemistry inherent advantages.[10] Nanotubes, and particularly, carbon nanotubes are also incorporated in electrochemical- and catalytic-based sensors in protein detection.[11] Their physical characteristics and electronic properties converted them into an ideal material to improve sensitivity in small molecule and protein detection. In this way, the detection of proteins such as streptavidin, bovine serum albumin, prostate-specific antigen, HIV-1 protease and others at detection ranges between fM to pM concentration levels have demonstrated that nanotubes are a promising material in the electrochemical detection of proteins.[7,8,11 – 14] Therefore, in this subsection, a special emphasis is made on those protein detection methods based on nanostructured materials such as nanotubes, nanoparticles or other nanostructures regardless on the type of detection employed (e.g. mass, optical or electrochemical detection). However, as mentioned before, some outstanding protein detection methods that are not based on nanostructured materials but represent an important breakthrough in terms of limit of detection, time of analysis or assay simplicity are also discussed.

Wong and collaborators[15] demonstrated in 1998 that nanotube tips with the capability of biological discrimination could be created by coupling biomolecular probes to the carboxyl groups that are present at the open tip ends. They used these modified nanotubes as Atomic Force Microscopy (AFM) tips to detect single protein-ligand interactions. This breakthrough opened up the possibility to both detect a specific protein at the single-molecule level as well as to measure for the first time the strength of the interaction between a protein and its ligand. Unfortunately, the elevated cost of the AFM technique seriously represents a limitation for its widespread use in research or clinical diagnostic. In the same year, Chan and Nie[16] developed highly luminescent semiconductor quantum dots (zinc sulfide-capped cadmium selenide) covalently coupled to biomolecules for their use in ultrasensitive biological detection. QDs labeled with the protein transferrin underwent receptor-mediated endocytosis in cultured cervical cancer cells (HeLa cells). Moreover, QD labeled with

Immunoglobulin G (IgG) were able to recognize some proteins such as the bovine serum albumin (BSA). The use of luminescent QD in biosensing opened up the possibility to customizable portable protein detection kits. Moreover, the versatility of QD to be adapted into different sensing platforms (e.g. electrochemical detection platforms) allowed innumerable applications in both protein and pathogen detection at fM levels.[10]

In 1999, Rowe et al.[17] developed an array biosensor for the simultaneous detection of bacteria, viruses and proteins. The sensor was based on the recognition of the analytes by antigen-specific antibodies previously immobilized in a patterned array on the surface of a planar waveguide. Bound analyte was subsequently detected using fluorescent tracer antibodies. The sensor was capable of detecting viral, bacterial, and protein analytes in a 14 minutes assay with limits of detection for *Bacillus globigii*, MS2 bacteriophage, and staphylococcal enterotoxin B (SEB) of about 10^5 colony-forming units (CFU)/mL, 10^7 plaque-forming units (PFU)/mL, and 10 ng/mL, respectively. Despite the advantages presented by the multiplexed detection of several targets in terms of time of analysis, such a biosensing platform was limited by the use of fluorescent labels which resulted in affected limits of detection.

In 2001, Wu and collaborators[18] demonstrated that microcantilevers of different geometries in combination with polyclonal antibodies could be used in the label-free detection of prostate-specific antigen (PSA) over a wide range of concentrations (0.2 ng/mL to 60 µg/mL) in a background of human serum albumin (HSA) and human plasminogen (HP) at 1 mg/ml, making this a clinically relevant diagnostic technique for detecting prostate cancer. In this case, intermolecular nanomechanics involved in the target-recognition event bent the cantilever, which can be optically detected. Lieber's group[19] published in the same year the development of boron-doped silicon nanowires able to detect streptavidin at a pM concentration range using biotin as a biorecognition molecule and field-effect transistors (FET) as detection technique. The combination of these technologies opened up the possibility for large-scale studies of protein interactions with other biomolecules.[20] Unfortunately, the complexity and high cost involved in the construction of silicon nanowires and microcantilevers

represents a limitation for their ample use in either point-of-care or research sensing applications.

Star and co-workers[21] used in 2003, nanoscale field-effect transistor devices with carbon nanotubes as the conducting channel to detect protein binding. Biotin molecules were used as the biorecognition element in the detection of streptavidin. FETs are transistors that rely on an external field to control the conductivity of a channel of one type of carrier in a semiconductor material.[22] In the case of analytical sensors, these external fields have an electrochemical origin. Consequently, the origin of the current change is a variation in the potential, which in turn is affected by the analyte concentration in the test sample.[23] In the same year, Chen et al.[24] developed FETs for the specific detection of monoclonal antibodies (mAbs) to the human autoantigen U1A, a prototype target of the autoimmune response in patients with systemic lupus erythematosus and mixed connective tissue disease. FET-based sensors experienced a constant growth within further years as a versatile platform for the detection of different protein targets.[11-13] Unfortunately, the need of expensive devices and the complicated processes involved in sensor construction is a serious limitation for FET applications in 'real life' biosensing. Nam and collaborators[25] also developed in the same year a method for detecting PSA using magnetic microparticle probes with antibodies that specifically bind to PSA and nanoparticle probes that are encoded with DNA that is unique to the protein target of interest and antibodies that can sandwich the target captured by the NP probes. Magnetic separation of the complex target-probe followed by dehybridization of the oligonucleotides on the NP probe surface allowed the determination of the presence of the target protein by identifying the oligonucleotide sequence released from the NP probe. Magnetic separation of biological targets represented an interesting option for biosensing applications in complex matrices. Nowadays magnetic nanoparticle probes represent a platform which is applied in many other different fields such as catalysis.[26]

Savran and others[27] reported in 2004 the label-free detection of Taq DNA polymerase proteins at pM concentration levels using a microfabricated cantilever-based sensor that was functionalized with DNA aptamers to act as receptor molecules. The sensor used two adjacent cantilevers that constituted a sensor/reference pair and

allowed direct detection of the differential bending between the two cantilevers. One cantilever was functionalized with the aptamers while the other was blocked with single-stranded DNA. However, as in the previous examples of cantilever-based sensors, the complexity and cost involved in sensor construction is again an important limitation for its ample use. That year, Dierksen and co-workers[28] developed a cytosensor based on living chromatophores from *Betta splendens* (Siamese fighting fish) for the detection of bacterial toxins. The agents tested were *Streptococcus pyogenes* toxins streptolysin S and streptolysin O, *Clostridium tetani* tetanolysin, *Staphylococcus aureus* alpha-toxin and *Vibrio parahemolyticus* hemolysin. Such an interesting biosensing technique exhibited minimum detectable concentration values in the order of nM to μM level in a 5 minutes assay. However, the special cautions needed to maintain the chromatophores alive, restricted this biosensing format only to limited applications under highly controlled conditions.

In 2005, Hianik and collaborators[29] showed that methylene blue (MB) could be used as an electrochemical indicator in the detection of thrombin with high sensitivity and selectivity using aptamers. In the same work, the binding of thrombin to aptamers was detected also by the quartz-crystal microbalance (QCM) method in a continuous-flow system. The use of electrochemical indicators is a versatile approach that has been exploited for years in different electrochemical biosensing formats.[22] Unfortunately, the detection of proteins by quartz-crystal microbalance-based methods require of a precise control of the laboratory conditions during measurements. In that same year, Rodríguez, Kawde and Wang[30] reported the label-free recognition of proteins by aptamer-modified electrodes using impedance spectroscopy. So and co-workers[31] also reported in 2005 the first successful demonstration of a single-walled carbon nanotube field effect transistor (SWNT-FET) biosensor using aptamers as an alternative to protein-based sensing elements. In that report, the authors detected thrombin at nM concentrations using thrombin-specific aptamers. Label-free electrochemical biosensing methods based on nanostructured materials offer several advantages in protein detection. The reduced time of analysis and improved limits of detection originated by the outstanding transducing properties

exhibited by nanostructured materials represent an interesting option for biosensor design.

Gu et al.[32] demonstrated in 2006 a general strategy to generate biofunctional magnetic nanoparticles useful in protein separation and pathogen detection, with a high sensitivity and high selectivity using antibodies and other biorecognition molecules. The authors were able to sense down to the nM concentration level of proteins in a 5 minutes assay. Such an interesting technique demonstrated that biosensors based on magnetic nanoparticles are useful for target extraction from complex matrices. Byon and Choi[33] also reported the creation of highly sensitive FETs based on antibodies as recognition elements able to detect 1 pM of the Protein A from *Staphylococcus aureus*. Moreover, Saá, Castilla and Soto[34] developed a method for the rapid detection of the PrP^{Sc} (misfolded prion protein), the main component of the prions responsible for transmissible spongiform encephalopathies (e.g. Creutzfeldt-Jakob disease in humans, bovine spongiform encephalopathy, scrapie in sheep and chronic wasting disease in other animals).[35] The authors used the protein misfolding cyclic amplification (PMCA),[36] a technique that produces accelerated prion replication in order to amplify the quantity of PrPSc present in sample. In this way, they reported the detection of as low as 20 to 50 molecules of monomeric hamster PrP in blood, which corresponded to a single unit of infectious oligomeric PrP^{Sc}.

In 2007, Maehashi and co-workers[37] reported the detection of Immunoglobulin E proteins (IgE) using a label-free protein biosensor based on aptamer-modified carbon nanotube FETs. The authors were able to detect as low as 250 pM of IgE in one hour. In the same year, Mehta et al.[38] detected proteins and bacteria using an array of feedback capacitance sensors. An integrated array of micron-dimension capacitors, originally developed for biometric applications (fingerprint identification), was engineered for biodetection of proteins and bacteria. Upon functionalization with antibodies and in conjunction with signal amplification schemes that result in perturbation of the dielectric constant around the captured antigens, this system was used as a detector of biological agents. You and collaborators[39] reported in that same year nanoparticle-fluorescent polymer 'chemical nose' sensors for the detection, identification and quantification of proteins. The authors created a sensor array

containing six non-covalent gold nanoparticle-fluorescent polymer conjugates. The biosensing platform was based on the polymer fluorescence quenching by gold nanoparticles. The presence of proteins disrupted the nanoparticle-polymer interaction, producing distinct fluorescence response patterns. The method represents an important advance in multiple protein detection and given the simplicity of the technique its incorporation into commercial protein detection kits seems to be possible in a future.

Numnuam et al.[40] reported in 2008, the first example of an aptamer-based potentiometric sandwich assay of proteins at nM concentration levels using thrombin as a prototype example. The measurements were based on CdS quantum dot labels of a secondary aptamer, which were determined with a novel solid-contact Cd^{2+}-selective polymer membrane electrode after dissolution with hydrogen peroxide. The electrode exhibited cadmium ion detection limits of 100 pM in 100 mL samples and of 1 nM in 200 µL microwells, using a calcium-selective electrode as a pseudoreference electrode. Unfortunately, the latter sandwich-type detection method may offer serious limitations in protein detection as well as possible false positive results when samples containing oxidative species are analyzed. Evtugyn and others[41] also reported in 2008 the potentiometric detection of DNA-protein interactions at nM concentration levels using polymeric phenothiazine dyes, methylene blue (MB) and methylene green (MG) electrochemically deposited onto a glassy carbon electrode and covered with a DNA aptamer specific to human α-thrombin. Despite of the simplicity in both the biosensing platform and the potentiometric detection approach used, the dependence on several consecutive steps in order to perform the electromotive force measurements (initial preconditioning, first EMF measurement, sample incubation, second EMF measurement, assessment of the ΔEMF) have limited the technique from high-throughput and real-time protein detection applications. Lee and co-workers[42] demonstrated in that same year the rapid and accurate measurement of biomarkers in tissue and fluid samples using a chip-NMR biosensor based on a miniaturized diagnostic magnetic resonance (DMR) system for multiplexed, quantitative and rapid analysis. By using magnetic particles as a proximity sensor to amplify molecular interactions, the handheld DMR system could perform measurements on unprocessed

biological samples. They showed the capability of the DMR system by using it to detect bacteria in real time, as well as to measure a series of protein biomarkers. This latter technique is a promising tool in point-of-care biosensing applications.

In 2009, a great amount of high-quality scientific papers on the field of protein biosensing platforms were reported. Fukasawa and collaborators[43] reported in that year an aptamer bound/free separation system for thrombin and IgE detection. The complementary strand was immobilized onto beads and the aptamer was labeled with pyrroquinoline quinone glucose dehydrogenase (PQQGDH). In the absence of a target, the aptamer was trapped by beads, whereas in the presence of a target, the aptamer bound to the target was not trapped. The aptamer-target complexes were then recovered easily and detected by PQQGDH activity. The system allowed the detection of 270 pM thrombin and 1 nM IgE. Zhang and co-workers[44] also reported in that year the detection of platelet-derived growth factor protein (PDGF) at pg/mL concentrations. The authors used a voltammetric aptasensor based on proximity-dependent surface hybridization assay consisting of a pair of aptamer probes with a short complementary sequence that recognizes different sites of target PDGF. Simultaneous recognition of a single PDGF molecule by the aptamer pair enabled the hybridization between the complementary sequences of both aptamer probes, which kept two tail sequences of both aptamer probes in close proximity and promoted cooperative annealing of the aptamer-protein-aptamer sandwiched complex on capture probes immobilized on the electrode. Ferrocene tags, previously introduced at the terminus of one aptamer probe, were drawn in close contact with the electrode providing a strong redox signal in voltammetric detection. Voltammetric sensing-based methods are relatively simple and allow to reach very low detection limits. However, the dependence of the above reported biosensing platform on a pair of aptamer probes complicates the possibility of the technique to be tailored against a wide range of protein targets. Such a limitation comes from the fact that each aptamer must bind to different epitopes on the target molecule, which is in contrast, a more complicated task in aptamer synthesis (see for example, Shamah et al. 2008[45] and subsection ***1.2.3*** in this chapter). Cash, Ricci and Plaxco[46] demonstrated in the same year the use of a voltammetric sensor for the detection of protein-small molecule interactions directly

in serum with limits of detection at the nM concentration level. The small molecule recognition elements biotin and digoxigenin were used in the detection of streptavidin and anti-digoxigenin antibodies. Chen and others[47] also reported in 2009 a nanoplasmonic label-free biosensing platform for the label-free detection of the extracellular adherence protein (EAP) found on the outer surface of the bacterium *Staphylococcus aureus* and of the PSA cancer biomarker with detection limits at the fM concentration level. De and co-workers[48] developed conjugate proteins of nanoparticles and green fluorescent proteins for protein differentiation using linear discriminant analysis (LDA). The sensor was based on a hybrid synthetic-biomolecule that used arrays of green fluorescent protein (GFP) and nanoparticles to detect proteins at nM concentrations in both buffer and human serum. Distinct and reproducible fluorescence-response patterns were obtained from five serum proteins (human serum albumin, IgG, transferrin, fibrinogen and α-antitrypsin), both in buffer and spiked into human serum. The distinct response patterns resulted from the differences on the molecular interactions between the five target proteins and the GFP-NP conjugates. Fan et al.[49] also published the development of nanofluidic proteomic immunoassays for the serial analysis of oncoprotein activation in clinical specimens. The technique allowed the quantification of picograms of total and low-abundance oncoprotein isoforms in nanoliter volumes. Gaster and collaborators[50] also developed in 2009 a magnetic nanosensor technology that was matrix insensitive and capable of rapid, multiplex protein detection with resolution down to attomolar concentrations. Park et al.[51] developed combined viral nanoparticles, which were engineered to have dual affinity for troponin antibodies and nickel, with three-dimensional nanostructures including nickel nanohairs. The authors were able to detect troponin levels (a protein biomarker for myocardial infarction[52]) in human serum samples at attomolar concentrations.

In 2010, Estrela and others[53] developed a metal-oxide-semiconductor field-effect transistors (MOSFETs) to achieve label-free target protein detection at fM level of concentrations, using peptide aptamers that recognize highly related protein partners of the cyclin-dependent kinase family. Unfortunately, the requirement of clean room facilities as well as the complicated procedures required for FET construction limits the

wide use of this type of sensors. Kara, Merkoçi and co-workers[54] reported in the same year the label-free bioelectronic detection of aptamer-thrombin interaction based on electrochemical impedance spectroscopy (EIS) technique at the pM concentration level. The authors used multiwalled carbon nanotubes (MWCNT) as modifiers of screen-printed carbon electrotransducers. However, the relative high cost and complexity of the EIS instruments limit this type of aptamer-based electrochemical biosensors to only research applications. An et al.[55] also published in that year the real-time electrical detection of protein molecules using dielectrophoretically aligned SWCNT-film FET aptasensors. This device allowed the detection of thrombin down to the pM concentration levels. In that same year, Düzgün and collaborators[56] performed an exploratory attempt to study the potentiometric response of a SWCNT-based aptasensor in terms of the conformational changes of the aptamer molecules during the target recognition event in the detection of a free protein such as thrombin at nM concentrations in diluted buffer solutions. Unfortunately, despite the simplicity of this latter mentioned technique, its applications in more complex matrices at lower concentration values remained an open question.

In 2011, Atarashi and others[57] reported a new PrP^{Sc} amplification assay, called real-time quaking-induced conversion, which allowed the detection of ≥1 fg of PrP^{Sc} in diluted Creutzfeldt-Jakob disease brain homogenate. Such a technique exhibits a great sensitivity in PrP^{Sc} detection. Nevertheless the method can only be used in prion-related protein detection, variations to the technology may contribute to the creation of a similar method in the detection of other types of protein. Ogi et al.[58] reported in that same year the nM detection of human IgG with *Staphylococcus aureus* protein A nonspecifically immobilized on the film surfaces thin-film oscillator biosensors using a picosecond ultrasound method. In this method, ultrashort light pulses are focused on the surfaces of the films to excite the through-thickness resonance vibrations, which were detected by the delayed probe-light pulses using an optoelastic effect. Unfortunately, the use of the technique with different biorecognition elements in order to expand its biosensing capabilities have not been explored in that work.

1.1.2. Methods for bacterial detection

Effective prevention of infectious diseases caused by bacteria is possible when an adequate monitoring is implemented at the critical points for potential hazards. In critical situations as in an outbreak, the opportune achievement of information is crucial and thus, the use of rapid methods for the identification of pathogens are a necessity in order to trace their source and characteristics.[59] Unfortunately, the detection of bacteria has remained for years based on standard microbiological methods.[60] These methods have been a typical practice in clinical diagnostics as well as in ensuring the safety of food and water to be consumed all around the world for almost one century. These techniques make use of specific media for selective enrichment and culturing of bacteria, followed by further isolation steps, and finally confirmatory biochemical tests are also needed (Scheme 1.1). The process duration depends on the target pathogen, but in most of the cases a confirmatory result can take from a few days to even weeks.[61]

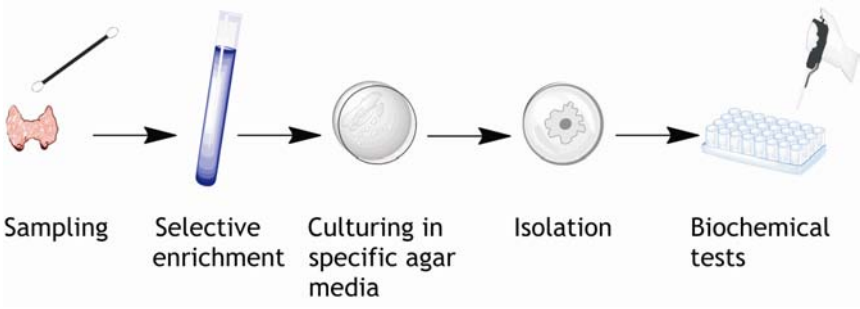

Scheme 1.1. Standard protocols for pathogen detection usually include several steps.

Numerous biosensing platforms have incorporated nanostructured materials as a strategy for reducing the limits of detection or the assay times in the detection of bacteria.[14] As a result, different approaches have been proposed, that include flow cytometry,[62] miniaturized biochemical tests, physicochemical methods for bacteriological metabolite measurements,[63] capillary electrophoresis,[64,65] ELISA[66] and fluorescence resonance energy transfer assays[67]. Methods based on electrochemical assays have been also developed. As an example, several electrochemical-based platforms have been reported, such as chip-based devices with

electrochemical impedance spectroscopy detection,[68] amperometric[69] and potentiometric[70] measurements by means of diverse types of both functionalized and simple electrodes. In any case, an ideal useful assay is supposed to detect, at least, the minimum number of living microorganism cells that are able to cause an infection in the body in a reasonable time of analysis. Nowadays, several biosensors have been developed for microorganism detection, improving substantially the analysis time and detection limit, showing promising results as 100 CFU/mL of bacteria in a 1 hour assay for ideal conditions.[71] Currently available ultrafast PCR detection methods are able to detect 5 CFU in only 7 minutes. [72] An important advance was achieved in this field, using a B cell-based sensor for the rapid identification of pathogens, reaching detection limits of 500 CFU/g in less than 5 minutes.[73] Unfortunately, the applications of those reported methods in high-throughput pathogen detection is challenged by the need of trained staff and the use of expensive devices.[74] Therefore, this subsection deals with the state of the art in analytical techniques for bacteria detection with a special focus on those methods with outstanding performance characteristics in terms of limit of detection, time of analysis or assay simplicity.

In 1999, Belgrader et al.[72] published an ultrafast PCR detection method for pathogen sensing at very low concentration levels (5 CFU) in 7 minutes, within a total reaction volume of 25 mL. This technique allowed the rapid detection of pathogenic DNA sequences using real time PCR analysis monitored by a spectrofluorometric thermal cycler.[75] The total assay required at least 20 minutes to be completed. The technique represented a breakthrough in bacteria detection at zero-tolerance levels. However, the method requires preprocessing steps for prior bacteria lysis and subsequent DNA extraction. This makes the overall procedure both expensive and complicated.

In 2000, Tu and others[76] reported the use of streptavidin coated magnetic beads for detecting 10^3-10^4 CFU of pathogenic bacteria by light addressable potentiometric sensors (LAPS). Streptavidin coated magnetic beads, partially labeled with biotinylated anti *Escherichia coli* O157 antibodies, were used to capture *Escherichia coli* O157:H7. Captured bacteria were further labeled with fluorescein-conjugated anti-*E. coli* O157:H7 antibodies and urease-labeled anti-fluorescein antibody. Magnetically

concentrated bacteria-containing complexes were then immobilized through streptavidin-biotin interactions on biotinylated nitro-cellulose membranes assembled as sample sticks for the instrument. The rate of pH change associated with the production of NH_3, by the urease in urea-containing solution was measured by a LAPS. Such an interesting technique demonstrated that magnetic beads can be successfully used in the extraction of bacteria from complex samples. However, the dependence of the technique on the detection of NH_3 as the reaction by-product challenged its deployment into more complex samples. As an example, samples with a strong pH buffering effect or samples that might be containing urea as an interfering agent would either lead to false-negatives or false-positives, respectively.

In 2001, Ilic and co-workers[77] demonstrated the single-cell detection with micromechanical oscillators. *E. coli*-cell-antibody binding events were detected using a resonant frequency-based mass sensor, comprised of low-stress silicon nitride cantilever beams. The binding events involved in the interaction between anti-*E. coli* O157:H7 antibodies immobilized on the cantilever beam and the O157 antigen present on the surface of pathogenic *E. coli* O157:H7 were measured in that manner. Such a platform facilitated the studies of bacteria-antibody interactions in mechanical terms for the first time. However, the incorporation of this biosensing platform as a quotidian tool for bacteria detection was limited by the device construction complexity.

Ruan, Yang and Li developed in 2003 electrochemical sensors for the detection of bacteria. Using the electrochemical impedance spectroscopy technique for measuring bacteria recognition events, the authors developed immunosensor chips for the detection of 10^3 CFU/mL *E. coli* O157:H7.[78] The authors also developed an electrochemical sensor for the detection of viable *Salmonella typhimurium* in a selective medium by monitoring oxygen consumption with cyclic voltammetry.[79] Using this method, the authors were able to detect changes on the voltammetric curves originated by the presence of 1-2 CFU/mL in a total assay time of 10 h. Despite the limit of detection achieved by this latter example, the assay still depended on the correct sample enrichment with bacteria. Baeumner and collaborators[80] also developed in the same year a highly sensitive and specific RNA biosensor for the rapid

detection of 40 CFU/mL of *Escherichia coli* in water in 15-20 minutes. Viable *E. coli* were identified and quantified via a 200 nucleotide long target sequence from mRNA. The limits of detection and time of analysis achieved by this method simplified enormously the detection of *E. coli* in aqueous samples. That same year, Rider and others[73] reported the use of genetically engineered cells in a pathogen identification sensor. This sensor used B lymphocytes that have been engineered to emit light within seconds of exposure to specific bacteria. The biosensor was able to sense 500 CFU/g bacteria in less than 5 minutes. This breakthrough in bacteria detection represented one of the first examples of bacteria detection methods in close to real time conditions.

In 2004, Zhao et al.[81] developed a rapid bioassay for single bacterial cell quantitation in 20 minutes using bioconjugated nanoparticles. The bioconjugated nanoparticles provided an extremely high fluorescent signal for bioanalysis when conjugated with antibodies. The antibody-conjugated nanoparticles were used to identify a variety of bacterium, such as *Escherichia coli* O157:H7, through antibody-antigen interaction and recognition. The previous example facilitated the design of portable biosensing platforms based on light-emitting nanoparticles which may represent in a future, a universal bacteria detection method. Moreover, Baeumner et al.[82] also reported in that same year the detection of 10 viable spores of *Bacillus anthracis* in 4 h targeting RNA sequences of the pathogen. The biosensor was based on an oligonucleotide sandwich-hybridization assay format. It used a membrane flow-through system with an immobilized DNA probe that hybridized with the target sequence. Signal amplification was provided when the target sequence hybridized to a second DNA probe that was coupled to liposomes encapsulating a dye. The amount of liposomes captured in the detection zone could be read visually and quantified with a hand-held reflectometer. The extremely low detection limit achieved demonstrated that the previously described biosensing platform is a promising tool with interesting applications not only in biowarfare agent detection but also for the development of diagnostic tools of a wide range of human and animal diseases.

In 2005, Zaytseva and others[83] developed a microfluidic biosensor module for pathogen detection. The biosensor recognition principle was based on DNA/RNA

hybridization and liposome signal amplification. Superparamagnetic beads were incorporated into the system as a mobile solid support. However, the dependence on expensive equipment for the construction of the microfluidic systems may represent a limitation in the deployment of this sensor in high throughput applications. Ochoa et al.[84] also reported the immunomagnetic isolation of enterohemorrhagic *Escherichia coli* O157:H7 from ground beef and its identification by matrix-assisted laser desorption-ionization time-of-flight mass spectrometry (MALDI-TOF) and database searches. Using this method, the authors were able to detect 10^6 CFU/mL in 25 minutes. Unfortunately, the dependence of the technique on accurately developed databases, as well as the high cost of the spectrometry-based techniques represented a serious limitation for its ample use. Kulagina and co-workers[85] used the antimicrobial peptide magainin I as a recognition element for *Escherichia coli* O157:H7 and *Salmonella typhimurium* detection on an array-based biosensor. They immobilized magainin I on silanized glass slides using biotin-avidin chemistry, as well as through direct covalent attachment. Immobilized magainin I was able to bind *Salmonella* and *E. coli* at detection limits ranging between 10^4 to 10^5 CFU/mL. Despite the limit of detection achieved, such an interesting platform represented the first example of antimicrobial peptides as recognition elements in a biosensing platform aimed for pathogen detection, which opened up the possibilities for this class of molecules to be used in different biosensing device formats.

Gao and collaborators[86] reported in 2006 the development of biofunctional magnetic nanoparticles combined with fluorescent probes for the detection of bacteria in blood. The authors were able to detect *E. coli* and *Staphlococcus aureus* at 100 CFU/mL concentrations in blood samples. The use of fluorescent probes demonstrated that easy-to-use magnetic nanoparticles could be used in optical biosensing platforms at very low concentration levels. Yu et al[87] have also reported in the same year a mid-IR biosensor for the detection and fingerprinting of pathogens on gold island functionalized chalchogenide films. Anti-*E. coli* O157:H7 and anti-*Salmonella* antibodies were immobilized on gold islands previously deposited on the surface of IR-transparent Ge-containing chalcogenide glass films. The films functionalized with anti-*E. coli* O157:H7 and anti-*Salmonella* antibodies were used to detect as low as 10^3

CFU/mL *E. coli* O157:H7 and *Salmonella enteriditis* through label-free IR fingerprinting in a 90 minute assay. Regardless of the rapidness and simplicity of the assay, the requirement for an IR device represents a limitation for this technique. Tok and co-workers[88] demonstrated that metallic striped nanowires could be used in multiplexed fluorescence-based immunoassay platforms for pathogen detection. The authors detected *Bacillus globigii* spores to simulate *Bacillus anthracis* and other bacterial species with a limit of detection of 10^5 CFU/mL in a 3-4 h assay. The method developed represented an important advance in rapid pathogen detection methods. The technique allowed discriminating between different targets in a biosensing format similar to an electronic barcode readout. In that year, Ko and Grant[89] developed a novel fluorescence resonance energy transfer-based optical fiber biosensor for the rapid detection of *Salmonella typhimurium* in ground pork samples. Labeled antibody–protein G complexes were formed via the incubation of anti-*Salmonella* antibodies labeled with FRET donor fluorophores and protein G labeled with FRET acceptor fluorophores. The signal detected by the fiber optic portable biosensor allowed the detection of 10^3 CFU/g of the pathogen. Such a portable biosensing platform represented an interesting example of FRET-based biosensor. Unfortunately, the detection system depended on a correct selection of the suitable recognition element, otherwise, unspecific responses may be achieved. Subramanian et al.[90] investigated as well the capability of alkane monothiol and dithiol dendritic tether based SAMs in conjunction with surface plasmon resonance (SPR) for the detection of 10^5 CFU/mL of *Staphylococcus aureus* using antibodies as recognition elements.

In 2007, Maalouf et al.[91] compared an EIS-based biosensing platform with a SPR-based biosensor in the detection of *E. coli* using polyclonal antibodies for the biorecognition of the pathogen. In this way, the detection limit of *E. coli* found by SPR spectroscopy was 10^7 CFU/mL while the EIS technique allowed the detection of 10^3 CFU/mL. In this way, the authors demonstrated that electrochemical biosensors are a powerful tool in the development of highly sensitive detection platforms. In that same year, Balasubramanian and others[92] demonstrated that lytic phage could be used as a specific and selective probe for the detection of *Staphylococcus aureus* by SPR spectroscopy. The biosensor developed was able to sense as low as 10^4 CFU/mL. This

latter example demonstrated that virus can be used as biorecognition elements in pathogen detection while the possible applications of such a platform are enormous. Escamilla-Gómez and collaborators[93] developed an amperometric immunosensor for the quantification of *Staphylococcus aureus* using SAM-modified electrodes as immobilization platforms. In this technique, the limit of detection was $1.6x10^5$ CFU/mL. Self-assembled monolayers are a useful tool in biosensor construction and allow the construction of reduced biosensors. Morales et al.[94] also reported an amperometric biosensor for simultaneous detection and identification of *Escherichia coli*, *Staphylococcus aureus* and *Salmonella choleraesuis* using a glucose oxidase-peroxidase composite biosensor. The biosensor was able to detect $6.5x10^2$ CFU/mL after an incubation period of 3 h, however, the limit of detection was lowered down to 6.5 CFU/mL when the samples were incubated for 7 h. In both latter examples, the simplicity of amperometric immunosensors are exploited to open up the possibility to construct smaller biosensors for pathogen detection.

In 2008, Laczka and collaborators[95] developed capacitive immunosensors based on interdigitated microelectrodes for the detection of 10^4-10^5 CFU/mL of *E. coli* and *Salmonella typhimurium*. Shabani et al.[96] also demonstrated in the same year, the use of bacteriophage-modified microarrays for the direct impedimetric detection of 10^4 CFU/mL of *Salmonella* typhimurium in 20 minutes. Villamizar and co-workers[71] reported the detection of 100 CFU/mL *Salmonella infantis* in 1 h using carbon nanotube FETs and antibodies. So and others[97] also published in the same year the detection and quantification of *Escherichia coli* using aptamer-functionalized single-walled carbon-nanotube FETs. The minimum amount of bacteria detected by this method was $2x10^3$ CFU/mL (0.93 CFU in 5 µL) in 20 minutes. These latter FET-based biosensors demonstrated that electrochemical biosensing platforms based on nanostructured materials may help on reducing both the limit of detection and time of analysis.

In 2009, Lee et al.[98] demonstrated that core–shell nanoparticles in combination with a NMR-filter system could be used as an efficient tool for pathogen detection. Using the bacillus Calmette-Guérin (BCG) as a surrogate for *Mycobacterium tuberculosis*, the authors demonstrated an unprecedented detection speed and

sensitivity of as few as 20 colony-forming units (CFU) in sputum (1 mL) in a 30 min assay. In the same year, Abu-Rabeah and others[99] reported a highly sensitive amperometric immunosensor for the detection of *Escherichia coli* (10 CFU/mL). Liébana et al.[100] detected *Salmonella* in milk by electrochemical magneto-immunosensing. In this approach, the bacteria was captured and preconcentrated from milk samples with magnetic beads through an immunological reaction. A second antibody labeled with peroxidase was used as serological confirmation with electrochemical detection based on a magneto-electrode. In this way, the biosensing platform detected 10^3 CFU/mL in 50 minutes. However, when the technique was combined with a preenrichment step of 6 h, the limit of detection reported was 1.4 CFU/mL. In all the previously described examples, nanostructures played the central role for a dramatic reduction of extremely low limits of detection and reduced times of analysis, thus suggesting that lower limits of detection may be achieved if the biosensing platforms are optimized.

Dharmasiri and co-workers[101] reported in 2010 an antibody modified microfluidic chip for the enrichment and detection of *Escherichia coli* O157:H7 from water samples with a lowest detected concentration of 6 CFU/mL. In that year, Grossi et al.[102] also developed an embedded portable biosensor system for bacterial concentration detection. The sensor was based on the measurement of changes in the impedance when bacteria were present. In this manner, the platform was able to detect 10^6 CFU/mL in 3 h. Both examples of target concentration demonstrated that lower limits of detection may be reached when a pre-processing step is incorporated in the detection process.

In 2011, Miranda and collaborators[103] reported a supramolecular enzyme nanoparticle biosensor for the colorimetric detection of bacteria. Using this strategy, the authors were able to quantify bacteria at concentrations of 10^2 CFU/mL. Cationic gold NPs featuring quaternary amine headgroups were electrostatically bound to an enzyme [β-galactosidase (β-Gal)], inhibiting enzyme activity. When analyte bacteria bound to the NP, β-Gal was released and its activity was consequently restored, providing an enzyme-amplified colorimetric readout of the binding event. García-Aljaro et al.[104] reported in the same year the development of carbon nanotube-based

chemiresistive biosensors for detection of 10^3 CFU/mL of *E. coli* O157:H7 in 60 minutes. Wan and others[105] developed in the same year an impedimetric immunosensor doped with reduced graphene sheets fabricated by controllable electrodeposition for the non-labelled detection of pathogenic sulphate-reducing bacteria at a limit of detection of $1.8x10^1$ CFU/mL.

1.2. Fundamentals

This section aims to set the fundamental basis and theoretical background of materials and techniques so that the reader can perfectly follow the performance of the biosensors developed in this Thesis. Subsection ***1.2.1***, includes a description of the physical properties of carbon nanotubes that are of a particular interest for a full comprehension of the sensors herein developed. In subsection ***1.2.2***, the theoretical background of the potentiometric sensors based on carbon nanotubes as ion-to-electron transducers is discussed. Finally, in subsection ***1.2.3***, a description of the aptamers as biorecognition elements is mentioned.

1.2.1. Carbon nanotubes

Since the rediscovery of carbon nanotubes (CNT) by S. Iijima in 1991,[106] this new allotropic form of carbon has been of interest in many fields of science, from basic science research to advanced materials. There are basically two types of CNTs, single walled and multi-walled. Single walled carbon nanotubes (SWCNT) can be seen as a seamless graphene rolled sheet and can be of metallic or semiconducting behavior, depending on the rolling orientation of the graphene sheet. Multi-walled carbon nanotubes (MWCNT) are coaxial SWCNTs rolled-up all together in a single tube, and in all cases, they show metallic behavior. Both CNT types are of interest on the fields of nanoelectromechanical systems, composite materials, chemical sensing, molecular electronics and energy storage, due to their outstanding properties. The properties of CNTs are originated by their chemical structure and their extremely high surface-to-volume ratio. This is precisely what suits CNTs as perfect molecules for sensing and transducing, since they have a huge capability to support electron transfer between heterogeneous phases.[107] As a result of such properties, CNTs have been used as elements in FETs,[108,109] capacitors,[110] nanoelectrodes in voltammetric analysis[111] and recently, our research group has demonstrated that they also can be used as transducers[112] in potentiometric analysis. CNTs can be produced in various ways, such as arc discharge, chemical vapor deposition, and others. Regarding to their purification, it could be done by many ways for example sonication, filtering and annealing, among others.[113]

Carbon nanotubes (Figure 1.1a) are an allotropic form of carbon, formed by end tips with the molecular structure of fullerene (Figure 1.1b), and a large folded graphene-like wall at the length of the molecule. Their length is usually up to several dozens of microns and their diameter ranges between less than one nanometer to a few nanometers. They can be seen as a nearly one-dimensional form of fullerenes (Figure 1.1c).[114]

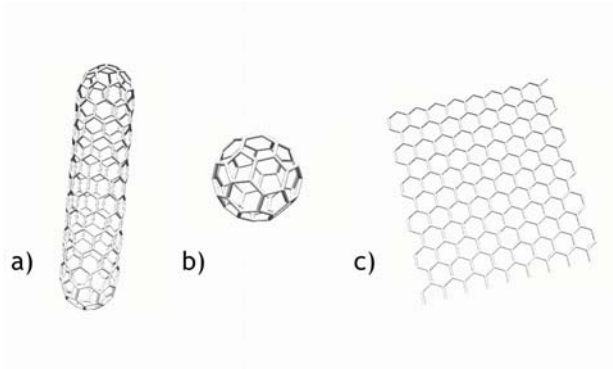

Figure 1.1. a) Basic structure of a single-walled carbon nanotube. b) Fullerene molecule (C_{60}). c) Basic structure of a graphene sheet.

Single walled carbon nanotubes can be formed by folding the graphene sheet along lattice vectors (a_1, a_2). The (a_1, a_2) indices determine the diameter and chirality, which are key parameters of a nanotube. As an example, in (Figure 1.2), the two basis vectors a_1 and a_2 are shown. Folding of the (8,8), (8,0), and (10,-2) vectors lead to armchair (Figure 1.2b), zigzag (Figure 1.2c), and chiral (Figure 1.2d) nanotubes, respectively. Depending on this, they have dissimilar properties such as optical activity, mechanical strength and electrical conductivity. Multi-walled carbon nanotubes (Figure 1.3) can be considered as a collection of concentric single walled carbon nanotubes with different diameters. The distance between layers of the MWCNT is about 0.34 nm. The length and diameter of these structures differ a lot from those of single walled and their properties are also very different.[107]

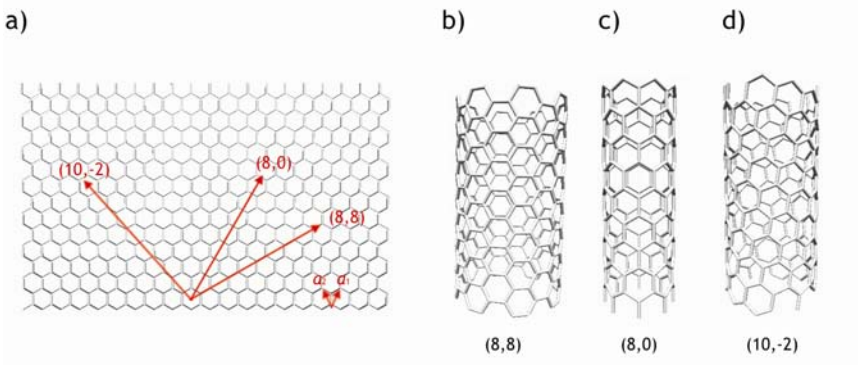

Figure 1.2. a. Schematic honeycomb structure of a graphene sheet. b. Armchair structure. c. Zigzag. d. Chiral.

CNTs display an improved chemical reactivity, compared with a graphene sheet, as a consequence of the curvature of the carbon nanotube surface. Carbon nanotube reactivity is directly related to the π-orbital divergence caused by an increased curvature. Consequently, there is a difference between the sidewall and the end caps of a nanotube. Therefore, the smaller the nanotube diameter is, the greater the observed reactivity. This reactivity allows chemical modification of either sidewalls or end caps.[115]

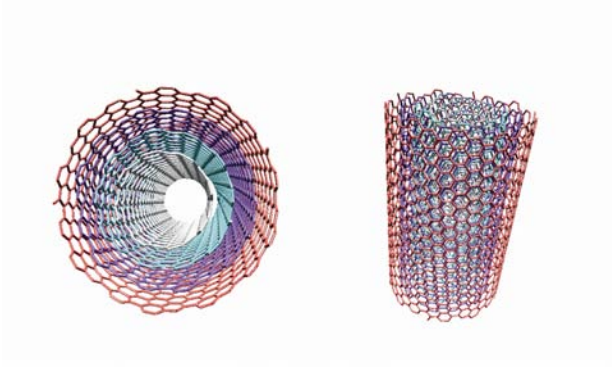

Figure 1.3. Representation of a multi-walled carbon nanotube.

Electrical properties are different depending on the type of carbon nanotube. Multi-walled carbon nanotubes are always metallic. However, single-walled carbon nanotubes can exhibit different electrical properties depending on their lattice vector.

The differences in conducting properties are caused by the molecular structure that results in a different band structure and thus a different band gap. Single walled carbon nanotubes can be either metallic or semiconductors, with band gaps that are relatively large (approximately 0.5 eV for typical diameter of 1.5 nm) or small (approx. 10 meV), even if they have nearly identical diameters. It has been shown that a nanotube is metallic when vector parameters (a_1, a_2) fulfill the equation: $a_1 = a_2$ or ($a_1 - a_2$) = 3i, where i is an integer. When this does not account, nanotubes are semiconducting.[116] Thus, armchair nanotubes are always metallic while both chiral and zigzag molecules are either metallic or semiconducting. For the same-chirality semiconducting nanotubes, the band gap is inversely proportional to the diameter. The differences in conductivity can easily be derived from the graphene sheet properties.[117] The resistance to conduction is determined by quantum mechanical aspects and was proved to be independent of the nanotube length.[118] Thus, there are infinite possibilities in the type of carbon nanotube molecules, and each nanotube could exhibit distinct physical properties.

According to some theoretical studies with chiral nanotubes,[119] optical activity disappears if the nanotubes become larger. In this sense, it is expected that other physical parameters are also biased by these properties. Carbon nanotubes have large values of Young modulus in their axial direction. The nanotube molecule is very flexible due to the length.[115] For that reason, these molecules are appropriate for applications in composite materials that need anisotropic properties.

1.2.2. Potentiometric sensors based on carbon nanotubes as ion-to-electron transducers

Electrochemical detection techniques are generally preferred over others due to the offered advantages such as rapid response, low-cost and ease of use.[120] Depending on which aspects of the electrochemical cell are controlled and which are measured, electrochemical methods can be classified in three major categories: 1) potentiometric methods, in which the difference in potential (voltage) between two electrodes is measured; 2) coulometric methods, which are based on the measurement of the amount of electricity consumed or produced in the cell; and 3)

voltammetric methods, where the current is measured while maintaining controlled the potential in the cell in a fixed or variable mode.[121]

Among the potentiometric techniques, electromotive force measurements based on solid state electrodes represent an attractive tool for chemical analysis in liquid samples. The technique is based on the passive measurement of the electric potential of a solution between two electrodes, a reference electrode and an indicator (working) electrode, while the solution composition is barely affected. The reference electrode consists on an electrode with a well-known and stable electrode potential. The stability in the reference electrode is reached by using a redox system with constant concentrations of two redox component (eg. Ag^0/AgCl in saturated KCl). The indicator electrode is an electrode whose potential varies according to the composition of the solution. If a recognition element is incorporated at the transducer/solution interface, the indicator electrode can be selective for a particular target (e.g. ions or other charged species). When the recognition element consists of an ionophore able to recognize a particular ion, and such ionophore is embedded in a permeable membrane between the transducer and the solution (as in the ion-selective membranes), the potentiometric electrode is therefore termed as an ion-selective electrode (ISE). However, other recognition elements such as biorecognition molecules can be included in the construction of an electrode instead of using selective membranes. In such a case, the indicator electrode can be tailored to detect different targets as long as the transducer part is able to detect the electrochemical variations occurred during the recognition process. In potentiometric analysis, the electric potential (electromotive force) is related to the analyte concentration when a thermodynamic equilibrium is reached between the free analyte at the solution and the analyte present at the recognition element (e.g. the ion concentration within the ion-selective membrane or the analyte molecules tethered by a biorecognition element). In the steady state, the decrease on free energy produced when the analyte diffused from the solution to the recognition layer is compensated by an increase on free energy at the recognition layer/transducer interface by the repulsion of charges of the same charge at the transducer. This change on free energy is therefore measured as a change in voltage by a high impedance voltmeter. In a rapid-kinetic stabilization

process, this equilibrium can be reached almost in real-time, and thus, the measurement of voltage between the reference electrode and the indicator electrode gives a parameter of reference for analyte concentration.[22,121– 123]

As mentioned earlier, carbon nanotubes can be used as transducers in potentiometric analysis.[112] Both, multi-walled and single-walled carbon nanotubes can be perfectly used in the construction of solid-state potentiometric sensors. As an example, a SWCNT-based solid-state ion-selective electrode has been developed by Hernández, Riu and Rius for the direct detection of Ca^{2+} in sap, while a MWCNT-based solid-state ISE able to detect ClO_4^- has been reported by Parra, Rius and collaborators. [124,125] Solid-state potentiometric sensors present more advantages than their counterparts with an internal solution, especially in terms of versatility during measurements and their ability to be miniaturized. Moreover, in the case of ion-selective electrodes with internal solutions, leakage of the ions from the internal solution may occur in long-term measurements, which evidently cannot occur in a solid state ISE. In the same way, many authors have reported the use of different materials such as electroactive polymers,[126 – 130] macroporous carbon,[131] fullerenes[132] or platinized porous silica[133] as transducers in solid-state ion-selective electrodes. Among the transducers previously mentioned, electroactive polymers have represented the mainstay for years in the construction of solid-state ISE. Unfortunately, this latter type of material presents some important disadvantages. As an example, the major drawback of many conducting polymers is their sensitivity to light. However, such a problem can be overcome by the use of light-insensitive transducers, such as carbon nanotubes.[23,112]

The chemical structure of carbon nanotubes, their high surface-to-volume ratio, their extraordinary capacity to promote electron and charge transfer between heterogeneous phases and the presence of mobile electrons on the surface of the nanotubes makes them particularly suited for electrochemical field sensing at the nanoscale.[107] Charge transfer processes in carbon nanotubes are driven by the high double layer capacitance resulting from the large interface between the nanomaterial and the solution (Figure 1.4).[134]

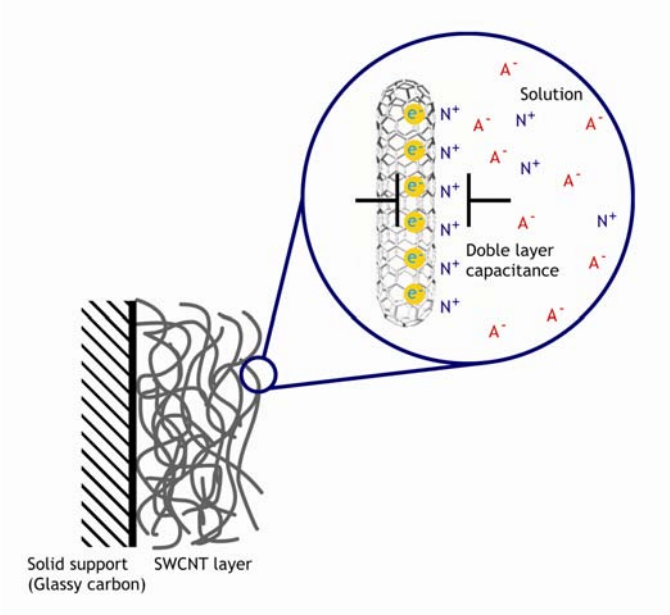

Figure 1.4. Schematic description of the ion-to-electron transduction process of the SWCNT/electrolyte system. N^+ = cation, A^- = anion, e- = electron.

1.2.3. Aptamers as biorecognition elements

A relatively novel approach for selective and high proficiency detection of a wide range of small molecules, proteins, virus and bacteria are special nucleotide-type sequences also called aptamers. These molecules are nucleic acid segments or similar structures (such as peptide nucleic acids) that have been engineered through repetitive cycles of *in vitro* selection (Figure 1.5), well known as systematic evolution of ligands by exponential enrichment (SELEX) to bind selectively to over 150 targets including small molecules, proteins, cell adhesion molecules, virus and bacteria.[45,135] The SELEX process starts with a chemically synthesized DNA library containing about 10^{14} to 10^{15} different individual molecules. The library is designed to contain a contiguous region of random sequences between two fixed sequence regions. The fixed sequences are primer binding sites used during the PCR amplification process. Aptamers can be synthesized from both DNA and RNA libraries. When RNA aptamers

are to be obtained, DNA libraries are previously converted to RNA libraries. In such a case, one of the fixed sequences flanking the random section of the DNA molecules within the library are engineered to contain a promoter for a RNA polymerase.[136] The random sequence oligonucleotide library is then exposed to the target under controlled buffer conditions. The sequences that do not bind to the target are then discarded from the solution by an appropriate partitioning method. The bound sequences are recovered from the target. Such a population contains a mixture of both high- and low-affinity binding molecules to the target. Further screening is needed in order to eliminate the sequences with low-affinity binding. Therefore, this mixture of aptamer candidates is amplified directly by PCR (in the DNA aptamer synthesis) for the next round of selection. RNA aptamer sequences are amplified by PCR after reverse transcription in order to convert such a sequence into its DNA complementary sequence. Afterwards, a single stranded DNA population is obtained by strand separation of PCR products. The previous mixture is then incubated with a new solution containing the target in order to start a new round of selection. The RNA population is obtained by *in vitro* transcription. Several iterations of the selection process are carried out while the medium conditions are increasingly stringed so that the high-affinity sequences may be enriched at the expense of the low-affinity binders. The progress of the enrichment of high-affinity binders can be determined by carrying out binding analysis of enriching populations against the target. The cycle is stopped once an enriched library reaches the affinity saturation. Finally, the PCR products are accordingly cloned and sequenced.[135,137]

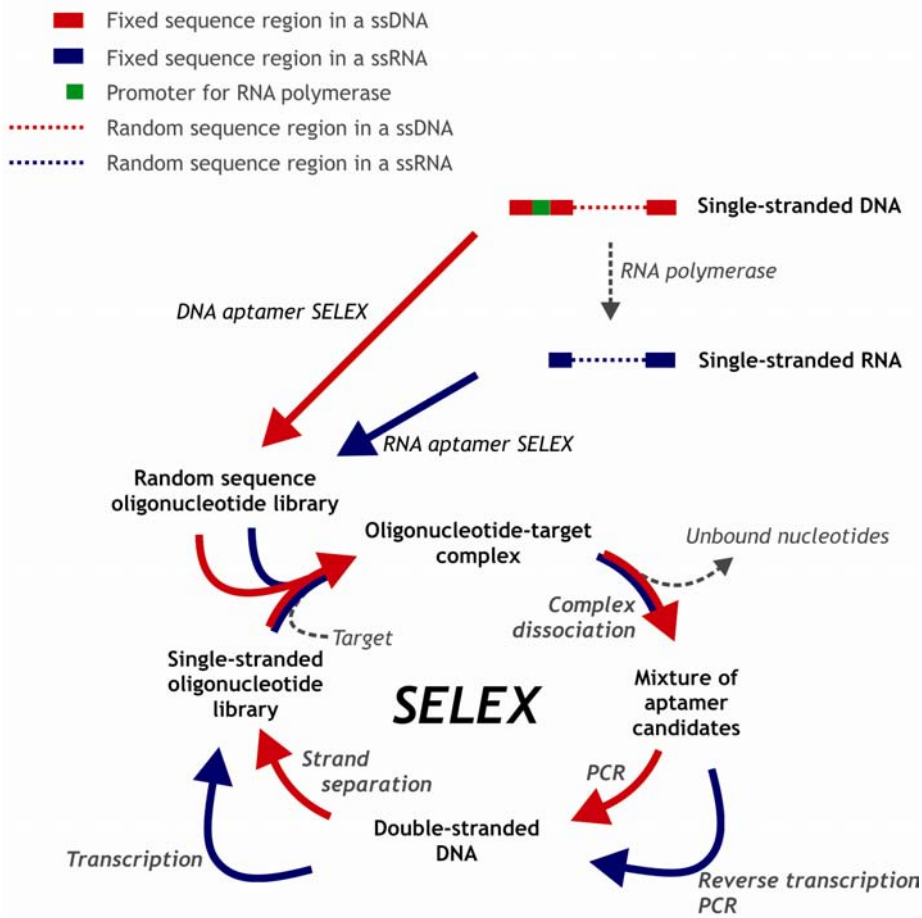

Figure 1.5. The SELEX process: (red arrows) DNA aptamer selection; (blue arrows) RNA aptamer selection.

This class of molecules is a promising tool that rivals both, antibodies in diagnostics and drugs in treatment for diseases. Aptamers are more advantageous and display fewer drawbacks, compared to antibodies. Because of these properties, aptamers are completely suitable as molecular recognition elements in the field of biosensors, making it possible to perform detection of complex targets.[138 – 141] In recent times, novel applications of the aptamer technology are rapidly arising in the field of electrochemical methods for detection of biochemical elements at very low concentration levels.[142] It has been recently demonstrated that potentiometric sensors based on solid state microelectrodes allow the quantification of proteins in the

subnanomolar concentration range, by means of sandwich aptamer-protein assays.[40] Additionally, some research groups have been able to develop novel carbon-based materials with similar aims and more promising results in electroanalytical chemistry, using carbon nanotube modified electrodes and aptamers.[143] Nevertheless, despite of the recent advances in the development of electrochemical aptasensors and sensors based on carbon nanotubes for rapid monitoring of proteins and bacteria, there is not yet any application of a reagentless, real-time, reusable and highly-selective potentiometric biosensor for the direct detection of whole-bacteria at zero-tolerance levels or proteins at attomolar concentrations.[142,144 – 147]

1.3. References

[1] J. M. Walker (ed.), *The protein protocols handbook*. Humana Press, Totowa NJ. 1146 p. (**2002**).

[2] B.T. Kurien, R.H. Scofield (eds.), *Protein Blotting and Detection: Methods and Protocols*. Humana Press, Totowa NJ. 588 p. (**2009**).

[3] M.J. Barber, D.C. Eichler, L.P. Solomonson, *Biochem. Soc. T.* **1985**, *13*, 624-625.

[4] E. Engvall E, P.E. Perlmann, *Immunochemistry* **1971**, *8*, 871-874.

[5] E. Engvall, *Clin. Chem.* **2010**, *56*, 319-320.

[6] S.L. Taylor, J.A. Nordlee, L.M. Niemann, D.M. Lambrecht, *Anal. Bioanal. Chem.* **2009**, *395*, 83-92.

[7] S. Song, Y. Qin, Y. He, Q. Huang, C. Fan, H.-Y. Chen, *Chem. Soc. Rev.* **2010**, *39*, 4234-4243.

[8] J. Durner, *Angew. Chem. Int. Ed.* **2010**, *49*, 1026-1051.

[9] L.R. Goulart, C.U. Vieira, A.P. Freschi, F.E. Capparelli, P.T. Fujimura, J.F. Almeida, L.F. Ferreira, I.M. Goulart, A.G. Brito-Madurro, J.M. Madurro, *Crit. Rev. Immunol.* **2010**, *30*, 201-222.

[10] A. de la Escosura-Muniz, A. Merkoçi, *Expert Opin. Med. Diagn.* **2010**, *4*, 21-37.

[11] C.B. Jacobs, M.J. Peairs, B.J. Venton, *Anal. Chim. Acta* **2010**, *662*, 105-127.

[12] H.R. Byon, S. Kim, H.C. Choi, *NANO* **2008**, *3*, 415-431.

[13] B.L. Allen, P.D. Kichambare, A. Star, *Adv. Mater.* **2007**, *19*, 1439-1451.

[14] W. Yang, K.R. Ratinac, S.P. Ringer, P. Thordarson, J.J. Gooding, F. Braet, *Angew. Chem. Int. Ed.* **2010**, *49*, 2114-2138.

[15] S.S. Wong, E. Joselevich, A.T. Woolley, C.L. Cheung, C.M. Lieber, *Nature* **1998**, *394*, 52-55.

[16] C.W.C. Chan, S. Nie, *Science* **1998**, *281*, 2016-2018.

[17] C.A. Rowe, L.M. Tender, M.J. Feldstein, J.P. Golden, S.B. Scruggs, B.D. MacCraith, J.J. Cras, F.S. Ligler, *Anal. Chem.* **1999**, *71*, 3846-3852.

[18] G. Wu, R.H. Datar, K.M. Hansen, T.Thundat, R.J. Cote, A. Majumdar, *Nat. Biotechnol.* **2001**, *19*, 856-860.

[19] Y. Cui, Q. Wei, H. Park, C.M. Lieber, *Science* **2001**, *293*, 1289-1292.

[20] N. Ramachandran, D.N. Larson, P.R.H. Stark, E. Hainsworth, J. LaBaer, *FEBS J.* **2005**, *272*, 5412-5425.

[21] A. Star, J.-C.P. Gabriel, K. Bradley, G. Grüner, *Nano Lett.* **2003**, *3*, 459-463.

[22] D.C. Harris, *Quantitative Chemical Analysis.* W. H. Freeman and Co. New York, NY. 928 p. (**2003**).

[23] A. Düzgün, G.A. Zelada-Guillén, G.A. Crespo, S. Macho, J. Riu, F.X. Rius, *Anal. Bioanal. Chem.* **2011**, *399*, 171-181.

[24] R.J. Chen, S. Bangsaruntip, K.A. Drouvalakis, N.W.S. Kam, M. Shim, Y. Li, W. Kim, P.J. Utz, H. Dai, *Proc. Natl. Acad. Sci.* **2003**, *100*, 4984-4989.

[25] J.-M. Nam, C.S. Thaxton, C.A. Mirkin, *Science* **2003**, *301*, 1884-1886.

[26] A.-H. Lu, E.L. Salabas, F. Schüth, *Angew. Chem. Int. Ed.* **2007**, *46*, 1222-1244.

[27] C.A. Savran, S.M. Knudsen, A.D. Ellington, S.R. Manalis, *Anal. Chem.* **2004**, *76*, 3194-3198.

[28] K.P. Dierksen, L. Mojovic, B.A. Caldwell, R.R. Preston, R. Upson, J. Lawrence, P.N. McFadden, J.E. Trempy, *J. Appl. Toxicol.* **2004**, *24*, 363-369.

[29] T. Hianik, V. Ostatná, Z. Zajacová, E. Stoikova, G. Evtugyn, *Bioorg. Med. Chem. Lett.* **2005**, *15*, 291-295.

[30] M.C. Rodriguez, A.N. Kawde, J. Wang, *Chem. Commun.* **2005**, 4267-4269.

[31] H.-M. So, K. Won, Y.H. Kim, B.-K. Kim, B.H. Ryu, P.S. Na, H. Kim, J.-O Lee, *J. Am. Chem. Soc.* **2005**, *127*, 11906-11907.

[32] H. Gu, K. Xu, C. Xu, B. Xu, *Chem. Commun.* **2006**, 941-949.

[33] H.R. Byon, H.C. Choi, *J. Am. Chem. Soc.* **2006**, *128*, 2188-2189.

[34] P. Saá, J. Castilla, C. Soto, *Science* **2006**, *313*, 92-94.

[35] S.B. Prusiner, *Proc. Natl. Acad. Sci. U.S.A.* **1998**, *95*, 13363-13383.

[36] J. Castilla, P. Saá, C. Soto, *Nat. Med.* **2005**, *11*, 982-985.

[37] K. Maehashi, T. Katsura, K. Kerman, Y. Takamura, K. Matsumoto, E. Tamiya, *Anal. Chem.* **2007**, *79*, 782-787.

[38] M. Mehta, C.S. Hanumanthaiah, P.A. Betala, H. Zhang, S. Roh, W. Buttner, W.R. Penrose, J.R. Stetter, V.H. Pérez-Luna, *Biosens. Bioelectron.* **2007**, *23*, 728-734.

[39] C.-C. You, O. R. Miranda, B. Gider, P. S. Ghosh, I.-B. Kim, B. Erdogan, S. A. Krovi, U. H. F. Bunz, V. M. Rotello, *Nat. Nanotechnol.* **2007**, *2*, 318-323.

[40] A. Numnuam, K.Y. Chumbimuni-Torres, Y. Xiang, R. Bash, P. Thavarungkul, P. Kanatharana, E. Pretsch, J. Wang, E. Bakker, *Anal. Chem.* **2008**, *80*, 707-712.

[41] G.A. Evtugyn, A.V. Porfireva, T. Hianik, M.S. Cheburova, H.C. Budnikova, *Electroanalysis* **2008**, *20*, 1300-1308.

[42] H. Lee, E. Sun, D. Ham, R. Weissleder, *Nat. Med.* **2008**, *14*, 869-874.

[43] M. Fukasawa, W. Yoshida, H. Yamazaki, K. Sode, K. Ikebukuro, *Electroanalysis* **2009**, *21*, 1297-1302.

[44] Y.-L. Zhang, P.-F. Pang, J.-H. Jiang, G.-L. Shen, R.-Q. Yu, *Electroanalysis* **2009**, *21*, 1327-1333.

[45] A.M. Shamah, J.M. Healy, S.T. Cload, *Acc. Chem Res.* **2008**, *41*, 130-138.

[46] K.J. Cash, F. Ricci, K.W. Plaxco, *J. Am. Chem. Soc.* **2009**, *131*, 6955-6957.

[47] S. Chen, M. Svedendahl, M.Käll, L. Gunnarsson, A. Dmitriev, *Nanotechnology* **2009**, *20*, 434015/1-434015/9.

[48] M. De, S. Rana, H. Akpinar, O.R. Miranda, R.R. Arvizo, U.H.F. Bunz, V.M. Rotello, *Nat. Chem.* **2009**, *1*, 461-465.

[49] A.C. Fan, D. Deb-Basu, M.W. Orban, J.R. Gotlib, Y. Natkunam, R. O'Neill, R.A. Padua, L. Xu, D. Taketa, A.E. Shirer, S. Beer, A.X. Yee, D.W. Voehringer, D.W. Felsher, *Nat. Med.* **2009**, *15*, 566-571.

[50] R.S. Gaster, D.A. Hall, C.H. Nielsen, S.J. Osterfeld, H. Yu, K.E. Mach, R.J. Wilson, B. Murmann, J.C. Liao, S.S. Gambhir, S.X. Wang, *Nat. Med.* **2009**, *15*, 1327-1332.

[51] J.-S. Park, M.K. Cho, E.J. Lee, K.-Y. Ahn, K.E. Lee, J.H. Jung, Y. Cho, S.-S. Han, Y.K. Kim, J. Lee, *Nat. Nanotechnol.* **2009**, *4*, 259-264.

[52] J.E. Adams 3d, G.S. Bodor, V.G. Davila-Roman, J.A. Delmez, F.S. Apple, J.H. Ladenson, A.S. Jaffe, *Circulation* **1993**, *88*, 101-106.

[53] P. Estrela, D. Paul, Q. Song, L.K. Stadler, L. Wang, E. Huq, J.J. Davis, P. Ko Ferrigno, P. Migliorato, *Anal. Chem.* **2010**, *82*, 3531-3536.

[54] P. Kara, A. de la Escosura-Muñiz, M. Maltez-da Costa, M. Guix, M. Ozsoz, A. Merkoçi, *Biosens. Bioelectron.* **2010**, *26*, 1715-1718.

[55] T. An, K.S. Kim, S.K. Hahn, G. Lim, *Lab Chip* **2010**, *10*, 2052-2056.

[56] A. Düzgün, A. Maroto, T. Mairal, C. O'Sullivan, F. X. Rius, *Analyst* **2010**, *135*, 1037-1041.

[57] R. Atarashi, K. Satoh, K. Sano, T. Fuse, N. Yamaguchi, D. Ishibashi, T. Matsubara, T. Nakagaki, H. Yamanaka, S. Shirabe, M. Yamada, H. Mizusawa, T. Kitamoto, G. Klug, A. McGlade, S.J. Collins, N. Nishida, *Nat. Med.* **2011**, *17*, 175-178.

[58] H. Ogi, T. Kawamoto, N. Nakamura, M. Hirao, M. Nishiyama, *Biosens. Bioelectron.* **2011**, *26*, 1273-1277.

[59] C.A. Batt, *Science* **2007**, *316*, 1579-1580.

[60] P. Gerhardt, R.G.E. Murray, R.N. Costilow, E.W. Nester, W.A. Wood, N.R. Krieg, G.B. Philips (Eds.), *Manual of methods for general bacteriology*. American Society for Microbiology, Washington, D.C. p. 524 (**1981**).

[61] P. Vasavada, *J. Dairy Sci.* **1993**, *76* , 3101-3113.

[62] K. Hibi, A. Abe, E. Ohashi, K. Mitsubayashi, H. Ushio, T. Hayashi, H. Ren, H. Endo, *Anal. Chim. Acta* **2006**, *158*, 573-574.

[63] G. Mazza, *Appl. Environ. Microbiol.* **1983**, *45*, 1949-1952.

[64] E. Avaniss-Aghajani, K. Jones, D. Chapman, C. Brunk, *BioTechniques* **1994**, *17*, 144-149.

[65] C.Y Turenne, S.E. Sanche, D.J. Hoban, J.A. Karlowsky, A.M. Kabani, *J. Clin. Microbiol.* **1999**, *37*, 1846-1851.

[66] I. González, R. Martín, T. García, P. Morales, B. Sanz, P.E. Hernández, *J. App. Bacteriol.* **1993**, *74*, 394-401.

[67] S. Ko, S.A. Grant, *Biosens. Bioelectron.* **2006**, *21*, 1283-1290.

[68] R. Maalouf, C. Fournier-Wirth, J. Coste, H. Chebib, Y. Saïkali, O. Vittori, A. Errachid, J.P. Cloarec, C. Martelet, N. Jaffrezic-Renault, *Anal. Chem.* **2007**, *79*, 4879-4886.

[69] H.J. Kim, H.P. Bennetto, M.A. Halablab, C. Choi, S. Yoon, *Sens. Act. B Chem.* **2006**, *B119*, 143-149.

[70] D. Ivnitski, E. Wilkins, H.T. Tien, A. Ottova, *Electrochem. Commun.* **2000**, *2*, 457-460.

[71] R.A. Villamizar, A. Maroto, F.X. Rius, I. Inza, M.J. Figueras *Biosens. Bioelectron.* **2008**, *24*, 279-283.

[72] P. Belgrader, W. Benett, D. Hadley, J. Richards, P. Stratton, R. Mariella, F. Milanovich, *Science* **1999**, *284*, 449-450.

[73] T.H. Rider, M.S. Petrovick, F.E. Nargi, J.D. Harper, E.D. Schwoebel, R.H. Mathews, D.J. Blanchard, L.T. Bortolin, A.M. Young, J. Chen, M.A. Hollis, *Science* **2003**, *301*, 213-215.

[74] L. Yang, R. Bashir, *Biotechnol. Adv.* **2008**, *26*, 135-150.

[75] C.A. Heid, J. Stevens, K.J. Livak, P.M. Williams, *Genome Res.* **1996**, *6*, 986-994.

[76] S.-I Tu, J. Uknalis, P. Irwin, L.S.L. Yu, *J. Rapid Meth. Autom. Microbiol.* **2000**, *8*, 95-109.

[77] B. Ilic, D. Czaplewski, M. Zalalutdinov, H.G. Craighead, *J. Vac. Sci. Technol. B* **2001**, *19*, 2825-2828.

[78] C. Ruan, L. Yang, Y. Li, *Anal. Chem.* **2002**, *74*, 4814-4820.

[79] C. Ruan, L. Yang, Y. Li, *J. Electroanal. Chem.* **2002**, *519*, 33-38.

[80] A.J. Baeumner, R.N. Cohen, V. Miksic, J. Min, *Biosens. Bioelectron.* **2003**, *18*, 405-413.

[81] X. Zhao, L.R. Hilliard, S.J. Mechery, Y. Wang, R.P. Bagwe, S. Jin, W. Tan, *Proc. Natl. Acad. Sci.* **2004**, *101*, 15027-15032.

[82] A.J. Baeumner, B. Leonard, J. McElwee, R.A. Montagna. *Anal. Bioanal. Chem.* **2004**, *380*, 15-23.

[83] N.V. Zaytseva, V.N. Goral, R.A. Montagna, A.J. Baeumner, *Lab Chip* **2005**, *5*, 805-811.

[84] M.L. Ochoa, M.B. Harrington, Anal. Chem. **2005**, *77*, 5258-5267.

[85] N.V. Kulagina, M.E. Lassman, F.S. Ligler, C.R. Taitt, *Anal. Chem.* **2005**, *77*, 6504-6508.

[86] J. Gao, L. Li, P.-L. Ho, G.C. Mak, H. Gu, B. Xu, *Adv. Mater.* **2006**, *18*, 3145-3148.

[87] C. Yu, A. Ganjoo, H. Jain, C.G. Pantano, J. Irudayaraj, *Anal. Chem.* **2006**, *78*, 2500-2506.

[88] J.B.-H. Tok, F.Y.S. Chuang, M.C. Kao, K.A. Rose, S.S. Pannu, M.Y. Sha, G. Chakarova, S.G. Penn, G.M. Dougherty, *Angew. Chem. Int. Ed.* **2006**, *45*, 6900-6904.

[89] S. Ko, S.A. Grant, *Biosens. Bioelectron.* **2006**, *21*, 1283-1290.

[90] A. Subramanian, J. Irudayaraj, T. Ryan, *Sens. Act. B Chem.* **2006**, *B114*, 192-198.

[91] R. Maalouf, C. Fournier-Wirth, J. Coste, H. Chebib, Y. Saïkali, O. Vittori, A. Errachid, J.P. Cloarec, C. Martelet, N. Jaffrezic-Renault, *Anal. Chem.* **2007**, *79*, 4879-4886.

[92] S. Balasubramanian, I.B. Sorokulova, V.J. Vodyanoy, A.L. Simonian, *Biosens. Bioelectron.* **2007**, *22*, 948-955.

[93] V. Escamilla-Gómez, S. Campuzano, M. Pedrero, J.M. Pingarrón, *Electroanalysis* **2007**, *19*, 1476-1482.

[94] M.D. Morales, B. Serra, A. Guzmán-Vázquez de Prada, A.J. Reviejo, J.M. Pingarrón *Analyst* **2007**, *132*, 572-578.

[95] O. Laczka, E. Baldrich, F.X. Muñoz, F.J. del Campo, *Anal. Chem.* **2008**, *80*, 7239-7247.

[96] A. Shabani, M. Zourob, B. Allain, C.A. Marquette, M.F. Lawrence, R. Mandeville, *Anal. Chem.* **2008**, *80*, 9475-9482.

[97] H.-M. So, D.-W. Park, E.-K. Jeon, Y.-H. Kim, B.S. Kim, C.-K. Lee, S.Y. Choi, S.C. Kim, H. Chang, J.-O Lee, *Small* **2008**, *4*, 197-201.

[98] H. Lee, T.-J. Yoon, R. Weisslederet, *Angew. Chem. Int. Ed.* **2009**, *48*, 5657-5660.

[99] K. Abu-Rabeah, A. Ashkenazi, D. Atias, L. Amir, R.S. Marks, *Biosens. Bioelectron.* **2009**, *24*, 3461-3466.

[100] S. Liébana, A. Lermo, S. Campoy, M.P. Cortés, S. Alegret, M.I. Pividori, *Biosens. Bioelectron.* **2009**, *25*, 510-513.

[101] U. Dharmasiri, M.A. Witek, A.A. Adams, J.K. Osiri, M.L. Hupert, T.S. Bianchi, D.L. Roelke, S.A. Soper, *Anal. Chem.* **2010**, *82*, 2844-2849.

[102] M. Grossi, M. Lanzoni, A. Pompei, R. Lazzarini, D. Matteuzzi, B. Riccò, *Biosens. Bioelectron.* **2010**, *26*, 983-990.

[103] O.R. Miranda, X. Li, L. Garcia-Gonzalez., Z.-J. Zhu, B. Yan, U.H.F. Bunz, V.M. Rotello, *J. Am. Chem. Soc.* **2011**, DOI:10.1021-ja2021729.

[104] C. García-Aljaro, L.N. Cella, D.J. Shirale, M. Park, F.J. Muñoz, M.V. Yates, A. Mulchandani, *Biosens. Bioelectron.* **2011**, *26*, 1437-1441.

[105] Y. Wan, Z. Lin, D. Zhang, Y. Wang, B. Hou, *Biosens. Bioelectron.* **2011**, *26*, 1959-1964.

[106] S. Iijima, *Nature* **1991**, *354*, 56-58.

[107] H. Dai, *Acc. Chem. Res.* **2002**, *35*, 1035-1044.

[108] S.J. Tans, A.R. Verschueren, C. Dekker, *Nature* **1998**, *393*, 49-52.

[109] R. Martel, T. Schmidt, H.R. Shea, T. Hertel, P. Avouris, *Appl. Phys. Lett.* **1998**, *73*, 2447-2449.

[110] E.S. Snow, F.K. Perkins, E.J. Houser, S.C. Badescu, T.L. Reinecke, *Science* **2005**, *307*, 1942-1945.

[111] Y. Tu, Y. Lin, W. Yantasee, Z. Ren, *Electroanalysis* **2005**, *17*, 79-84.

[112] G.A. Crespo, S. Macho, F.X. Rius, *Anal. Chem.* **2008**, *80*, 1316-1322.

[113] M. Daenen, R.D. de Fouw, B. Hamers, P.G.A. Janssen, K. Schouteden, M.A.J. Veld, *The Wondrous World of Carbon Nanotubes 'a review of current carbon nanotube technologies'*. Eindhoven University of Technology, The Netherlands. 93 p. (**2003**).

[114] P.M. Ajayan, *Chem. Rev.* **1999**, *99*, 1787-1799.

[115] H. Dai, *Sur. Sci.* **2002**, *500*, 218-241.

[116] W. Kim, H.C. Choi, M. Shim, Y. Li, D. Wang, H. Dai, *Nano Lett.* **2002**, *2*, 703-708.

[117] P. Avouris, *Chem. Phys.* **2002**, *281*, 429-445.

[118] S.J. Tans, M.H. Devoret, H. Dai, A. Thess, R.E. Smalley, L.J. Geerligs, C. Dekker, *Nature* **1997**, *386*, 474-477.

[119] M. Damnjanovic, I. Milosevic, T. Vukovic, R. Sredanovic, *Phys. Rev. B* **1999**, *60*, 2728-2739.

[120] I. Palchetti, M. Mascini, *Anal. Bioanal. Chem.* **2008**, *391*, 455-471.

[121] D.A. Skoog, D.M. West, F.J. Holler, *Fundamentals of Analytical Chemistry*. Harcourt Brace College Publishers, Texas, USA. 992 p. (**1993**).

[122] J.O'M. Bockris, A.K.N. Reddy, *Modern Electrochemistry vol. 2*. Reverté, Barcelona, Spain. 1521 p. (**1980**).

[123] C.H. Hamann, A. Hamnett, W. Vielstich, *Electrochemistry*, Wiley-VCH, Weinheim, Germany. 531 p. (**2007**).

[124] R. Hernández, J. Riu, F.X. Rius, *Analyst* **2010**, *135*, 1979-1985.

[125] E.J. Parra, G.A. Crespo, J. Riu, A. Ruiz, F.X. Rius, *Analyst* **2009**, *134*, 1905-1910.

[126] R. De Marco, G. Clarke, B. Pejcic, *Electroanalysis* **2007**, *19*, 1987-2001.

[127] E. Bakker, D. Diamond, A. Lewenstam, E. Pretsch, *Anal. Chim. Acta* **1999**, *393*, 11-18.

[128] 11 A.K. Jain, J. Raisoni, S. Jain, *Int. J. Environ. Anal. Chem.* **2008**, *88*, 209-221.

[129] T. Lindfors, A. Ivaska, *Anal. Chim. Acta* **2000**, *404*, 101-110.

[130] A. Michalska, A. Konopka, M. Maj-Zurawska, *Anal. Chem.* **2003**, *75*, 141-144.

[131] C.Z. Lai, M.M. Joyer, M.A. Fierke, N.D. Petkovich, A. Stein, P. Buhlmann, *J. Solid State Electrochem.* **2009**, *13*, 123-128.

[132] M. Fouskaki, N. Chaniotakis, *Analyst* **2008**, *133*, 1072-1075.

[133] Z.Q. Zhu, J. Zhang, J.Z. Zhu, W. Lu, J. Zi, *IEEE Sens. J.* **2007**, *7*, 38-42.

[134] G.A. Crespo, S. Macho, J. Bobacka, F.X. Rius, *Anal. Chem.* **2009**, *81*, 676-681.

[135] A.D. Ellington, J. Szostak, *Nature* **1990**, *346*, 818-822.

[136] J.F. Milligan, D.R. Groebe, G.W. Witherell, O.C. Uhlenbeck, *Nucleic Acids Res.* **1987**, *15*, 8783-8798.

[137] C. Tuerk, L. Gold, *Science* **1990**, *249*, 505-510.

[138] S. Tombelli, M. Minunni, M. Mascini, *Biosens. Bioelectron.* **2005**, *20*, 2424-2434.

[139] J.-O. Lee, H.-M. So, E.-K. Jeon, H. Chang, K. Won, Y.H. Kim, *Anal. Bioanal. Chem.* **2008**, *390*, 1023-1032.

[140] N. de-los-Santos-Álvarez, M.J. Lobo-Castañón, A.J. Miranda-Ordieres, P. Tuñón-Blanco, *Tr. Anal. Chem.* **2008**, *27*, 437-446.

[141] F. Chen, J. Zhou, F. Luo, A.-B. Mohammed, X.-L. Zhang, *Biochem. Biophys. Res. Comm.* **2007**, *357*, 743-748.

[142] A.B. Iliuk, L. Hu, W.A. Tao, *Anal. Chem.* **2011**, *83*, 4440-4452.

[143] L. Agüí, P. Yáñez-Sedeño, J.M. Pingarrón, *Anal. Chim. Acta* **2008**, *622*, 11-47.

[144] J. Zhou, M.R. Battig, Y. Wang, *Anal. Bioanal. Chem.* **2010**, *398*, 2471-2480.

[145] Y. Xu, G. Cheng, P. He, Y. Fang, *Electroanalysis* **2009**, *21*, 1251-1259.

[146] A. Sassolas, L.J. Blum, B.D. Leca-Bouvier, *Electroanalysis* **2009**, *21*, 1237-1250.

[147] T. Hianik, J. Wang, *Electroanalysis* **2009**, *21*, 1223-1235.

Chapter 2

Objectives

Objectives

The main objective of this Thesis is to demonstrate for the first time that potentiometric biosensors based on carbon nanotubes, as ion-to-electron transducers, and aptamers, as biorecognition elements, can be used as powerful tools in the real-time detection of pathogens and related biomolecules.

This general objective is achieved through the implementation of a series of specific objectives: the design of the biosensors for different targets and their development, validation and application in real samples. Additionally, this Thesis aims to show that the applications portfolio of this new generation of aptamer-based biosensors (also called aptasensors) can be customized for the detection of microorganisms with very different characteristics. In this way, biosensors for the determination of *Salmonella enterica* serovar Typhi and *Escherichia coli*, targeted as gram-negative bacteria models, are described in *Chapter 4* and *Chapter 6* respectively. The aptasensor for *Staphylococcus aureus*, used as a gram-positive bacteria example, is described in *Chapter 5* while a biosensor for the trypanosomal Variable Surface Glycoprotein is described in *Chapter 7*. This protein is employed as a model for the detection of pathogenic exoantigen proteins, opening in this way the applicability of the biosensing platform for further targets such as parasites or protein biomarkers.

The proof of concept for the real-time detection of bacteria in phosphate buffer solutions, in which the biosensor is addressed towards a specific protein anchored to the surface of the microorganism, is the specific objective of *Chapter 4*.

The comparison of two different methodologies for the immobilization of the aptamers onto the surface of the carbon nanotubes, using covalent and non-covalent linkages, is the specific objective in *Chapter 5*. In this chapter, the pathogen is targeted

in phosphate buffer solutions and the biosensors-target interactions analyzed according to the resulting performance parameters. Additionally, the behavior of the biosensor is also evaluated in real contaminated skin samples.

The detection of pathogens in foodstuff samples is addressed in *Chapter 6*. To demonstrate the possibility to use the biosensors for the detection of microorganisms in complex food matrices such as beverages, a rapid and simple sample pre-treatment protocol is developed, validated and tested with real fruit juice and milk samples.

Finally, two major specific objectives are addressed in *Chapter 7*: The demonstration that the identification of a particular protein in highly complex matrix conditions, such as blood, is possible in real-time without the need of complicated sample pre-treatment procedures; and the proof that the biosensing platform can be used for the ultrasensitive and specific detection of exoantigens such as trypanosomal Variable Surface Glycoproteins in clinical samples.

Chapter 3

Experimental Part

3.1. Materials, chemicals, culturing media and microorganisms

In this section, all the chemicals, microorganisms, materials and instruments used in the experimental part of the Thesis are described in detail. This section also includes a brief description of the purpose of some substances and culturing media as well as useful references for further information. However, the particular applications of the materials and the solutions prepared with each substance or culturing media are indicated in ***Chapters 4*** to ***7***.

3.1.1. List of materials and instruments

The following materials and instruments have been used:

- Bacteriological transfer and inoculating loop, model S-33, JP Selecta, Barcelona, Spain.
- Balance, model GR-120-EC, A&D Instruments, Abingdon, UK.
- Biosafety level II cabinet, model BIO II A, Telstar Industrials, Terrassa, Spain.
- Centrifuge, model EBA 20, Hettich Zentrifugen, Tuttlingen, Germany.
- Double junction reference electrode (Ag/AgCl/KCl 3 M) containing a 1 M LiAcO electrolyte bridge, type 6.0729.100, Metrohm AG, Herisau, Switzerland.
- Environmental scanning electron microscope (ESEM) with Everhart-Thornley Detector (ETD), model 600, FEI Quanta, Hillsboro, USA.
- Glass filtration system with a capacity for 250 mL, model 5810, Fisher Scientific, Madrid, Spain.
- Glassy carbon cylindrical rods, length 50 mm and diameter 3 mm, HTW Hochtemperatur-Werkstoffe GmbH, Thierhaupten, Germany.

- High speed micro centrifuge, model 5417 R, Eppendorf AG, Hamburg, Germany.
- High-input impedance voltmeter (10^{15} Ω), model EMF-16, Lawson Laboratories Inc, Malvern, PA, USA.
- High-input impedance voltmeter (10^{15} Ω), model M6514, Keithley, London, UK.
- Infrared sterilizer, model Sterilbio, JP Selecta, Barcelona, Spain.
- Integral Water Purification System, model Milli-Q plus, Millipore, Molsheim, France.
- Magnetic stirring system, model Agimatic-N, JP Selecta, Barcelona, Spain.
- Magnetic stirring system, model ANM-10006, SBS SL, Sabadell-Barcelona, Spain.
- MALDI-TOF spectrometer, Voyager-DE STR, Applied Biosystems, Carlsbad CA, USA.
- Microbiological incubator with natural convection system, model 100-800, Memmert GmbH Co KG, Schwabach, Germany.
- Nylon and Polycarbonate filtration membranes, 47 mm diameter, pore size 0.45 µm, Albet Lab science, Dassel, Germany.
- pH selective electrode, Model GLP21, Crison Instruments SA, Barcelona, Spain.
- Polishing alumina, 25 and 1 micron grain size, Buehler, Lake Bluff, USA.
- Silica furnace chamber, HST 12/600, Carbolite, Hope Valley, UK.
- Steam sterilizer (autoclave), model Med 12, JP Selecta, Barcelona, Spain.

- Sterile cellulose acetate filters, 13 mm diameter and 0.45 µm pore size, General Electric, Brussels, Belgium.

- Teflon rods, 7 mm diameter and 1000-2000 mm length, Amidata SA, Madrid, Spain.

- Thermostatic circulator, model 9112, Polyscience, Niles, USA.

- Tip-sonicator, Ultraschallprocessor UP200S, Dr. Hielscher, Teltow, Germany.

- Transmission Electron Microscope, model JEM-1011, JEOL Ltd, Tokio, Japan.

- Triple vent polystirene Petri dishes, 90x16 mm, model P101VR20, Sterilin Ltd, Newport, UK.

- Variable volume Micropipettes, models 3111 000.157, 3111 000.165 and 3111 000.181 (capacities 20-200 µL, 100-1000 µL and 0.1-10.0 µL, respectively), Eppendorf AG, Hamburg, Germany.

- Water-jacketed glass cell, 14 mL, model Zelada 1.0, designed by the author (Reference number V64863) and fabricated by the Fisher Scientific Glassblowing services, Madrid, Spain.

- Common laboratory glassware and plasticware such as volumetric pipettes, volumetric flasks, boiling flasks, Erlenmeyer flasks, filtering flasks, volumetric burettes, graduated cylinders, glass funnels, centrifuge tubes, watch glasses, beakers, non-sterile and sterile test tubes, weighing bottles, vials, condensers, microcentrifuge tubes, Teflon stirring rods, as well as other materials such as support stands, clamp holders, sterile plastic syringes of several sizes, stainless steel needles of different lengths and gauges, micropipette tips, sterilization indicator labels and tapes, latex and silicon rubber tubing of different gauges were purchased from Fisher Scientific, Madrid, Spain.

3.1.2. Carbon nanotubes

The single walled carbon nanotubes used in the development of all the sensors and biosensors were purchased in bulk form from HeJi (Zengcheng, China) with >90% purity, 150 µm average length and 1.4-1.5 nm diameter. Unless other conditions are indicated in further chapters, the carbon nanotubes were oxidized in a silica furnace chamber at 365 °C, with synthetic air flow-rate of 100 cm^3 min^{-1} during 90 min, in order to selectively remove the amorphous carbon. Subsequently, SWCNTs were refluxed in 2.6 M nitric acid for 4 h to oxidize the metallic impurities remaining from the synthesis.[1] The carbon nanotubes became carboxylated after this latter oxidation step. The SWCNTs in nitric acid solution were filtered and thoroughly rinsed with water to remove the acid completely. The filtered SWCNTs were dried overnight at 80°C, and stored under dry conditions until needed.

In the specific case of those biosensors prepared by non covalent linkage of pyrenil-modified aptamers on the sidewalls of SWCNT described in ***Chapter 5*** (subsections ***5.2.3*** and ***5.2.6***), the acidic carboxylation step was omitted in order to use non-carboxylated nanotubes as the transducing material.

3.1.3. Aptamers

Unless otherwise mentioned, the aptamers used in the development of the different biosensors were purchased from Eurogentec (London, UK) and their sequences and modifications are described in this subsection.

- The *Salmonella* Typhi type IVB Pili binding RNA aptamer of 71-mer was supplied with the sequence[2] 5'-GGG AAC AGU CCG AGC CUC ACU GUU AUC CGA UAG CAG CGC GGG AUG AGG GUC AAU GCG UCA UAG GAU CCC GC-3', and modified with a $-(CH_2)_5NH_2$ at the 3'-terminal. Once received, the aptamer was resuspended in MilliQ water and stored at -80 °C until needed. This aptamer was used in the experimental part of ***Chapter 4***.

- Two *S. aureus*-binding DNA aptamers of 88-mer with similar ligand-target affinity values[3] were supplied with the sequences 5'-GCA ATG GTA CGG

TAC TTC CTC CCA CGA TCT CAT TAG TCT GTG GAT AAG CGT GGG ACG TCT ATG ACA AAA GTG CAC GCT ACT TTG CTA A-3'-$(CH_2)_6NH_2$ (NH_2-Aptamer) and 5'-GCA ATG GTA CGG TAC TTC CGC GCC CTC TCA CGT GGC ACT CAG AGT GCC GGA AGT TCT GCG TTA TCA AAA GTG CAC GCT ACT TTG CTA A-3'-C3-Pyr (Pyr-C3-Aptamer, Pyr-C3- = pyrenil moiety with a phosphoramidite spacer). Once received, the aptamers were resuspended in MilliQ water and stored at -80 °C until needed. The aptamers were used in the experimental part of ***Chapter 5***.

- The *E. coli* CECT 675 binding DNA aptamer of 81-mer with the sequence[4] was supplied with the sequence 5'-GGG AGA GCG GAA GCG UGC UGG GUC GCA GUU UGC GCG CGU UCC AAG UUC UCU CAU CAC GGA AUA CAU AAC CCA GAG GUC GAU-3', and modified with a -$(CH_2)_5NH_2$ moiety at the 3' terminal. The aptamer was resuspended in MilliQ water and stored at -80°C until needed. This aptamer was used in the experimental part of ***Chapter 6***.

- The VSG-specific RNA aptamer (cl57) of 78-mer with the sequence 5'-GGG AGA CGA UAU UCG UCC AUC AGC GCG CAC CUA CUG UGA UGU AGA AGU CAC AGC AAG GCC CCG CUG UCC GAC UGA AUU-3' was synthesized by run off *in vitro* transcription in the presence of 2'-F-uridine-5'-triphosphate and 2'-F-cytidine-5'-triphosphate (2 mM each) as previously described by Lorger et al.[5] This aptamer was synthesized by the research group of Prof. H. Ulrich Göringer at the Department of Genetics, Darmstadt University of Technology, Germany. The aptamer was modified by oxidation of its 3'-terminal ribose moiety and further converted into a hydrazide derivative using adipic acid dihydrazide (ADH).[6] Chemical modification steps are further described in detail in ***Chapter 7***. Once received, the aptamer was resuspended in MilliQ water and stored at -80°C until needed.

3.1.4. Culturing media and microorganisms

The following culturing media were purchased from Becton, Dickinson and Company (Sparks, USA), prepared according to indications and used in the experimental parts of ***Chapters 4*** to ***6***:

- Lactobacilli MRS (deMan, Rogosa and Sharpe) agar. This medium was used in the isolation, enumeration and cultivation of *Lactobacillus* species. [7,8]
- Lactobacilli MRS (deMan, Rogosa and Sharpe) broth. This medium was used in the isolation, enrichment and cultivation of *Lactobacillus* species.[7,8]
- Mannitol salt agar (MSA). This medium was used for the selective isolation and enumeration of *Staphylococci* from clinical and nonclinical materials.[7]
- Tryptic soy agar (TSA). This non-selective medium was used in the enumeration and cultivation of pure strains of *Salmonella* Typhi, *Staphylococcus aureus*, *Staphylococcus epidermidis* and *Escherichia coli*. [7]
- Tryptic soy broth (TSB). This non-selective medium was used in the enrichment and cultivation of pure strains of *Salmonella* Typhi, *Staphylococcus aureus*, *Staphylococcus epidermidis* and *Escherichia coli*. [7]
- XLD (xylose-lysine-deoxycholate) agar. This medium was used for isolation, differentiation and confirmatory growth of the *Salmonella* group. [7,9 – 12]
- MacConkey agar. This medium was used for isolation, differentiation and confirmatory growth of *Escherichia coli*. [7]
- Lysogeny broth and agar (Luria-Bertani medium, LB). This medium was used for maintainance, enumeration and growth of *Escherichia coli* strains.[7]

The following microorganisms were used in the experimental part of the Thesis and cultured according to the procedures mentioned in subsection ***3.2.2***. The bacteria

were used in the experimental parts of ***Chapters 4*** to ***6***, while the parasites were used in ***Chapter 7***:

- Lyophilized strains of *Salmonella* Typhi (CECT 409), *Lactobacillus casei* subsp. *casei* (CECT 4180), *Escherichia coli* (CECT 675), *Staphylococcus aureus* (CECT 4630) and *Staphylococcus epidermidis* (CECT 231) were purchased from Colección Española de Cultivos Tipo (Valencia, Spain).

- Agar-supported colonies of *Escherichia coli* (CECT 4558) were kindly donated by the Biotechnology Department of the URV (Tarragona, Spain).

- *T. brucei* Lister 427 – MiTat serodeme,[i,13,14] variant clones 1.4 and 1.2 are part of the strain bank of Prof. H. U. Göringer and were used in the VSG protein extraction experiments by his team.[ii]

- *T. b. gambiense* LiTat 1.1, LiTat 1.3, LiTat 1.5, LiTat 1.6, *T. b. rhodesiense* ETat 1.2 and *T. evansi* RoTat 1.2 were kindly provided by Philipp Bücher, Antwerp for further VSG protein extraction by the research group of Prof. H. U. Göringer.[ii]

3.1.5. Other reagents

Unless otherwise indicated, the following molecular biology grade reagents (>99.5% purity) were purchased from Sigma-Aldrich (Tres Cantos, Spain) and were used as received:

- Sodium dodecyl sulphate (SDS). This surfactant is used for dispersing the carbon nanotubes in water before the deposition step during the construction of the sensors.

- N-(3-dimethylaminopropyl)-N′-ethylcarbodiimide hydrochloride (EDC). This substance is used in the activation of the carboxylic groups at the sidewalls of the carbon nanotubes via the formation of an *O*-acylisourea

[i] A serodeme is a population of trypanosomes, each of which can express the same range of variant antigen types.
[ii] Meaning for each serodeme classification can be found in the ***Abbreviations*** section.

intermediate[15] during the covalent functionalization of carboxylated nanotubes with NH_2-modified aptamers. [16,17]

- N-hydroxysuccinimide (NHS). This substance is used in the activation of the carboxylic groups at the sidewalls of the carbon nanotubes via the displacement of the *O*-acylisourea intermediates in order to form a stable NHS-ester. Such an intermediate can be further displaced by the NH_2-moieties of the modified aptamers in the formation of amide bonds between the aptamers and the carboxylated nanotubes.[16,17]

- 2-(N-morpholino) ethanesulfonic acid (MES). This substance is used as a pH buffering agent in the preparation of solutions involved in the carbodiimide-mediated covalent functionalization of carboxylated nanotubes with NH_2-modified aptamers.[6]

- Cetyltrimethylammonium bromide (CTAB). This positively charged surfactant is used to reduce the electrostatic repulsion between the remaining non-activated carboxylic groups at the sidewalls of the carbon nanotubes and the negatively charged phosphate groups of the aptamer backbone at pH 7.4 during the carbodiimide-mediated functionalization process.[18]

- Potassium dihydrogen phosphate (KH_2PO_4). This salt is used in the preparation of the phosphate buffer solutions with pH 7.4.

- Disodium hydrogen phosphate (Na_2HPO_4). This salt is used in the preparation of the phosphate buffer solutions with pH 7.4.

- Bovine serum albumin (BSA). This protein is used in ***Chapter 7*** for selectivity assays.

- Human serum Immunoglobulin G (IgG). This protein is used in ***Chapter 7*** for selectivity assays.

- Potassium ferricyanide ($K_3Fe(CN)_6$). This substance is used as a stable redox-agent[19–21] in the preparation of the tailored buffer for protein detection in blood samples in ***Chapter 7***.

- Potassium ferrocyanide ($K_4Fe(CN)_6$). This substance is used as a stable redox-agent[19–21] in the preparation of the tailored buffer for protein detection in blood samples in ***Chapter 7***.

- Sodium chloride (NaCl). Used for the preparation of several NaCl-based solutions (e.g. 2 M NaCl aptasensors' regeneration solution, 0.85 % isotonic NaCl solutions).

- Ethylenediaminetetraacetic acid (EDTA). This complexing agent[19,20] is used in the preparation of the tailored buffer for protein detection in blood samples in ***Chapter 7***.

- Trans-1,2-Cyclohexanediamine-N,N,N',N'-tetraacetic acid (CDTA). This substance is a complexing agent[19,20] used in the preparation of the tailored buffer for protein detection in blood samples in ***Chapter 7***.

- Human α-thrombin was supplied by Haematologic Technologies, Vermont, USA. This protein is used in ***Chapter 7*** for selectivity assays.

- Dry air 99.999% purity, Carburos Metálicos, Barcelona, Spain. Used in carbon nanotube purification experiments.

- Ethanol 70%. This substance is used in the surface sterilization process for microbiological experiments.

3.2. General procedures

This section includes all the basic procedures followed in the experimental part of the Thesis. Variations to the steps mentioned here, if any, are adequately mentioned in further chapters. This section also includes a brief description of the aim of each procedure as well as useful references for further information of the technique used.

3.2.1. Preparation of the biosensors

The solid contact electrode was made of a 3 mm diameter glassy carbon cylindrical rod covered by a Teflon jacket of 7 mm diameter. The surface of the glassy carbon was successively polished using 25 and 1 µm grain size polishing alumina before the SWCNT layer was deposited on the same surface. For the spraying process (Figure 3.1), we used sonication for 30 minutes at 0.5 s^{-1} to prepare a solution of 25 mg of purified SWCNT dispersed in 10 mL of MilliQ water containing 100 mg of SDS. The SWCNT/SDS/H_2O solution was sprayed under a high temperature (200°C) air blow, and washed with MilliQ water to progressively remove the SDS.

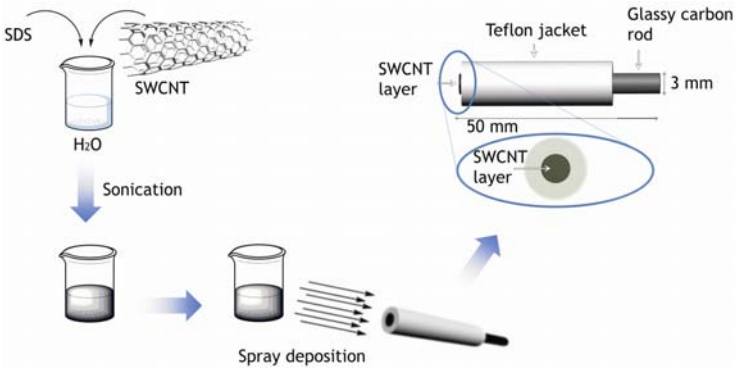

Figure 3.1. Carbon nanotube deposition on the surface of a glassy carbon electrode.

In most of the biosensors built in this Thesis, the carboxylic groups that are on the sidewalls of the deposited SWCNTs are activated using a solution of 100 nmol of EDC and 25 nmol of NHS in a 50 mM MES buffer pH 5 for 30 minutes (only in ***Chapter 5*** a different strategy of functionalization was tested).[15–17] Subsequently, the electrodes were soaked overnight into 500 µL of a 1 µM aptamer solution, which also consisted of

PBS pH 7.4 (1 mM) and CTAB (0.2 mM). Finally, the sensors were washed in MilliQ water and stored in PBS 1.7 mM pH 7.4 until needed.

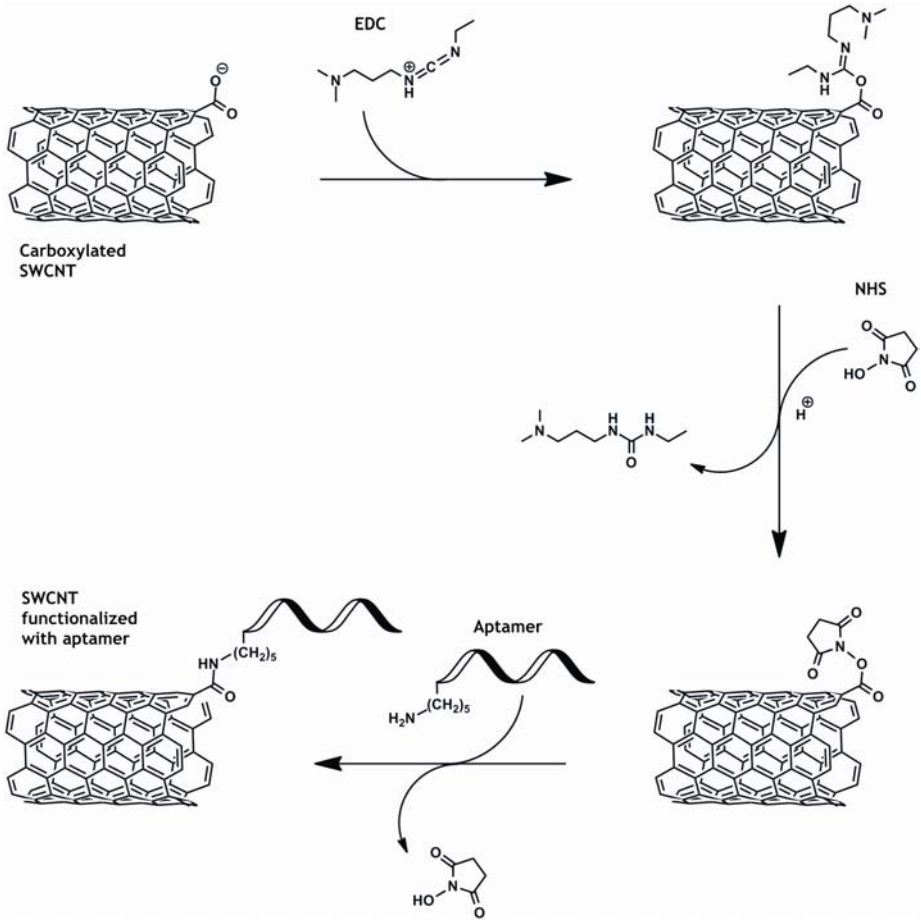

Figure 3.2. Functionalization of carboxylated carbon nanotubes with amine-modified aptamers via carbodiimide-mediated chemistry.[15-17,22,23]

3.2.2. Microorganism culturing

All the bacteria strains were cultured following standard microbiological techniques, using adequately sterilized materials, solutions and culturing media. Variations to the procedures mentioned in this section are indicated in further chapters, depending on the particular experiment carried out.

- Lyophilized pure strains of *Salmonella* Typhi (CECT 409), *Lactobacillus casei* subsp. *casei* (CECT 4180), *Escherichia coli* (CECT 675), *Staphylococcus aureus* (CECT 4630) and *Staphylococcus epidermidis* (CECT 231) were reactivated with NaCl 0.85 % and further incubated in broth for 24-48 h at 37 °C. The pellet was then transferred to selective agar medium and sub-cultured for 24-48 h at 37 °C in order to confirm the purity of the strains. The selective medium used in this latter step depended on the cultured bacteria, according to section 3.1.4. Characteristic colonies were transferred to non-selective broth and agar media and cultured for 24-48 h at 37 °C. Colonies obtained in agar cultures were then transferred to Glycerol/TSB 20:80 and stored at -20 °C until needed and reactivated by inoculating the bacteria in 10 mL of sterile broth medium at 37 °C for 24 h. Bacteria grown in non-selective broth was used for different purposes (e.g. testing of biosensors, inoculation of samples).

- Agar-supported colonies of *Escherichia coli* (CECT 4558) were transferred to MacConkey agar medium and incubated for 24-48 h at 37 °C in order to confirm the purity of the strains. Characteristic colonies were transferred to non-selective (LB) broth and agar media and cultured for 24-48 h at 37 °C. Colonies obtained in agar cultures were then transferred to Glycerol/LB 20:80 and stored at -20 °C until needed and reactivated by inoculating the bacteria in 10 mL of sterile broth medium at 37 °C for 24 h. Bacteria grown in non-selective broth was used for different purposes (e.g. testing of biosensors, inoculation of samples).

- The bloodstream life cycle stage of *Trypanosoma brucei brucei* Lister 427 – MiTat serodeme, variant clones 1.4 and 1.2 were cultivated at 37 °C in HMI-9 medium[24] supplemented with 10% (v/v) heat inactivated bovine fetal calf serum. This part was performed by the research group of Prof. H. U. Göringer in Darmstadt University of Technology.

- *T. b. gambiense* LiTat 1.1, LiTat 1.3, LiTat 1.5, LiTat 1.6, *T. b. rhodesiense* ETat 1.2 and *T. evansi* RoTat 1.2 were also cultivated by the research group of Prof. Göringer following similar procedures.

For the bacteria enumeration assays, testing of biosensors and preparation of standard solutions, the selected bacteria were inoculated in 10 mL of sterile broth medium at 37 °C for 24 h. Then, the bacteria samples were centrifuged at 6000 rpm for 15 minutes and the supernatant was discarded. The precipitate was resuspended in 10 mL of sterile buffer (e.g. PBS 1.7 mM in ***Chapters 4*** to ***6***), and the resulting solution was 1:10 diluted eightfold to provide a series of 10^{-1} to 10^{-8} stock solutions of bacteria. Each stock solution was quantified with the standard plate count method by triplicate,[7] in appropriate culturing agar medium (e.g. TSA for *S.* Typhi/*S. aureus*/*S.epidermidis*, LB for *E. coli* and MRS for *L. casei*).

3.2.3. Potentiometric analysis

Potentiometric analysis was performed by real-time measurements of the electromotive force (EMF)[25–27] between the terminals of a two-electrode system (Figure 3.2) consisting of a carbon nanotube-based sensor as the working electrode, and a double-junction Ag/AgCl/KCl electrode as the reference electrode at isothermal conditions (22 ± 0.5 °C) in a water-jacketed glass cell under constant stirring conditions (300 rpm). A high-input impedance voltmeter was used in all the cases to measure the difference in electromotive force.

The electrolyte used in the cell depended on the experiment. As an example, the electrolyte used in ***Chapters 4*** to ***6*** was PBS 1.7 mM pH 7.4, whereas in ***Chapter 7***, the electrolyte was a more complex buffer. The EMF value was recorded automatically with the software provided by the company. Modifications to this previous part are adequately mentioned in further chapters. This analytical technique helps us to monitor the potentiometric response of the sensors prepared towards the target and interfering agents.

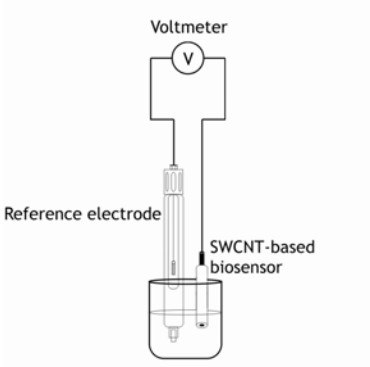

Figure 3.3. Two-electrode system for the measurements of electromotive force (voltage) including the double-junction Ag/AgCl/KCl (3 M) reference electrode, the SWCNT-based biosensor (working electrode) and the high-input impedance voltmeter.

3.2.4. Other procedures

Calibration of micropipettes (Eppendorf AG, Hamburg, Germany) and laboratory glassware was validated every 6 months according to standard calibration protocols.[28,29] Materials, culturing media and solutions were sterilized by autoclaving at 121°C for 15 minutes in a J.P. Selecta autoclave model Med 12 (Barcelona, Spain). All the microbiological cultures were incubated in an incubator model 100-800, Memmert GmbH Co KG (Schwabach, Germany).

Microscopic characterization of carbon nanotubes was performed by Transmission electron microscopy (TEM) analysis[30,31] by prior dispersion in tetrahydrofuran or SDS/H_2O and further deposition on the TEM grid. This step was done in order to verify the structure of the nanotubes after the chemical modification steps.

Microscopic characterization of carbon nanotube-based sensors and biosensors was performed by ESEM analysis[31–33] by directly supporting the specimen on the ESEM holder. This step was done to verify the physical structure of the deposited nanotubes as well as in the analysis of bacteria adsorbed onto the sensor surface.

3.3. References

[1] C.A. Furtado, U.J. Kim, H.R. Gutierrez, L. Pan, E.C. Dickey, P.C. Eklund, *J. Am. Chem. Soc.* **2004**, *126*, 6095-6105.

[2] Q. Pan, X.L. Zhang, H.Y. Wu, P.W. He, F. Wang, M.S. Zhang, J.M. Hu, B. Xia, J Wu, *Antimicrob. Agents Chemother.* **2005**, *49*, 4052-4060.

[3] X. Cao, S. Li, L. Chen, H. Ding, H. Xu, Y. Huang, J. Li, N. Liu, W. Cao, Y. Zhu, B. Shen, N. Shao, *Nucl. Ac. Res.* **2009**, *37*, 4621-4628.

[4] H.-M. So, D.-W. Park, E.-K. Jeon, Y.-H. Kim, B.S. Kim, C.-K. Lee, S.Y. Choi, S.C. Kim, H. Chang, J.-O Lee, *Small* **2008**, *4*, 197-201.

[5] M. Lorger, M. Engstler, M. Homann, H. U. Göringer, *Eukaryot. Cell* **2003**, *2*, 84-94.

[6] G. T. Hermanson, *Bioconjugate techniques*. Academic Press, Oxford, UK. 1323 p. (**2008**).

[7] P. Gerhardt, R.G.E. Murray, R.N. Costilow, E.W. Nester, W.A. Wood, N.R. Krieg, G.B. Philips (Eds.), *Manual of methods for general bacteriology*. American Society for Microbiology, 524 p. (**1981**).

[8] J.C. de Man, M. Rogosa, M.E. Sharpe, *J. Appl. Bacteriol.* **1960**, *23*, 130-135.

[9] W.J. Taylor, *Am. J. Clin. Pathol.* **1965**, *44*, 471-475.

[10] W.J. Taylor, B. Harris, *Am. J. Clin. Pathol.* **1965**, *44*, 476-479.

[11] W.J. Taylor, B. Harris, *Am. J. Clin. Pathol.* **1967**, *48*, 350-355.

[12] W.J. Taylor, D. Schelhart, *Am. J. Clin. Pathol.* **1967**, *48*, 356-362.

[13] M. Turner, *Nature* **1983**, *303*, 202-203.

[14] K. Vickerman, *Nature* **1978**, *273*, 613-617.

[15] N. Nakajima, Y. Ikada, *Bioconjugate Chem.* **1995**, *6*, 123-130.

[16] S. S. Wong, E. Joselevich, A. T. Woolley, C. L. Cheung, C. M. Lieber, *Nature* **1998**, *394*, 52-55.

[17] D.-H. Jung, B. H. Kim, Y. K. Ko, M. S. Jung, S. Jung, S. Y. Lee, H.-T. Jung, *Langmuir* **2004**, *20*, 8886-8891.

[18] A. Düzgün, A. Maroto, T. Mairal, C. O'Sullivan, F.X. Rius, *Analyst* **2010**, *135*, 1037-1041.

[19] A. Ringbom, *Complexation in analytical chemistry.* Wiley (Interscience), New York USA. 395 p. (**1963**).

[20] G. Charlot, *Les Réactions chimiques en solution : l'analyse qualitative minerale.* Masson, Paris, France. 468 p. (**1969**).

[21] G. Charlot, *Les réactions électrochimiques: les méthodes électrochimiques d'analyse.* Masson, Paris, France. 395 p. (**1959**).

[22] W.A. Anderson, J.E. Zimmerman, F.M. Callahan, *J. Am. Chem. Soc.* **1964**, *86*, 1839-1842.

[23] Y. Lapidot, S. Rappoport, Y. Wolman, *J. Lipid Res.* **1967**, *8*, 142-145.

[24] H. Hirumi, K. Hirumi, *Parasitol. Today* **1994**, *10*, 80-84.

[25] J.O'M. Bockris, A.K.N. Reddy, *Modern Electrochemistry vol. 2*. Reverté, Barcelona, Spain. 1521 p. (**1980**).

[26] C.H. Hamann, A. Hamnett, W. Vielstich, *Electrochemistry*, Wiley-VCH, Weinheim, Germany. 531 p. (**2007**).

[27] D.C. Harris, *Quantitative Chemical Analysis.* W. H. Freeman and Co. New York, NY. 928 p. (**2003**).

[28] ISO 4787, *Laboratory glassware – Volumetric glassware – Methods for use and testing of capacity* (**1984**).

[29] ISO 8655-1/2/6, *Piston-operated volumetric apparatus* (**2002**).

[30] P.R. Busek, J.M. Cowley, L. Eyring (Eds.), *High-resolution transmission electron microscopy and associated techniques*. Oxford University Press, Oxford UK. 645 p. (**1988**).

[31] D. Brandon, W.D. Kaplan, *Microstructural characterization of materials*. John Wiley & Sons, Chichester UK. 550 p. (**2008**).

[32] G. González-Mancera, M.E. Noguez-Amaya, *Principios de microscopía electrónica de barrido y microanálisis por rayos X característicos.* UNAM, Mexico City. 97 p. (**2006**).

[33] J. Goldstein, D. Newbury, D. Joy, C. Lyman, P. Echlin, E. Lifshin, L. Sawyer, J.Michael, *Scanning electron microscopy and X-ray microanalysis*. Kluwer Academic, Plenum Press, New York, USA. 689 p. (**2003**).

Chapter 4

Real-time detection of bacteria in buffer solutions

4.1. Introduction

In this chapter, biosensors based on carbon nanotubes as ion-to-electron potentiometric transducers and aptamers as biorecognition elements are demonstrated as a completely novel biosensing platform with great capabilities in real-time pathogen detection at zero-tolerance levels in phosphate buffer solutions, solving most of the drawbacks inherent to the current methods of detection of pathogens reviewed in Chapter 1. Aptamers specifically tailored for the molecular recognition of type IVB pili of *Salmonella enterica* serovar Typhi (also known as *Salmonella* Typhi, or ST) are used as biorecognition elements chemically linked to the transducing layer of nanotubes. The hybrid material nanotube/aptamer is able to both recognize the target and to translate the binding event into a measurable electrical signal in real-time. The main relevance of this part of the work is the demonstration for the first time that a particular bacteria can be detected with an open circuit potentiometric biosensor and thus pathogen detection is therefore converted into a very simple and rapid task. The implications of this part of the work lie on the very low limits of detection achieved, the rapid response time observed and the customizability that aptamers offer as tailorable biorecognition elements, thus opening the door to infinite applications in real-time biosensing. The content of this chapter has been published in the journal *Angewandte Chemie International Edition*, year 2009, volume 48, pages 7334-7337, and co-authored by Jordi Riu, Ali Düzgün, and F. Xavier Rius.

4.2. Immediate detection of living bacteria at ultralow concentrations using a carbon nanotube based potentiometric aptasensor

The control of diseases has been one of the most important public health concerns of our society for decades. Typical standard methods that are used to assess the presence of microbiological threats consist of specific enrichment media to separate, identify and count bacterial cells. This process takes at least two days after the test sample has been obtained. In recent years, several research groups have tried to attain zero tolerance detection systems within much shorter overall response times.[1] Currently available ultrafast polymerase chain reaction (PCR) detection methods are able to sense 5 CFU (colony-forming units) in an assay time of 20 minutes,[2] which is a major achievement, as is the detection of biowarfare pathogen genes with a DNA-based nanobarcode using a one-minute test.[3] However, these methods require pre-treatment steps to condition the test samples and to perform cell lysis in order to extract the suitable target DNA, a process that significantly complicates these assays. To overcome these drawbacks, there has been a continuing search for methods that allow the direct detection of whole microorganisms. The detection of one cell perched on the tip of a micromechanical oscillator[4] was an important approach for detecting single cells, although the assay was performed at high concentrations of heat-killed bacteria (10^5 CFU/mL) and without a sample matrix. Moreover, the instrumental complexity of this method is high enough to prevent its widespread use. Further progress was made when scanning electron and fluorescence microscopy techniques were used to detect biofunctional magnetic nanoparticles during the extraction and counting of 4 to 10 CFU.[5] Nevertheless, the special care needed when examining the samples by microscopy and the time invested in each observation barely permit a reasonable sample throughput. A fast and versatile method was reported by Rider et al. in 2003 when they detected 500 CFU/g in only 5 minutes using a B cell-based sensor modified to act as a photo-emitter.[6] However, the main shortcomings in this case are the expensive and time-consuming processes involved in fabricating the device.

Therefore, there is still a demand for a fast, sensitive, selective, inexpensive and easy-to-use method for detecting and quantifying pathogenic bacterial cells.

Electrochemical detection techniques have a series of advantages such as rapid response, ease of use, low-cost and small sized commercial detectors. Among the electrochemical techniques, the simplest, most widespread and field-portable methodologies are based on potentiometry. The new wave of potentiometric solid state electrodes represents an attractive tool for real-time bioanalysis in liquid samples.[7] However, to date, it has been difficult to carry out the specific and direct electrochemical detection at ultra low levels of whole living bacterial cells without chemical labeling because the interaction receptor-bacteria does not provide a measurable electrochemical signal.

Recently, Crespo et al.[8] showed that single walled carbon nanotubes (SWCNT) can act as efficient ion-to-electron transducers in potentiometric analysis. The notable charge-transfer capability between heterogeneous phases of SWCNT[9] together with their remarkable double layer capacitance[10] explain their transducing behavior. Moreover, they are easily deposited over many surfaces making them ideal for solid contact electrode design.[11] However, in order to selectively detect a particular target, SWCNT must be coupled to the suitable receptor. Aptamers are highly suitable receptors for the selective and high proficiency detection of a wide range of molecular targets, including bacteria.[12–14] Moreover, aptamers can self-assemble to carbon nanotubes via π-π stacking interaction between the nucleic acid bases and the carbon nanotubes walls,[15] thus constituting a hybrid material that has been applied to nanobiosensors.[16,17] Also, Pan et al. recently obtained a high-affinity RNA aptamer that specifically binds to type IVB pili of *Salmonella* Typhi (ST).[18]

With these developments in mind, we report a potentiometric biosensor for selectively detecting one single CFU of ST close to real time. This aptamer was modified with a five carbon spacer and an amine group ($–(CH_2)_5NH_2$) at the 3' end and was covalently immobilized into a layer of previously carboxylated SWCNT.[19] This step used a well-known carbodiimide mediated wet-chemistry to form amide bonds between the amine spacer and the carboxylic moieties on the sidewalls of the

nanotubes.[20,21] Before linking the aptamers to the carboxylated SWCNT, a 30 µm thick layer of nanotubes were sprayed onto the polished surface of a glassy carbon (GC) rod that was electrically contacted to a potentiometer.[10] We used an Ag/AgCl/KCl double junction electrode as reference for the electromotive force (EMF) measurements. Further information about materials and methods is also included in subsection ***4.2.1***.

The hybrid material aptamer-SWCNT acts as both the sensing and the transducing layer of the biosensor. In the absence of the target analyte (Figure 4.1a), the aptamers are self-assembled to carbon nanotubes via π-π stacking interaction between the puric and pyrimidic bases and the carbon nanotubes walls.[22] The presence of the target bacteria promotes a conformational change in the aptamer that separates the phosphate groups, largely ionized at pH 7.4, from the SWCNT sidewalls, inducing a charge change to the SWCNT and the subsequent change of the recorded potential (Figure 4.1b). The bacteria linked to the aptamer could also lean towards the carbon nanotubes establishing a charge transfer between the highly concentrated H^+ ions that surround the cell wall[23] and the carbon nanotubes. Both mechanisms occur simultaneously and are currently being investigated.

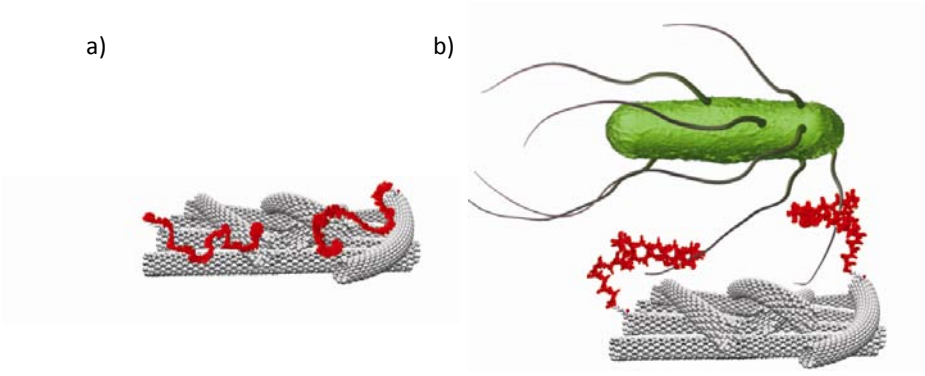

Figure 4.1. a) Possible conformations of the aptamers that are self-assembled to carbon nanotubes. b) Schematic representation of the interaction between the target bacteria and the hybrid system aptamer-SWCNT.

To explore the response of the biosensor to stepwise additions of living ST in phosphate buffer solution (PBS, 1.7 mM, pH = 7.4), we performed consecutive inoculations. All the electromotive force measurements were performed at low ionic strength (1.7 mM PBS) and at neutral pH with a high-input impedance voltmeter M6514 (London, U.K.) in an isothermal vessel at (22 ± 0.5)°C, using 5 mL of sterile and pure PBS before any inoculation of bacteria. The amount of bacteria that was contained in each aliquot was simultaneously standardized in quintuplicate using the agar plate count technique. Stock solutions of bacteria consisted of consecutive 1:10 dilutions in sterile PBS (the same matrix that is used for EMF measurements) of a suspension of bacteria cultured for 12-24 hours, that had been previously washed, precipitated and reconstituted in PBS. The initial EMF values (E_0) for each of the biosensors were in the interval of 80-130 mV; however this value does not exert any influence on the final response for either ST or any other type of bacteria. Figure 4.2 shows an environmental scanning electron microscopy (ESEM) image of a single ST cell placed on the SWCNT-aptamer layer.

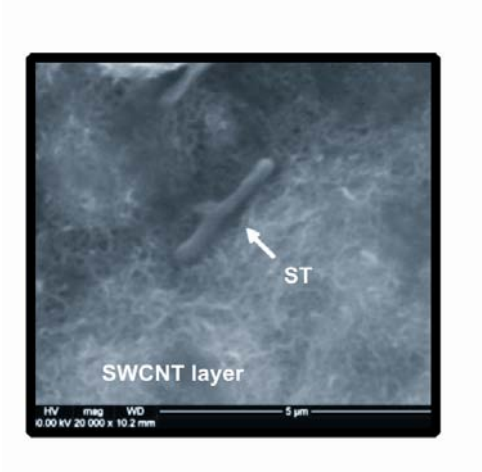

Figure 4.2. Environmental scanning microscope image obtained from an aptamer-functionalized SWCNT electrode after exposure to ST.

The potentiometric response of our biosensor was found to be immediate after each inoculation, ranging from 0.2 CFU mL^{-1} (1 CFU in 5 mL PBS) to 10^6 CFU mL^{-1}. Figure 4.3 shows that the response time is shorter than 60 s indicating a fast affinity

equilibrium between the aptamers and ST. The recorded potential does not decrease after the solution is diluted, indicating that the equilibrium is not easily reversed.

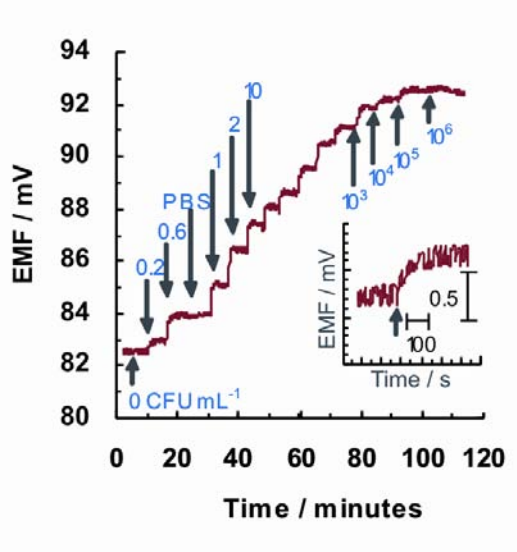

Figure 4.3. Aptamer-functionalized SWCNT electrode exposed to stepwise concentrations of ST and the corresponding potentiometric response; arrows represent the inoculations with ST; values are the final concentration of bacteria. Inset is amplification for the inoculation step at 0.2 CFU mL^{-1} to show the fast response; time is in seconds. The signal provided by the first aliquot containing 1 bacteria (0.2 CFU mL^{-1}) is high enough to be resolved from the instrumental limit of detection,[24] delimited by 3 x SD_{noise} [standard deviation of noise = ± 0.08 mV].

In all the tested sets of inoculations for all the tested sensors (5 sensors), a linear relationship existed between the EMF response and the logarithm of the bacteria concentration up to 10^3 CFU mL^{-1} (Figure 4.4). A sensitivity of 1.87 mV/decade (Standard Deviation=0.29 mV, N=5) has been obtained for this concentration range. However, the slope decreases considerably at higher levels, reaching a plateau at concentrations above 10^6 CFU mL^{-1}. This behavior can be explained by the progressive saturation of the available binding sites (Figures 4.3 and 4.4). After each set of inoculations, the sensors were easily regenerated by dissociating the aptamers from the bacteria in NaCl 2 M for 30 minutes, and then reconstituted by conditioning in PBS,

thus leaving the biosensor ready to take new measurements. Even though the saturation level of the electrodes decreased after 10 regeneration cycles, all the electrodes were able to detect the minimum bacteria concentration for at least 3 months.

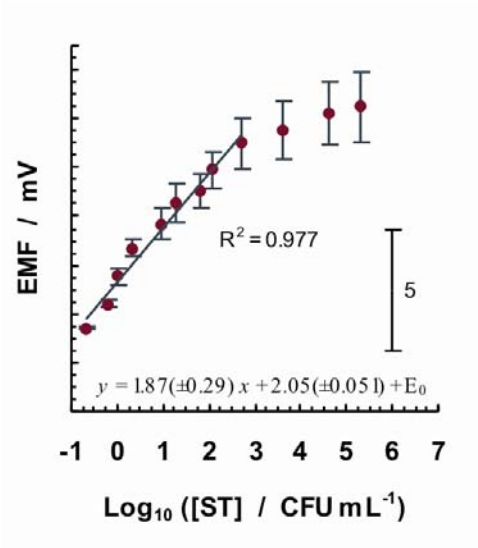

Figure 4.4. EMF response versus decade of concentration of ST. The solid line is the linear regression fit and the equation below was obtained for that range (E_0 is the corresponding sensor potential before any inoculation, and it is particular for each sensor). Error bars are SD of the response obtained at same concentrations for 5 different sensors. Error values in parenthesis are SD for the different regression equations obtained for 5 different sensors.

Our biosensor also shows a high degree of selectivity. No response was shown for parallel experiments using either *Escherichia coli* as a Gram-negative foodborne agent or *Lactobacillus casei* as a non-toxic Gram-positive microorganism. Moreover, control experiments confirmed that the responses are caused exclusively by the binding event between ST and the aptamer, and the subsequent transduction of the SWCNT layer. Several modified solid-contact sensors were tested in order to discard the possibility that the electric potential was originated by unspecific adsorptions. We tested carbon nanotube based electrodes functionalized with the 1-pentylamine molecule ($CH_3(CH_2)_4NH_2$) that represents the five-carbon spacer between the carbon nanotube and the aptamer, and carbon nanotube based electrodes without any other chemical

modification. We also examined the potentiometric response using only the original glassy carbon support as the sensor, which had been either aptamer-functionalized or 1-pentylamine-modified. There was no potentiometric response under any of these conditions, showing that the EMF change is only generated when aptamers attached to SWCNTs interact with ST (Figure 4.5).

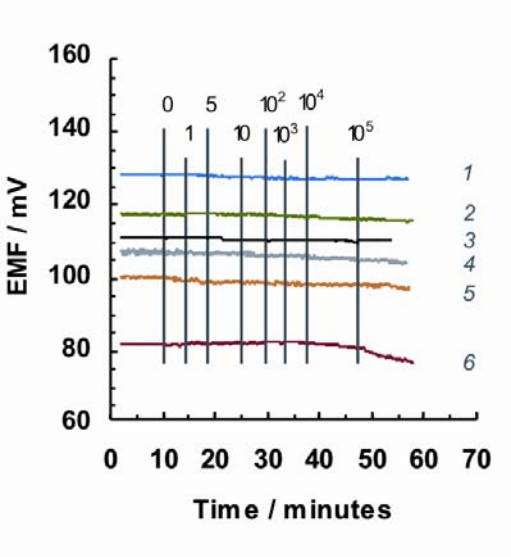

Figure 4.5. Controls and selectivity assays. EMF response versus recorded time, for stepwise concentrations of bacteria. Solid vertical lines represent inoculation with increasing amounts of bacteria. From top to down: *1*, carbon nanotube sensor functionalized with $CH_3(CH_2)_4NH_2$ using same procedure for amide bonding, exposed to ST; *2* and *3* SWCNT-Aptamer biosensors exposed to *E. coli* and to *L. casei*, respectively; *4*, glassy carbon electrode functionalized with $CH_3(CH_2)_4NH_2$, exposed to ST; *5*, carboxylated SWCNT sensor without any functionalization, exposed to ST; *6*, glassy carbon electrode after functionalization with the aptamer and exposed to ST.

In this chapter, we demonstrate that easy-to-build aptamer-based SWCNT potentiometric biosensors are highly selective and can be successfully used to detect living microorganisms in an assay close to real time, thus making the detection of pathogens as easy as measuring the pH value. As demonstrated herein, a highly accurate linear response can be obtained with good reproducibility and without any kind of pretreatment, starting at ultra-low concentrations of bacteria and a dynamic

range of 4 logarithmic units (0.2-10^3 CFU mL^{-1}), and progressing in just a few seconds to concentrations far below those reported previously. Higher concentrations of bacteria can also be detected but in a semiquantitative way. However, the most important strength of this biosensor is that simple positive/negative tests can be carried out in real zero-tolerance conditions and without cross reaction with other types of bacteria. The ease with which measurements are taken in potentiometric analysis opens the door to greater simplicity in microbiological analysis.

4.2.1. Supporting Information

The single walled carbon nanotubes (SWCNTs) were purchased in bulk form from HeJi (Zengcheng, China) with >90% purity, 150 μm average length and 1.4-1.5 nm diameter. The SWCNTs were oxidized in a HST 12/600 silica furnace chamber (Carbolite, Hope Valley, UK) at 365°C, with synthetic air flow-rate of 100 cm^3 min^{-1} and 90 min, in order to selectively remove the amorphous carbon. Subsequently, SWCNTs were refluxed in 2.6 M nitric acid for 4 h to oxidize the metallic impurities remaining from the synthesis[19]. The carbon nanotubes became carboxylated after this latter oxidation step. The SWCNTs in nitric acid solution were filtered and thoroughly rinsed with water to remove the acid completely. The filtered SWCNTs were dried overnight at 80°C.

The reagents sodium dodecyl sulphate (SDS), N-(3-dimethylaminopropyl)-N′-ethylcarbodiimide hydrochloride (EDC), N-hydroxysuccinimide (NHS), 2-(N-morpholino) ethanesulfonic acid (MES) and cetyltrimethylammonium bromide (CTAB) were purchased from Sigma-Aldrich (Tres Cantos, Spain). Potentiometric measurements were carried out in all cases in a 1.7 mM pH 7.4 phosphate buffer solution (PBS), which was prepared by a 1:100 dilution of a 0.17 M stock solution of corresponding amounts of KH_2PO_4 and Na_2HPO_4 (Sigma-Aldrich, Tres Cantos, Spain). All the substances were used as received. Water used to prepare the solutions was purified through a Milli-Q system (Millipore, Barcelona, Spain) and in all cases the resistivity level of purified water was 18.2 MΩ cm.

Eurogentec (London, UK) synthesized the *Salmonella* Typhi type IVB Pili binding aptamer of 71-mer with the sequence 5'-GGG AAC AGU CCG AGC CUC ACU GUU AUC CGA UAG CAG CGC GGG AUG AGG GUC AAU GCG UCA UAG GAU CCC GC-3', and $(CH_2)_5NH_2$-modified in the 3' end. The aptamer was resuspended in MilliQ water and stored at -80 °C.

Lyophilized strains of *Salmonella* Typhi (CECT 409) and *Lactobacillus casei* subsp. *casei* (CECT 4180) were purchased from Colección Española de Cultivos Tipo (Valencia, Spain) and reactivated by resuspension in saline solution 0.85% and later selective

enrichment in XLD agar (*Salmonella* Typhi) and MRS broth (*Lactobacillus casei*). *Escherichia coli* (CECT 4558) was kindly donated by the Biotechnology Department of the URV (Tarragona, Spain). Tryptic soy agar and Tryptic soy broth, Lactobacilli MRS (deMan, Rogosa and Sharpe) agar / broth and XLD (xylose-lysine-deoxycholate) agar were purchased from Becton, Dickinson and Company (Sparks, U.S.A.) and prepared according to indications. All bacteria strains were cultivated under the same experimental conditions, including incubation time and temperature, except for the growth medium of *Lactobacillus casei* (*Lactobacilli* MRS broth and agar). The original bacteria samples were stored at -20 °C in glycerol / broth medium (10% v/v) and reactivated by inoculating the bacteria in 10 mL of sterile broth medium at 37 °C for 24 h. The bacteria samples were then centrifuged at 6000 rpm for 15 minutes and the supernatant was discarded. The precipitate was resuspended in 10 mL of sterile PBS 1.7 mM pH 7.4, and the resulting solution was 1:10 diluted eight times to give a series of 10^{-1} to 10^{-8} stock solutions of bacteria. The stock solutions were quantified in quintuplicate using the standard plate count method, in an appropriate culturing agar medium (tryptic soy for *Salmonella* Typhi / *Escherichia coli* and MRS for *Lactobacillus casei*), and the same procedure was also applied to the standardization of the variable aliquots of stock solutions that were used to inoculate the solutions analyzed.[25]

The solid contact electrode was made of a 3 mm diameter glassy carbon cylindrical rod (HTW Hochtemperatur-Werkstoffe GmbH, Thierhaupten, Germany) covered by a Teflon jacket of 7 mm diameter. The surface of the glassy carbon was successively polished using 25 and 1 micron grain size polishing alumina (Buehler, Lake Bluff, USA) before the SWCNT layer was deposited on the same surface. For the spraying process, we used sonication for 30 minutes at 0.5 s^{-1} to prepare a solution of 25 mg of purified SWCNT dispersed in 10 mL of MilliQ water containing 100 mg of SDS. The SWCNT/SDS/H_2O solution was sprayed under a high temperature (200°C) air blow, and washed with MilliQ water to progressively remove the SDS.

The carboxylic groups that are on the sidewalls of the deposited SWCNTs are activated using a solution of 100 nmol of EDC and 25 nmol of NHS in a 50 mM MES buffer pH 5 for 30 minutes[21]. Subsequently, the electrodes were soaked overnight

into 500 µL of a 1 µM aptamer solution, which also consisted of PBS pH 7.4 (1 mM) and CTAB (0.2 mM).

Microscopic analysis of electrodes was carried out using a FEI Quanta model 600 environmental scanning electron microscope (ESEM) with ETD detector (Hillsboro, USA). The microscopic observations were performed in high vacuum mode (10^{-5} mbar) and with an accelerating voltage of 30 kV. The working distance was 10.2 mm. The attached cells of bacteria were directly observed without biological-specimen preparation. The electrode was immersed directly in 5 mL of PBS working solution containing a concentration of 10^5 CFU mL^{-1} of bacteria. Subsequently, the electrode was withdrawn from the solution and directly inserted to the ESEM sample holder. Sample drying was achieved using the ESEM vacuum system. The specimens were examined at a magnification of 20000x.

4.2.2. Acknowledgements

We would like to thank A. Maroto and R. Villamizar for their helpful comments and also S. Moreno for the loan of essential equipment. This study has been supported by the Spanish Ministry of Education and Science, MEC, through the project grants NAN2004-09306-C05-05 and CTQ2007-67570/BQU. G.A.Z.-G. would like to thank the Generalitat de Catalunya (Catalan Government) and European Social Fund for awarding the FI DGR fellowship.

4.3. References

[1] C.A. Batt, *Science* **2007**, *316*, 1579-1580.

[2] P. Belgrader, W. Benett, D. Hadley, J. Richards, P. Stratton, R. Mariella Jr., F. Milanovich, *Science* **1999**, *284*, 449-450.

[3] Y. Li, Y.T.H. Cu, D. Luo, *Nature Biotech.* **2005**, 23, 885-889.

[4] B. Ilic, D. Czaplewski, M. Zalalutdinov, H.G. Craighead, P. Neuzil, C. Campagnolo, C. Batt, *J. Vac. Sci. Technol. B* **2001**, *19*, 2825-2828.

[5] H. Gu, K. Xu, C. Xu, B. Xu, *Chem. Commun.* **2006**, 941-949.

[6] T.H. Rider, M.S. Petrovick, F.E. Nargi, J.D. Harper, E.D. Schwoebel, R.H. Mathews, D.J. Blanchard, L.T. Bortolin, A.M. Young, J.Chen, M.A. Hollis, *Science* **2003**, *301*, 213-215.

[7] E. Bakker, E. Pretsch, *Angew. Chem. Int. Ed.* **2007**, *46*, 5660-5668.

[8] G.A. Crespo, S. Macho, F.X. Rius, *Anal. Chem.* **2008**, *80*, 1316-1322.

[9] H. Dai, *Acc. Chem. Res.* **2002**, *35*, 1035-1044.

[10] G.A. Crespo, S. Macho, J. Bobacka, F.X. Rius, *Anal. Chem.* **2009**, *81*, 676-681.

[11] L. Agüí, P. Yáñez-Sedeño, J.M. Pingarrón, *Anal. Chim. Acta* **2008**, *622*, 11-47.

[12] S.M. Shamah, J.M. Healy, S. T. Cload, *Acc. Chem. Res.* **2008**, *41*, 130-138.

[13] S. Tombelli, M. Minunni, M. Mascini, *Biosens. Bioelectron.* **2005**, *20*, 2424-2434.

[14] N. de-los-Santos-Álvarez, M.J. Lobo-Castañón, A.J. Miranda-Ordieres, P. Tuñón-Blanco, *Trends Anal. Chem.* **2008**, *27*, 437-446.

[15] M. Zheng, A. Jagota, M.S. Strano, A.P. Santos, P. Barone, S.G. Chou, B.A. Diner, M.S. Dresselhaus, R.S. Mclean, G.B. Onoa, G.G. Samsonidze, E.D. Semke, M. Usrey, D.J. Walls, *Science* **2003**, *302*, 1545-1548.

[16] H.M. So, D.W. Park, E.K. Jeon,Y.H. Kim, B.S. Kim, C.K. Lee, S.Y. Choi, S.C. Kim, H. Chang, J.O. Lee, *Small* **2008**, *4*, 197-201.

[17] A. Star, E. Tu, J. Niemann, J.C.P. Gabriel, C.S. Joiner, C. Valcke, *Proc. Natl. Acad. Sci.* **2006**, *103*, 921-926.

[18] Q. Pan, X.L. Zhang, H.Y. Wu, P.W. He, F. Wang, M.S. Zhang, J.M. Hu, B. Xia, J Wu, *Antimicrob. Agents Chemother.* **2005**, *49*, 4052-4060.

[19] C.A. Furtado, U.J. Kim, H.R. Gutierrez, L. Pan, E.C. Dickey, P.C. Eklund, *J. Am. Chem. Soc.* **2004**, *126*, 6095-6105.

[20] S.S. Wong, E. Joselevich, A.T. Woolley, C.L. Cheung, C.M. Lieber. *Nature* **1998**, *394*, 52-55.

[21] D.H. Jung, B.H. Kim, Y.K. Ko, M.S. Jung, S. Jung, S.Y. Lee, H.T. Jung. *Langmuir* **2004**, *20*, 8886-8891.

[22] R.R. Johnson, A.T.C. Johnson, M.L. Klein, *Nano Lett.* **2008**, *8*, 69-75.

[23] Y. Hong, D.G. Brown, *Langmuir* **2008**, *24*, 5003-5009.

[24] L. A. Currie, *Pure Appl. Chem.* **1995**, *67*, 1699-1723.

[25] A.L. Koch, Growth measurement. In: P. Gerhardt et al. (eds.), *Manual of Methods for General Bacteriology*. American Society for Microbiology, Washington, D.C. pp. 179-207 (**1981**).

Chapter 5

Effect of the functionalization approach on the biosensor performance parameters

5.1. Introduction

In the previous chapter, the proof-of-principle for the potentiometric biosensors based on carbon nanotubes as potentiometric transducers and RNA aptamers as biorecognition elements was demonstrated with the detection of the gram-negative bacteria *Salmonella* Typhi in buffer solutions. In that chapter, the aptamer molecules were covalently attached to the carbon nanotubes by amide bonds formed between amine moieties previously introduced at the 3' end of the aptamers and carboxylic groups at the nanotubes' sidewalls. However, the possibility to detect gram-positive bacteria using this new generation of potentiometric biosensors was not demonstrated so far. Therefore, it is very interesting to investigate the possibilities to generalize the methodology for all types of bacteria. Moreover, the compatibility of simpler biosensor functionalization procedures with the potentiometric biorecognition phenomenon as well as their eventual effect on the biosensor performance parameters remained an open question.

Therefore, in this chapter we analyze the biosensor performance parameters in terms of the functionalization procedure followed and type of bacteria detected. A network of carbon nanotubes was used as the ion-to-electron potentiometric transducing layer whereas DNA aptamers are the recognition element used to target the gram-positive microorganism *Staphylococcus aureus*. The carbon nanotube layer was functionalized with the aptamer molecules by two different approaches (Scheme 5.1): 1) covalent bond formation between a primary amine-group introduced to one of the terminals of the aptamer molecules and the carboxylic groups at the sidewalls of the nanotubes following standard carbodiimide-mediated chemistry; and 2) non-covalent adsorption of drop-casted pyrenil-modified aptamer molecules onto the external walls of the nanotubes.

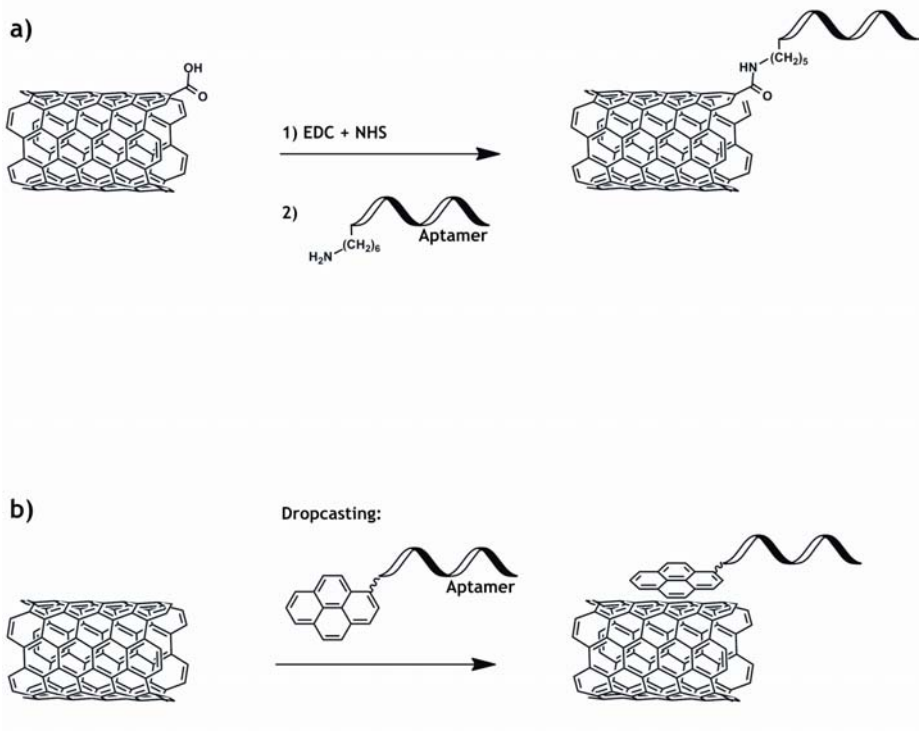

Scheme 5.1. a) Covalent functionalization of carboxylated carbon nanotubes with amine-modified aptamers. b) Non-covalent functionalization of carbon nanotubes with pyrenil-modified aptamers.

By comparing the performances of the biosensors prepared using these two strategies, we aimed to determine the best approach in terms of analytical performance and biosensor construction simplicity. The biosensors were finally assessed as potential tools for the detection of *Staphylococcus aureus* in human skin using, as a surrogate for human skin, freshly excised pig skin. The content of this chapter has been submitted for publication, and it has been co-authored by José Luis Sebastián-Ávila, Pascal Blondeau, Jordi Riu and F. Xavier Rius.

5.2. Label-free detection of Staphylococcus aureus in skin using real-time potentiometric biosensors based on carbon nanotubes and aptamers

5.2.1. Abstract

In this chapter we report the first biosensor that is able to detect *Staphylococcus aureus* (*S. aureus*) in real-time. A network of single-walled carbon nanotubes (SWCNTs) acts as an ion-to-electron potentiometric transducer and anti-*S. aureus* aptamers are the recognition element. Carbon nanotubes were functionalized with aptamers using two different approaches: 1) non-covalent adsorption of drop-casted pyrenil-modified aptamers onto the external walls of the SWCNTs; and 2) covalent bond formation between amine-modified aptamers and carboxylic groups previously introduced by oxidation at the ends of the SWCNTs. Both of these approaches yielded functional biosensors but there were large differences in the minimum detectable bacteria concentration and sensitivity values. With covalent functionalization, the minimum concentration detected was 8 x 10^2 Colony-Forming Units (CFU)/mL and the sensitivity was 0.36 mV/Decade. With the non-covalent approach, the sensitivity was higher (1.52 mV/Decade) but the minimum concentration detected was greatly affected (10^7 CFU/mL). In both cases, potential as a function of Decade of bacteria concentration was linear. Functional biosensors were used to test real samples from freshly excised pig skin, contaminated with the target microorganism, as a surrogate for human skin.

5.2.2. Introduction

Staphylococcus aureus (*S. aureus*) is a common Gram-positive pathogen that can be present on skin and mucous membranes of healthy humans or in inadequately treated food. In uncontrolled conditions, *S. aureus* can cause a wide range of diseases including several types of dermatitis and gastrointestinal tract infections and is widely involved in many cases of enterotoxin-related food poisoning worldwide. It is also an important cause of life-threatening infections such as pneumonia, septicemia, osteomyelitis, toxic shock syndrome and about a third of the total cases of

endocarditis worldwide. Moreover, is an important burden in critical sectors such as hospitals because of the high volume of acquired nosocomial-infections it causes, especially in immunodepressed patients or with post-operatory treatments. An increasing prevalence of Methicilin- and Vancomycin-resistant strains of *S. aureus* is now seriously challenging global monitoring platforms. Consequently, there is currently a huge demand for rapid methods of *S. aureus* detection.[1–4] *S. aureus* is traditionally detected using the gold standard technique known as the plate count method after selective enrichment in broth.[5] Despite the simplicity of this technique, however, the time needed to produce a confirmatory result ranges from 2 to 4 days. Also, further biochemical tests are usually needed for corroboration, which makes the existing detection protocols complicated and requires skilled staff and expensive laboratory facilities.

Several successful fast biosensing approaches have been developed for indirectly detecting *S. aureus* either by detecting pathogenic-nucleic acid sequences,[6–9] or the presence of toxins and other biomolecules produced by the pathogen at very low concentrations.[10–12] However, the techniques based on nucleic acid sequences detection usually require preprocessing steps for prior bacteria lysis and subsequent DNA extraction, amplification and detection. This makes the overall procedure both expensive and complicated. Moreover, indirect detection techniques are limited by the ability of *S. aureus* to produce target molecules and shed them into the sample matrix. Both are also influenced by intrinsic and extrinsic factors, so negative results are not necessarily related to the absence of the pathogen. Biosensing methods based on the direct detection of target pathogens are preferred over indirect detection methods because their results are directly related to the presence of the microorganism. Recent advances in biosensing platform development have led to novel biosensors for directly and rapidly detecting *S. aureus*. State-of-the-art techniques such as surface plasmon resonance biosensors based on antibodies[13] and phages[14] –able to detect 10^5 Colony-forming units (CFU)/mL in 2 h or 10^4 CFU/mL in about 20 minutes, respectively– or fluorescence-based immunoassays[15] –able to detect 10^4 CFU/mL in 15 minutes– represent a huge advance in the fast detection of this pathogen. However, biosensors based on electroanalytical methods are generally preferred

because electrochemical devices are cheap, portable, easy to use and easy to miniaturize, and afford lower detection limits than other techniques.[16] However, the thick polysaccharide layer of poly-N-acetylglucosamine on the surface of *S. aureus* and the low abundance of antigens that are externally exposed and available to biorecognition elements such as antibodies,[17,18] seriously limit in the development of biosensors for direct electrochemical detection. Consequently, only a few electrochemical biosensors for *S. aureus* detection have been developed to date, with detection limits ranging between 10^4 and 10^5 CFU/mL in the best case scenario.[19,20] Recent advances using amperometric detection techniques have enabled much lower detection limits of about 10^3 CFU/mL in a total analysis time of 50 minutes,[21] or $6.5x10^2$ CFU/mL in 3 hours[22] when selective enrichment steps are introduced. As in all the previous examples, in both of these cases enzymatic-labeling is essential and, unfortunately, the detection of *S. aureus* without the need for labels or complicated procedures such as ELISA-based methods remains a challenge. Several promising approaches have recently tried to solve this problem by targeting *S. aureus* using lectins as biorecognition elements in label-free biosensors based on electrochemical quartz crystal microbalance for the detection of 10^7 CFU/mL in one hour.[23]

Very recently, a new generation of DNA aptamers able to recognize conserved epitopes on the surface of *S. aureus*[24] has provided promising solutions for this important issue but platforms for the direct and label-free detection of *S. aureus* are still not completely resolved. The deployment of the above-reported *S. aureus*-biosensing platforms into clinical settings for the rapid detection of this life threatening pathogen in clinical samples such as infected wounds or skin biopsy specimens has remained unsolved for years. To address this challenge, in this chapter we report the first biosensor for the real-time and label-free potentiometric detection of *S. aureus*. We used a hybrid transducing/biosensing material[25] consisting of single-walled carbon nanotubes (SWCNT) as ion-to-electron potentiometric transducers and aptamers –tailored DNA or RNA segments acting as artificial recognition elements[26]– as biorecognition molecules. The transducing properties of this SWCNT/aptamer hybrid material derive from the remarkable SWCNT double-layer capacitance, the great ability to support charge transfer between the SWCNT/solution interface and the

ions that surround the cell wall of the target bacteria, and the extremely high surface-to-volume ratio of the nanotubes that are also able to sense conformational changes in the linked aptamers during the target-recognition event that switches the surface charge on the SWCNT layer.[27–29] To explore alternative methods for the functionalization of nanotubes with aptamers and thus open the door to easier functionalization procedures, we attached the aptamers to a homogeneous layer of SWCNT using two functionalization strategies –a covalent approach and a non-covalent approach– and analyzed the effects on the biosensors' performance parameters. The covalent approach consisted of linking the aptamers to the nanotubes chemically by amide bonds formed between the –COOH groups of previously carboxylated SWCNT and an amine moiety introduced at the 3' end of the aptamer by well-known carbodiimide mediated chemistry.[30,31] The non-covalent approach was performed by direct physisorption onto the SWCNT sidewalls of pyrenil moieties previously introduced to the 3' end of the aptamer. Pyrenil groups strongly interact with the sidewalls of the nanotubes by π-stacking, and this property is commonly used to fix pyrenil-modified biomolecules to carbon nanotubes by drop casting.[32] By comparing the performances of the biosensors prepared using these two strategies, we aimed to determine the best approach in terms of analytical performance and biosensor construction simplicity. Finally, we assessed the functional biosensors as potential tools for detecting *S. aureus* in human skin using, as a surrogate for human skin (based on the morphological similarity of the two skin types), freshly excised dorsal skin of the domestic pig.[33]

5.2.3. Materials and methods

5.2.3.1. Chemicals and aptamers

Solutions were prepared using deionized water purified through a Milli-Q system (Millipore, Madrid, Spain) with a resistivity level of 18.2 MΩ cm. The reagents sodium dodecyl sulphate (SDS), N-(3-dimethylaminopropyl)-N'-ethylcarbodiimide hydrochloride (EDC), N-hydroxysuccinimide (NHS), 2-(N-morpholino) ethanesulfonic acid (MES) and cetyltrimethylammonium bromide (CTAB), KH_2PO_4 and Na_2HPO_4 were purchased from Sigma-Aldrich (Tres Cantos, Spain). All substances were used as

received. Phosphate buffer solution (PBS) 1.7 mM pH 7.4 was prepared sterilely using a 1:100 dilution of a 0.17 M stock solution of corresponding amounts of KH_2PO_4 and Na_2HPO_4, and the pH was adjusted as required. The 88-mer *S. aureus*-binding DNA aptamers with similar affinities[24] and the sequences 5'-GCAAT-GGTAC-GGTAC-TTCCT-CCCAC-GATCT-CATTA-GTCTG-TGGATAAGCG-TGGGA-CGTCT-ATGAC-AAAAG-TGCAC-GCTAC-TTTGC-TAA-3'-$(CH_2)_6NH_2$ (NH_2-Aptamer) and 5'-GCAAT-GGTAC-GGTAC-TTCCG-CGCCC-TCTCACGTGG-CACTC-AGAGT-GCCGG-AAGTT-CTGCGTTATC-AAAAG-TGCAC-GCTAC-TTTGC-TAA-3'-C3-Pyr (Pyr-Aptamer, C3-Pyr = pyrenil moiety with a phosphoramidite spacer) were purchased from Eurogentec (London, UK). The aptamers were resuspended in deionized water and stored at -80 °C. All the materials and solutions were adequately sterilized and manipulated under sterile conditions.

5.2.3.2. Microorganism culturing

The manipulation of microorganisms was carried out in a biosafety level II cabinet, model BIO II A (Telstar Industrials, Terrassa, Spain). Information about culturing media, bacteria strains and culturing procedures can be found in subsection ***5.2.6***.

5.2.3.3. Instrumentation and materials

Electromotive force (EMF) measurements were automatically recorded with a high-input impedance voltmeter model EMF-16 (Lawson Laboratories, Inc., Malvern, PA, U.S.A.) using an Ag/AgCl/KCl (3 M) double junction reference electrode containing a 1 M LiAcO electrolyte bridge (type 6.0729.100, Metrohm AG, Herisau, Switzerland) and the biosensor or SWCNT-based electrode as the working electrode.

5.2.3.4. Development of the biosensors

The development of the biosensors prepared by both procedures, the covalent functionalization approach and the non-covalent functionalization method, as well as the preliminary viability tests performed with the biosensors are described in subsection ***5.2.6***.

5.2.3.5. Analytical procedure

Constant stirring (300 rpm) was applied during all the potentiometric measurements in an isothermal vessel at 22±0.5 °C containing 5 mL of sterile PBS working solution (1.7 mM and pH 7.4) before addition of the sample. The electrochemical cells were inoculated in a stepwise mode with the stock solutions of serially diluted bacteria (10^{-8} to 10^{-1} solutions prepared as mentioned in subsection ***5.2.6***) in order to progressively increase the bacteria concentration within the electrochemical cell and simultaneously monitor the EMF changes with the biosensors at periods of 10 s. The dilution was corrected for all the stepwise concentration experiments in order to calculate the concentration of bacteria within the electrochemical cell by considering the volume increase of buffer solution after each sample addition. The potentiometric response of the biosensors was evaluated following the EMF changes after stepwise inoculation with increasing concentrations of *S. aureus*. Selectivity assays were carried out by testing the biosensors against stepwise increasing concentrations of *Escherichia coli* (*E. coli*) and *Staphylococcus epidermidis* (*S. epidermidis*). Parallel control assays were performed by monitoring the potentiometric response of SWCNT sensors without aptamers against increasing concentrations of *S. aureus*. Biosensors were regenerated in a 2 M NaCl aqueous solution for 1 hour after each potentiometric measurement experiment in order to dissociate the bacteria from the aptamers. The regenerated biosensors were then washed for 15 minutes in sterile deionized water and stored in PBS working solution to prepare them for new measurements.

For the detection of *S. aureus* in a surrogate for human skin, 2 cm x 2 cm segments of freshly excised dorsal pig skin (purchased from a local butcher's) were successively washed with water and soap, rinsed with water, dried, further sterilized at the surface with 70% v/v ethanol/water, and finally dried for 10 minutes, always with sterile solutions and under sterile conditions. The surface was then inoculated with 50 µL of a 10^{8} CFU mL^{-1} *S. aureus* stock solution in PBS, distributed over the surface with a sterile microbiological loop, and dried for 30 minutes. Control pig skin without *S. aureus* inoculated was prepared following the same steps but substituting the bacteria-containing solution with sterile PBS. Finally, the inoculated pig skin was rubbed with

two sterile cotton swabs moistened with sterile PBS working solution. One of the swabs was used for growth control by smearing the adsorbed bacteria onto the solidified surface of Mannitol Salt Agar (MSA) contained in a Petri dish that was then incubated for 48 h at 37 °C. MSA is a selective solid medium for confirming the growth of *S. aureus* and the presence of the microorganism is evidenced when pale-yellow colonies surrounded by a yellow halo are found.[5] The other swab was introduced in a tube containing 2 mL of sterile PBS working solution in order to transfer the recovered microorganisms to the PBS by intense shaking and later detect the S. aureus present in an aliquot of this solution using the developed biosensors. The tube was shaken intensely and 500 µL of the solution was then transferred into an electrochemical cell containing the tested biosensor (Figure 5.1). Three functional biosensors for each type of functionalization were used in this experiment. Parallel quantification assays were carried out in order to estimate the amount of *S. aureus* recovered from pig skin by this procedure following the standard plate count method in TSA in triplicate applied to an aliquot of the solution within the tubes containing the recovered bacteria. Control pig skin without *S. aureus*, prepared as described previously, was used as a blank in both control quantification assays and control potentiometric assays of the tested biosensors following the latter swab-smearing based procedure. Finally, selectivity assays were performed by substituting *S. aureus* for *E. coli* and *S. epidermidis* in this same protocol. The biosensors were then tested in the same way to evaluate them with different microorganisms that could be present in real skin samples.

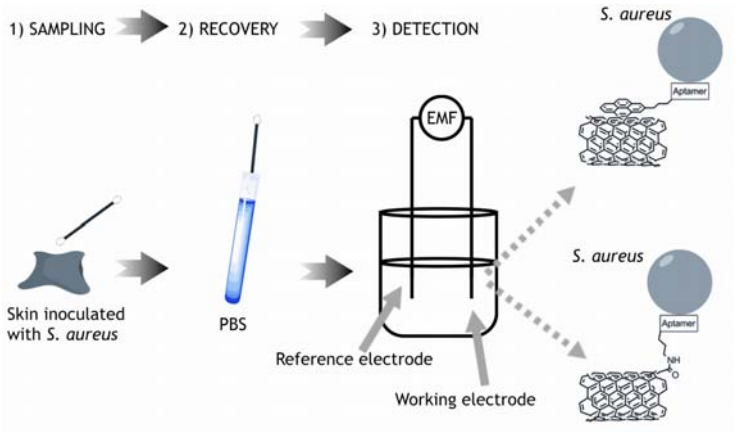

Figure 5.1. Experimental setup for the sample recovery steps required to analyze human skin surrogates using the potentiometric biosensor. 1) sampling from skin segments using a sterile swab moistened with PBS; 2) recovery by resuspension of the collected microorganisms in a tube containing PBS; 3) potentiometric detection of bacteria in aliquots of the recovery solution. Biosensors functionalized by both methods and the interaction with *S. aureus* are schematized on the right.

5.2.4. Results and discussion

Recognition of *S. aureus* by the biosensors following the covalent functionalization approach was evidenced when the biosensors were incubated for 30 minutes in a 10^8 CFU/mL solution of *S. aureus*, which was then thoroughly washed and smeared onto the solid surface of agar to yield positive growth after 48 h at 37 °C. Control tests with SWCNT sensors without aptamer did not produce colonies under these conditions. Non-covalently functionalized biosensors prepared by drop casting the Pyr-Aptamer solution also yielded positive growth on agar. This was confirmed by triplicate experiments of the previous assays. The instrumental limit of detection (3 x standard deviation of the noise) determined from electromotive force (EMF) measurements recorded using both biosensor types was 96 µV and 42 µV for the covalently prepared biosensors and non-covalently prepared biosensors, respectively. EMF variations above these values should be easily detected by the corresponding biosensor type.

In the case of non-covalently functionalized biosensors prepared by drop casting Pyr-Aptamer solution, the EMF response to *S. aureus* began at the relatively high concentration of 10^7 CFU/mL and lower concentrations did not change the EMF values (Figure 5.3a). The EMF response was linearly dependent on the bacterial concentration in Decade units with a slope of 1.52 mV/Decade in the very limited range of 1 order of magnitude between 10^7 CFU/mL and 10^8 CFU/mL (Figure 5.2b). The biosensor response time was about 120-200 seconds, but an immediate change was observed after the addition of *S. aureus* at concentrations above 10^7 CFU/mL. The EMF response was quite stable for at least 10 minutes after bacteria inoculation during the range explored. However, when exposed to concentrations above 10^8 CFU/mL, signal drift was observed and a progressively more pronounced decay on signal stability appeared as the concentration of bacteria increased. This effect may be attributed to colloidal agglomeration of the highly concentrated non-bound bacteria onto the surface of the biosensor. This behavior would limit the applicability of biosensors at higher concentrations. Sample dilution would not be an option for reducing such an effect in samples with a high bacterial load, since, as explained earlier, the working range of this non-covalently prepared biosensor is very limited. Biosensors prepared by this method and exposed to increasing concentrations of *E. coli* and *S. epidermidis* at the concentration range of 0 – 10^8 CFU/mL did lead to a clear change in EMF. Simultaneous control assays with non-functionalized SWCNT sensors also resulted in the same behavior.

Covalently prepared biosensors afforded much lower detectable concentrations when exposed to *S. aureus* since the first clear potentiometric change was observed at a concentration of 8 x 10^2 CFU/mL (Figure 5.2a). At concentrations above this value, EMF as a function of the concentration of bacteria in Decade units was linear and the sensitivity was 0.36 mV/Decade (Figure 5.2b). The signal was also stable in the concentration range analyzed. A response time of 6 to 11 minutes (90% of the total response, see amplification in Fig. 5.3a) was observed for the concentration range 8x102 CFU/mL to 10^8 CFU/mL and the signal was stable for at least one hour after the addition of the sample, which is enough time to perform any sample analysis with this type of biosensor. However, after inoculation with bacteria at concentrations above

10^8 CFU/mL stability dramatically decreased and EMF response remained stable for about 20 minutes before negative drift appeared. As mentioned previously, this effect was probably caused by stochastic charge transfer processes between the surface of the biosensor and the highly concentrated *S. aureus* not tethered to the biosensor by the aptamers. Control experiments conducted in parallel with non-functionalized SWCNT sensors did not lead to a clear change in EMF, which confirms that the potentiometric response is driven by the recognition of the target microorganism by the biosensors. When selectivity assays were carried out with functionalized biosensors exposed to stepwise increasing concentrations of *E. coli* and *S. epidermidis* between 0 and 10^8 CFU/mL, no change was observed in EMF (Fig. 5.2c). However, at concentrations above 10^7 CFU/mL, progressive drift was observed on the baseline after addition of the sample.

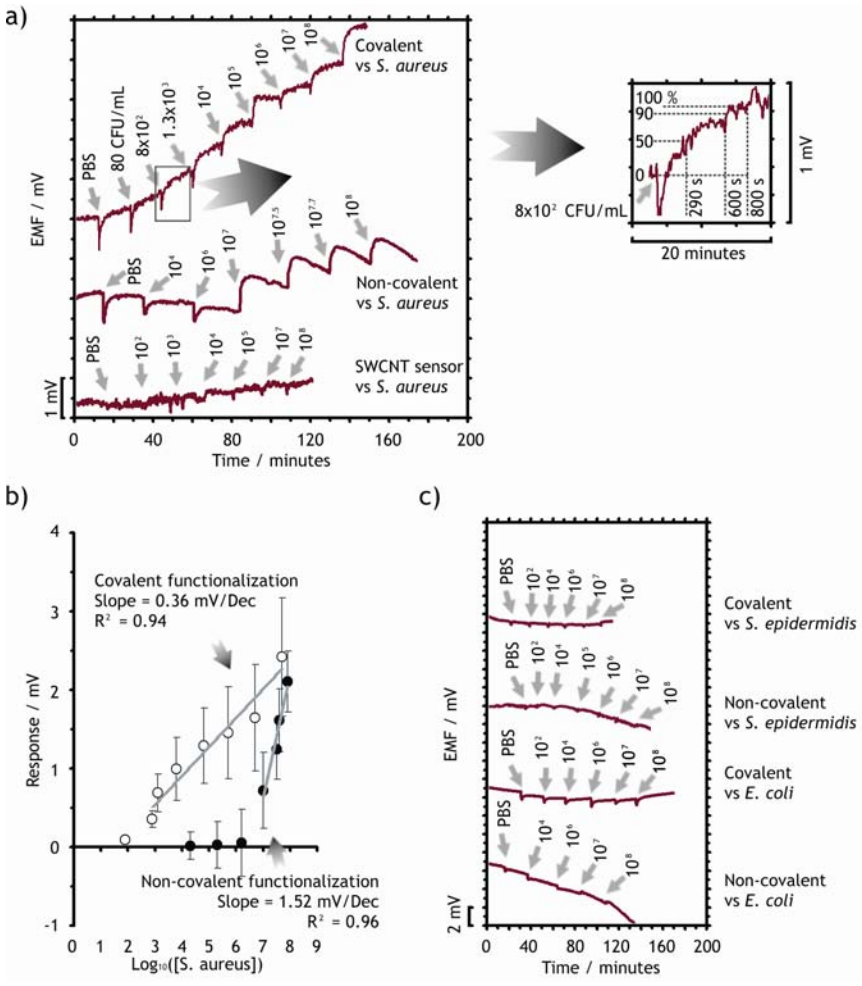

Figure 5.2. Performance of biosensors prepared by covalent functionalization with NH_2-Aptamer and non-covalent functionalization with Pyr-Aptamer. a) Change in EMF recorded as a function of time for different biosensors when exposed to *S. aureus* (right, amplification of the curve after inoculation with $8x10^2$ CFU/mL). b) Potentiometric response as a function of concentration of bacteria in Decade units (the circles represent the average responses of three different biosensors; error bars are standard deviation). c) Change in EMF recorded as a function of time, when biosensors were exposed to stepwise increasing concentrations of different microorganisms (values are in CFU/mL), *S. aureus*, *E. coli*, *S. epidermidis* and a SWCNT sensor without aptamer to *S. aureus*.

The different performances between of the two types of biosensor in terms of the minimum concentration detected and sensitivity are explained by the differences in the bacterial-adsorption profiles due to the functionalization procedure followed. This was demonstrated when the *S. aureus* linked to the biosensor surfaces of each biosensor type at a concentration of 10^8 CFU/mL was grown in TSA according to the standard plate count method. Using this procedure, differences in bacterial adsorption were observed for each biosensor type. While the biosensors prepared by the covalent method yielded a surface bacterial concentration of $9.1x10^6$ CFU (standard deviation, SD=$5x10^6$, with three biosensors tested), the biosensors prepared by the non-covalent approach only yielded a surface bacterial concentration of $2.4x10^3$ CFU (SD=$8x10^3$, three biosensors tested). The observed difference suggests that the bacteria remain more easily tethered to covalently functionalized biosensors by a difference of almost 4 orders of magnitude if compared with non-covalently functionalized biosensors. Several reasons may be behind this lower affinity of the biosensors prepared by non-covalent functionalization. An excess of Pyr-Aptamer molecules closely adsorbed during the drop casting procedure probably resulted in random molecular overlapping and so the recognition of the target bacteria by the biosensor was compromised by self-entanglement of Pyr-Aptamer molecules (which could clearly reduce the availability of aptamers that are able to recognize their target). Another possibility is the progressive leaching of the aptamer+bacteria complex, which was probably caused by an excessive accumulation of aptamer, which may have reduced the fixation strength of outer aptamer layers to the nanotube sidewalls by inner layers of more strongly adsorbed aptamers. Both possibilities are performance limiting factors for biosensor prepared by this procedure, and further theoretical/experimental research is needed in order to unravel this trend.

To assess the potential use of biosensors prepared by both of these methods in the detection of *S. aureus* in human skin, we used segments of freshly excised dorsal pig skin as a surrogate. These segments were inoculated with 50 µL of a 10^8 CFU/mL solution (corresponding to $5x10^6$ CFU). Aliquots of PBS containing the *S. aureus* recovered from pig skin segments using sterile cotton swabs were analyzed using functional biosensors prepared by both functionalization methods (Figure 5.3). The

biosensors prepared covalently showed a clear change in EMF of 390±16 µV (N=3) when 500 µL of this solution was inoculated into the electrochemical cell (Figure 5.3) but no evident change was observed when 500 µL of the same solution was added to the cell containing the sensors functionalized using the non-covalent approach. Control SWCNT sensors did not show any potentiometric response at these conditions either. The standard plate count method was used in triplicate to quantify the bacteria recovered in PBS solution by this swab-based technique. The amount of bacteria recovered using the swab-based protocol was $7.3x10^5$ CFU with a standard deviation of $5.1x10^5$ CFU (5 skin samples), which represents an average recovery rate of 15% with a very high standard deviation, because the amount of recovered *S. aureus* ranged from 1.6% to 29.6% the original load. Therefore, to correlate the EMF response with the concentration of target microorganism in the PBS solution recovered from skin and introduced into the electrochemical cell, we simultaneously quantified the bacteria within that solution by plate counting. Results obtained after culturing the PBS solution with the swab-recovered bacteria demonstrated that both covalently and non-covalently prepared biosensors were exposed to *S. aureus* concentrations ranging from $2.4x10^3$ CFU/mL to $2.0x10^4$ CFU/mL in the electrochemical cell. This range is in accordance with the working range of the biosensors prepared by the covalent approach and the positive change in EMF confirmed the compatibility of the sample recovery protocol with the potentiometric analysis using this type of covalently functionalized biosensors. Also, these values were far below the limit of detection of the biosensors prepared by the non-covalent method, which explains why no potentiometric response was observed in this type of biosensor. We also carried out selectivity assays by inoculating pig skin with either *E. coli* as a gram-negative pathogen or *S. epidermidis* as a non-pathogenic gram-positive microorganism that may also be present in real skin samples. The load of bacteria inoculated into the pig skin segments and swab-based sample recovery procedure remained constant for samples with *S. aureus*, *E. coli* and *S. epidermidis*. Neither the *E. coli* nor the *S. epidermidis* showed a change in EMF when the samples were analyzed with both biosensor types. The concentration of bacteria within the electrochemical cells after inoculation with 500 µL of the solution containing the recovered microorganisms ranged between $5.6x10^2$ CFU/mL and $9.1x10^4$ CFU/mL for *E. coli* and between $3.8x10^3$ CFU/mL and $3.1x10^4$

CFU/mL for *S. epidermidis*. The absence of a response in the biosensor covalently functionalized to these two microorganisms in pig skin suggests that biosensors functionalized by the covalent approach perform well in the identification of *S. aureus* in either skin or aqueous samples. The whole procedure, including sample recovery with swabs, resuspension in buffer and inoculation into the cell takes about 2 minutes while the EMF response value achieved after inoculating with the aliquot takes less than 6 minutes. However, an increase in EMF was immediately observed after the sample was added to the electrochemical cell, so a response was achieved in real-time.

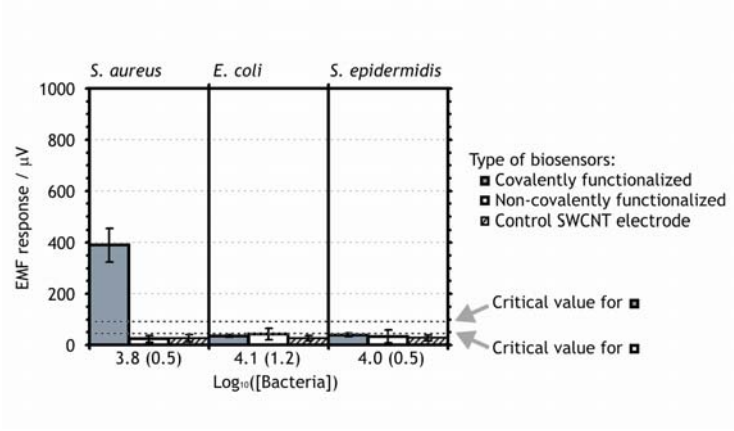

Figure 5.3. Average potentiometric response observed when biosensors were exposed to samples containing different microorganisms recovered from pig skin segments. All the skin samples were initially inoculated with $5x10^6$ CFU of the microorganism tested. Error bars are standard deviation for three different experiments. The average concentration (CFU/mL) in the electrochemical cell is given below the chart in logarithmic units (the values in parenthesis are SD, N=3).

5.2.5. Conclusions

In this chapter we have demonstrated that potentiometric biosensors based on single-walled carbon nanotubes as ion-to-electron transducers and aptamers as recognition elements are excellent biosensors for real-time detection of *S. aureus* as they improve on all the current detection methods for this pathogen. The biosensor performance parameters of two functionalization approaches were compared.

Important differences were observed between the biosensors prepared by covalently linking the aptamers to the SWCNTs by amide bonds and those prepared by the non-covalent adsorption of pyrenil-functionalized aptamers onto the nanotube sidewalls. The performance parameters depended on the functionalization approach used. Non-covalently functionalized biosensors detected the target microorganism at concentrations above 10^7 CFU/mL with a very limited working range. On the other hand, biosensors functionalized covalently detected *S. aureus* concentrations above $8x10^2$ CFU/mL, which represents a minimum detectable concentration five orders of magnitude below that of the biosensors prepared by the non-covalent approach. Biosensors prepared by the covalent method also showed a higher stability. Both biosensor types demonstrated great versatility in selectivity assays, which suggests the applicability of SWCNT/aptamer-based potentiometric biosensors in the highly selective identification of *S. aureus*. However, since the performance parameters of non-covalently functionalized biosensors are more limited, covalently functionalized biosensors are the best option in *S. aureus* detection in real samples. Finally, biosensors prepared covalently also showed many more advantages in terms of simplicity, analysis time and detection limit compared with both the standard detection methods and current state-of-the-art biosensing platforms for *S. aureus* detection. This was additionally demonstrated with the highly selective detection of *S. aureus* in human skin surrogates by a simple real-time assay that did not need require highly trained staff.

5.2.6. Supporting Information

Microorganism culturing:

Tryptic soy agar (TSA), Tryptic soy broth (TSB) and Mannitol Salt Agar (MSA) were purchased from Becton, Dickinson and Company (Sparks, U.S.A.). Lyophilized strains of *Staphylococcus aureus* (CECT 4630) and *Staphylococcus epidermidis* (CECT 231), were purchased from Colección Española de Cultivos Tipo (Valencia, Spain). *Escherichia coli* (CECT 4558) was kindly donated from the Biotechnology Department at URV (Tarragona, Spain). All bacteria strains were cultivated under the same experimental conditions, including incubation time and temperature. The bacteria lyophiles were

stored at -20 °C in glycerol/TSB medium (10% v/v) and reactivated by incubating the bacteria in 10 mL of sterile TSB at 37 °C for 24 h. The bacteria samples were then centrifuged at 6000 rpm for 15 minutes and the supernatant was discarded. The precipitate was successively washed with PBS 1.7 mM pH 7.4 following the same centrifugation conditions previously mentioned. The pellet was finally resuspended in sterile PBS 1.7 mM pH 7.4. The resulting solution (namely 10^0 solution) was eight-fold 1:10 diluted serially to give a series of 10^{-1} to 10^{-8} stock solutions of bacteria. The stock solutions were quantified in quintuplicate using the standard plate count method[5] in TSA and the same procedure was also applied to the standardization of the variable aliquots of stock solutions that were used to inoculate the samples to be analyzed. The bacteria concentration was measured in colony-forming units (CFU)/mL.

Development of the biosensors:

SWCNTs were purchased in bulk form from HeJi (Zengcheng, China) with > 90 % purity, 150 µm average length and 1.4-1.5 nm average diameter. SWCNTs were first oxidized in a quartz furnace chamber tube in order to selectively remove the amorphous carbon, under the following conditions: T = 365 °C; synthetic air flow-rate = 100 cm^3 min^{-1}; and t = 90 min. The electric contact and physical support for the SWCNT sensors consisted of a glassy carbon cylindrical rod 3 mm in diameter and 50 mm in length (HTW Hochtemperatur-Werkstoffe GmbH, Thierhaupten, Germany) covered by a Teflon jacket 6.2 mm in diameter and 40 mm in length. The surface of the glassy carbon was successively polished using 25, 1 and 0.3 µm grain size polishing alumina (Buehler, Lake Bluff, USA) before the SWCNT layer was deposited by spraying the nanotubes on the same surface. For the covalently functionalized biosensors, SWCNTs were refluxed, prior to aqueous dispersion and deposition onto the glassy carbon, in 2.6 M nitric acid for 4 h in order to carboxylate the carbon nanotubes.[34] The SWCNTs in nitric acid solution were filtered and thoroughly rinsed with water to completely remove the acid. The filtered SWCNTs were dried overnight at 80 °C. In the case of non-covalently functionalized biosensors, this acidic carboxylation step was omitted in order to use non-carboxylated nanotubes as the transducing material. Afterwards, either carboxylated or non-carboxylated SWCNTs were deposited onto one of the ends of the glassy carbon electrode depending on the biosensor functionalization procedure

to be followed. For the spraying process, we previously homogenized 25 mg of purified SWCNT in 100 mL of deionized water containing 100 mg SDS, using a tip-sonicator (amplitude 60%, 0.5 s^{-1}, Ultraschallprocessor UP200S, Dr. Hielscher, Teltow, Germany) for 30 min. Ten milliliters of the SWCNT aqueous solution were sprayed onto the exposed glassy carbon surface under a high temperature (200 °C) air blow and subsequently washed with deionized water to progressively remove the SDS. A 30 µm homogeneous layer of SWCNTs (measured with ESEM) was deposited after the spraying process. Residual SDS was finally removed selectively by heating[35]at 280 °C with an air flow rate of 100 cm^3 min^{-1} for 1 h (the Teflon jacket was temporarily removed during this step) and the SWCNT sensors were further washed with deionized water and dried overnight at 80° C.

For the covalent functionalization method, the carboxylic groups on the sidewalls of the deposited SWCNTs were activated using a solution containing 100 nmol of EDC and 25 nmol of NHS in a 50 mM MES buffer pH 5 for 30 min.[30,31] Subsequently, the electrodes were soaked overnight in 500 µL of a 1 µM NH_2-Aptamer solution that also consisted of PBS pH 7.4 (1 mM) and CTAB (0.2 mM). This well-known carbodiimide-mediated chemistry was followed to form stable amide bonds between the carboxylic moieties on the sidewalls of the SWCNTs and the primary amine spacer on the 3' end of the aptamers.

For the non-covalent functionalization approach, 25 µL of a 5 nM Pyr-Aptamer solution was deposited by drop casting on a SWCNT sensor prepared according to the procedure described in the first paragraph of this subsection. The drop casting procedure was carried out at a controlled room temperature (24 °C) in a closed system with constant humidity for 24 h to avoid total drop evaporation.

Preliminary viability tests were performed in triplicate to confirm that biosensors prepared by either method lead to workable biosensors capable of recognizing the target *S. aureus* (Figure 5.4). Both types of biosensors, non-covalently functionalized and covalently functionalized, were immersed in a vessel with 5 mL of PBS working solution with *S. aureus* at a concentration of 10^8 CFU/mL for 30 minutes under constant stirring (300 rpm) in order to allow free bacteria to be attached by the

aptamers on the biosensor surface. The biosensors were then washed with sterile deionized water for 15 minutes in a different cell to remove unbound bacteria. Finally, the tips of the biosensors were placed in contact with a TSA-containing Petri dish and incubated for 48 h at 37 °C. Parallel control assays were carried out using sensors containing a layer of SWCNTs without aptamers, following this same procedure in order to compare bacterial adherence between covalently/non-covalently functionalized biosensors and sensors without aptamer as blanks.

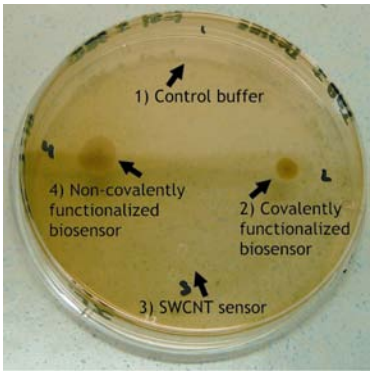

Figure 5.4. Example for the preliminary viability tests when biosensors were exposed to PBS solutions with *S. aureus* at a concentration of 10^8 CFU/mL. 1) Control PBS, without bacteria inoculated (no bacteria growth is observed). 2) *S. aureus* recovered from a covalently functionalized biosensor (growth of bacteria is observed). 3) *S. aureus* is not recovered from a SWCNT sensor without aptamer (no bacteria growth is observed). 4) *S. aureus* recovered from a non-covalently functionalized biosensor (growth of bacteria is observed).

Microscopic analysis:

Microscopic analysis of the bacteria attached to the biosensors (e.g. Figure 5.5) was carried out using a FEI Quanta model 600 (FEI Co., Inc., Hillsboro, U.S.) environmental scanning electron microscope (ESEM).

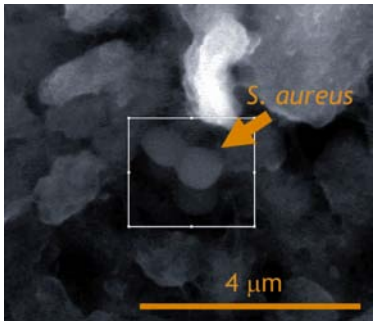

Figure 5.5. Example for a biosensor after the exposition to a 10^8 CFU/mL solution of *S. aureus*. The bacteria cells adsorbed to the biosensor's surface are indicated by the arrow. In this case, the example is for a covalently functionalized biosensor.

5.2.7. Acknowledgements

We thank S. Moreno (Department of Biochemistry, URV), S. Macho and T. Codera (Department of Analytical and Organic Chemistry, URV) for providing essential equipment and materials and for their unconditional support. This study has been supported by the Spanish Ministry of Science and Innovation (MICINN) through project grant CTQ2010-18717. G.A.Z.-G. thanks the Generalitat de Catalunya (Catalan Government) and the European Social Fund for awarding the FI-DGR fellowship.

5.3. References

[1] H.F. Chambers, F.R. DeLeo, *Nat. Rev. Microbiol.* **2009**, *7*, 629-641.

[2] A.L. Frank, J.F. Marcinak, P.D. Mangat, P.C. Schreckenberger, *Clin. Infec. Dis.* **1999**, *29*, 935-936.

[3] A.I. Hidron, J.R. Edwards, J. Patel, T.C. Horan, D.M. Sievert, D.A. Pollock, S.K. Fridkin, *Infect. Control Hosp. Epidemiol.* **2008**, *29*, 996-1011.

[4] F.D. Lowy, *N. Engl. J. Med.* **1998**, *339*, 520-532.

[5] P. Gerhardt, R.G.E. Murray, R.N. Costilow, E.W. Nester, W.A. Wood, N.R. Krieg, G.B. Philips (Eds.), *Manual of methods for general bacteriology*. American Society for Microbiology, Washington, D.C. p. 524 (**1981**).

[6] F. Farabullini, F. Lucarelli, I. Palchetti, G. Marrazza, M. Mascini, *Biosens. Bioelectron.* **2007**, *22*, 1544-1549.

[7] A. Niemz, A.M. Ferguson, D.S. Boyle, *Trends Biotechnol.* **2011**, *29*, 240-250.

[8] M.I. Pividori, A. Merkoci, S. Alegret, *Analyst* **2001**, *126*, 1551-1557.

[9] S. Tombelli, M. Minunni, A. Santucci, M.M. Spiriti, M. Mascini, *Talanta* **2006**, *68*, 806-812.

[10] P. Banerjee, A.K. Bhunia, *Biosens. Bioelectron.* **2010**, *26*, 99-106.

[11] N. Liu, Z. Gao, H.Y. Zhou, M. Yue, *Biosens. Bioelectron.* **2007**, *22*, 2371-2376.

[12] M. Yang, S. Sun, Y. Kostov, A. Rasooly, *Lab Chip.* **2010**, *10*, 1011-1017.

[13] A. Subramanian, J. Irudayaraj, T. Ryan, *Sens. Actuators B: Chem.* **2006**, *114*, 192-198.

[14] S. Balasubramanian, I.B. Sorokulova, V.J. Vodyanoy, A.L. Simonian, *Biosens. Bioelectron.* **2007**, *22*, 948-955.

[15] F.Y. Su, Y. Endo, H. Saiki, X.H. Xing, N. Ohmura, *Biosens. Bioelectron.* **2007**, *22*, 2500-2507.

[16] I. Palchetti, M. Mascini, *Anal. Bioanal. Chem.* **2008**, *391*, 455-471.

[17] D. McKenney, K.L. Pouliot, Y. Wang, V. Murthy, M. Ulrich, G. Döring, J.C. Lee, D.A. Goldmann, G.B. Pier, *Science* **1999**, *284*, 1523-1527.

[18] A. Kropec, T. Maira-Litran, K.K. Jefferson, M. Grout, S.E. Cramton, F. Götz, D.A. Goldmann, G.B. Pier, *Infect. Immun.* **2005**, *73*, 6868-6876.

[19] V. Escamilla-Gómez, S. Campuzano, M. Pedrero, J.M. Pingarrón, *Electroanal.* 2007, *19*, 1476-1482.

[20] B. Mirhabibollahi, J.L. Brooks, R.G. Kroll, *Appl. Microbiol. Biotechnol.* **1990**, *34*, 242-247.

[21] V. Escamilla-Gómez, S. Campuzano, M. Pedrero, J.M. Pingarrón, *Anal. Bioanal. Chem.* **2008**, *391*, 837-845.

[22] M.D. Morales, B. Serra, A. Guzman-Vazquez-de-Prada, A.J. Reviejo, J.M. Pingarron, *Analyst*, **2007**, *132*, 572-578.

[23] B. Serra, M. Gamella, A.J. Reviejo, J.M. Pingarron, *Anal. Bioanal. Chem.* **2008**, *391*, 1853-1860.

[24] X. Cao, S. Li, L. Chen, H. Ding, H. Xu, Y. Huang, J. Li, N. Liu, W. Cao, Y. Zhu, B. Shen, N. Shao, *Nucl. Ac. Res.* **2009**, *37*, 4621-4628.

[25] G.A. Zelada-Guillén, J. Riu, A. Düzgün, F.X. Rius, *Angew. Chem. Int. Ed.* **2009**, *48*, 7334-7337.

[26] N. de-los-Santos-Álvarez, M.J. Lobo-Castañón, A.J. Miranda-Ordieres, P. Tuñón-Blanco, *Trends Anal. Chem.* **2008**, *27*, 437-446.

[27] G.A. Crespo, S. Macho, J. Bobacka, F.X. Rius, *Anal. Chem.* **2009**, *81*, 676-681.

[28] A. Düzgün, G.A. Zelada-Guillén, G.A. Crespo, S. Macho, J. Riu, F.X. Rius, *Anal. Bioanal. Chem.* **2011**, *399*, 171-181.

[29] P. Yañez-Sedeño, J.M. Pingarrón, J. Riu, F.X. Rius, *Trends Anal. Chem.* **2010**, *29*, 939-953.

[30] D.H. Jung, B.H. Kim, Y.K. Ko, M.S. Jung, S. Jung, S.Y. Lee, H.T. Jung, *Langmuir* **2004**, *20*, 8886-8891.

[31] S.S. Wong, E. Joselevich, A.T. Woolley, C.L. Cheung, C.M. Lieber, *Nature* **1998**, *394*, 52-55.

[32] R.J. Chen, Y. Zhang, D. Wang, H. Dai, *J. Am. Chem. Soc.* **2001**, *123*, 3838-3839.

[33] W. Meyer, R. Schwarz, K. Neurand, *Curr. Probl. Dermatol.* **1978**, *7*, 39-52.

[34] C.A. Furtado, U.J. Kim, H.R. Gutierrez, L. Pan, E.C. Dickey, P.C. Eklund, *J. Am. Chem. Soc.* **2004**, *126*, 6095-6105.

[35] A.P. Washe, S. Macho, G.A. Crespo, F.X. Rius, *Anal. Chem.* **2010**, *82*, 8106-8112.

Chapter 6

Detection of bacteria in food matrices

6.1. Introduction

In ***Chapter 4***, the usefulness of the potentiometric biosensors based on carbon nanotubes and RNA aptamers was demonstrated in laboratory conditions with the detection of the gram-negative bacteria *Salmonella* Typhi. Moreover, in ***Chapter 5*** it was demonstrated that this biosensing platform can also be used for the detection of gram-positive microorganisms such as *Staphylococcus aureus*. In that chapter, it was observed that an optimum analytical performance can be achieved in this new generation of biosensors when DNA aptamers are linked to the carbon nanotubes at the transducing layer by a covalent bond. However, the eventual detection of a gram-negative pathogen with a DNA aptamer-based carbon nanotube biosensor would additionally support the universality and robustness of the technique indicating that this generation of potentiometric biosensors can be customized for the detection of virtually any pathogen.

In this chapter, we planned to expand the field of application for this new class of biosensors to real food samples. A potentiometric biosensor based on carbon nanotubes as ion-to-electron transducers and DNA aptamers as biorecognition elements is addressed against a non-pathogenic strain of *Escherichia coli* as a surrogate for pathogenic *Escherichia coli* O157:H7 in complex food matrices. In view of the benefits that covalent functionalization strategies offer in the construction of this type of sensors, the biosensor herein reported is prepared by covalently linking a DNA aptamer modified with an amine moiety at the 3' terminal to the carboxylic groups on the SWCNT sidewalls following standard carbodiimide-mediated chemistry. The pathogen is first detected using the developed biosensors in phosphate buffer solutions and the performance parameters are adequately evaluated. In order to assess the applicability of this biosensor into real samples with complex matrices, a new sample pre-treatment protocol is designed, developed, validated and deployed into real fruit juice and milk samples looking for the elimination of undesired electroactive species within the original matrix, which otherwise may lead to incorrect or inaccurate results in biosensing experiments. The pre-treatment procedure includes three steps for the consecutive filtration, washing and elution of the target

microorganism while the compatibility with the developed biosensor is evaluated by the analysis of real samples with known loads of the target bacteria. The principal importance of this part of the Thesis is the simplicity and rapidness with which the overall analytical procedure is carried out. Moreover, the simplicity afforded by this analytical method opens the possibility for high throughput real-time microbiological analysis of complex matrices, with a special focus on food and beverages, with acceptable performance parameters. Finally, with the detection of the gram-negative microorganism *Escherichia coli* using a DNA aptamer as the biorecognition element, the biosensing platform is demonstrated as a universal and robust customizable technique in pathogen detection. The content of this chapter has been published in the journal *Analytical Chemistry*, year 2010, volume 82, pages 9254-9260, and co-authored by Suryakant V. Bhosale, Jordi Riu, and F. Xavier Rius.

6.2. Real-time potentiometric detection of bacteria in complex samples

6.2.1. Abstract

Detecting and identifying pathogen bacteria is essential to ensure quality at all stages of the food chain and to diagnose and control microbial infections. Traditional detection methods, including those based on cell culturing, are tedious and time-consuming and their further application in real-samples generally implies more complex pre-treatment steps. Even though state-of-the-art techniques for detecting microorganisms enable the quantification of very low concentrations of bacteria, to date it has been difficult to obtain successful results in real-samples in a simple, reliable and rapid manner. In this report, we demonstrate that the label free detection and identification of living bacteria in real samples can be carried out in a couple of minutes and in a direct, simple and selective way at concentration levels as low as 6 colony forming units/mL (CFU) in complex matrices such as milk or 26 CFU/mL in apple juice where the pre-treatment step of samples is extremely easy. We chose *Escherichia coli* (*E. coli*) CECT 675 cells as a model organism as a nonpathogenic surrogate for pathogenic *E. coli* O157:H7 to test the effectiveness of a potentiometric aptamer-based biosensor. This biosensor uses single-walled carbon nanotubes (SWCNT) as excellent ion-to-electron transducers and covalently immobilized aptamers as biorecognition elements. The selective aptamer-target interaction significantly changes the electrical potential, thus allowing for both inter-species and inter-strain selectivity and enabling the direct detection of the target. This technique is therefore a powerful tool for the immediate identification and detection of microorganisms. We demonstrate the highly selective detection of living bacteria with an immediate linear response of up to 10^4 CFU/mL. The biosensor can be easily built and used, is regenerated without difficulty, and can be used at least 5 times with no loss in the minimum amount of detected bacteria.

6.2.2. Introduction

Microbial diseases represent the main cause of death in many countries. For example, each year, foodborne diseases cause at least 76 million illnesses in the United States alone.[1] In sanitary terms, time of analysis and reliability in the identification of pathogens are both critical, especially during outbreaks. The detection method followed to detect bacteria is essential for an early successful diagnosis. Detection methods must be able not only to detect extremely low concentrations of pathogens but also to succeed in both deploying the techniques in real-samples and identifying the particular strain of the pathogen in order to provide precise information that could be vital for an accurate diagnosis, successful prevention and correct therapeutic treatment. The whole process, however, generally requires the use of cell culturing-based methods that can take up to several days to provide specific results. The same drawback arises in microbiological control of foods/beverages and other sample types. Rapid and sensitive detection and identification of a particular bacteria strain are therefore particularly important in medical diagnosis, biotechnology and food safety.[2,3]

The classic plate count technique has been the mainstay of pathogen detection in recent decades and it is a very cheap tool; however, it takes one to three days to provide results. Available state-of-the-art bacteria-detection techniques use a wide range of approaches. Successful detection methods include the use of polymerase chain reaction (PCR),[4,5] micromechanical oscillators[6], biofunctional magnetic nanoparticles,[7,8] electrochemical-based methods (field-effect transistors,[9] amperometry,[10] square wave voltammetry[11]) and B-cell-based sensors,[12] among others. Nevertheless, most of these techniques are expensive to implement, do not have adequate limits of detection or the analyzed samples always need to be pre-treated, what makes the overall procedure in some cases extremely long and complex to deploy in "real-life". Even though there have been some recent interesting attempts to reduce the complexity of the pre-processing steps[2], most of these lead to analysis times in the order of hours and none of the reported cases is able to attain a close-to-real-time detection of pathogens in complex matrices.

Nanomaterials are excellent for developing label-free, high-sensitivity sensors. Very recently, our group has demonstrated that it is possible to use single-walled carbon nanotubes (SWCNT) in ion selective electrodes (ISEs) as ion-to-electron transducers in potentiometric analysis.[13,14] Moreover, this approach can be used not only to detect ions but also to elicit a potentiometric response in the presence of proteins and bacteria by using label-free SWCNT/aptamer-hybrid material based biosensors.[15,16] The transducing properties of this SWCNT/aptamer-hybrid material originate from the extremely high surface-to-volume ratio of the nanotubes, the material's ability to support charge transfer between the ions that surround the cell wall of the target bacteria, the SWCNT/aptamer-functionalized layer, the remarkable SWCNT double-layer capacitance and the conformational changes in the linked aptamers during the target-recognition step.[14 – 18] These reasons combined with the simplicity and portability that potentiometry offers to chemical/biological analysis in general[19] are precisely what makes SWCNT/aptamer a perfect material for detecting microorganisms;[20] that is, SWCNT/aptamer makes the detection procedure a simple task that does not require high technical skills. Nonetheless, until now, two main drawbacks remain unsolved. First, discriminating between different strains of a same pathogen has been an elusive task up to date and second, it has not been possible to successfully apply this material to identifying and detecting microorganisms in real samples because the electroactive species present in environmental and food/beverage sample solutions tend to produce either false positives or hinder the potentiometric response generated by the ionic screening of the target. In this study, it is demonstrated for the first time that a particular strain of a microorganism can be detected and identified in real samples with the minimum number of pretreatment steps, in close to-real-time and almost zero-tolerance conditions. This was achieved by developing a biosensor based on aptamers (also called aptasensor) chemically linked into a layer of previously carboxylated SWCNTs which was able to selectively detect *Escherichia coli* (*E. coli*) CECT 675 as a nonpathogenic surrogate for pathogenic *E. coli* O157:H7 in complex liquid samples such as milk and fruit juice.

Escherichia coli is one of the most common bacteria types and is a normal inhabitant of the large intestine of warm-blooded animals. Some of the strains of *E.*

coli are particularly virulent and, as is the case with *E. coli* O157:H7, cause a wide spectrum of human diseases, ranging from some types of hemorrhagic and non-hemorrhagic diarrhea, to occasional kidney failure or hemolytic uremic syndrome and death due to ingestion of contaminated food.[21,22] To demonstrate the plausibility of identifying targets using our biosensor, we assessed its selectivity against different microorganisms such as *Salmonella enterica*, *Lactobacillus casei* and a different strain of *Escherichia coli* (CECT 4558), and found that none of them gave a detectable potentiometric signal. Furthermore, in all the samples contaminated with the target microorganism and subsequently analyzed with our aptasensor, the minimum amount of bacteria detected was far below the lower limits allowed by the European Regulations 2073/2005 and 1441/2007, which demonstrates that the biosensor can be successfully used to analyze real samples with minimum pre-treatment steps, and that the change in the potentiometric response can be achieved in almost real-time.

6.2.3. Experimental section

6.2.3.1. Chemicals, aptamer and culturing media

Water used to prepare the solutions was purified through a Milli-Q system (Millipore, Madrid, Spain) and in all cases the resistivity level of purified water was 18.2 MΩ cm. The reagents sodium dodecyl sulphate (SDS), N-(3-dimethylaminopropyl)-N'-ethylcarbodiimide hydrochloride (EDC), N-hydroxysuccinimide (NHS), 2-(N-morpholino) ethanesulfonic acid (MES) and cetyltrimethylammonium bromide (CTAB), KH2PO4 and Na2HPO4 were purchased from Sigma-Aldrich (Tres Cantos, Spain). All the substances were used as received. Phosphate buffer solution (PBS) 1.7 mM pH 7.4 was prepared using a 1:100 dilution of a 0.17 M stock solution of corresponding amounts of KH_2PO_4 and Na_2HPO_4, and the pH was adjusted as required.

Tryptic soy agar (TSA) / broth (TSB), Lactobacilli MRS (deMan, Rogosa and Sharpe) agar/broth, XLD (xylose-lysine-deoxycholate) agar, MacConkey agar/broth and Luria-Bertani (LB) agar/broth were purchased from Becton, Dickinson and Company (Sparks, U.S.A.) and prepared according to indications. The *E. coli* CECT 675 binding aptamer of 81-mer with the sequence[9] 5'-GGG-AGA-GCG-GAA-GCG-UGC-UGG-GUC-GCA-GUU-

UGC-GCG-CGU-UCC-AAG-UUC-UCU-CAU-CAC-GGA-AUA-CAU-AAC-CCA-GAG-GUC-GAU-3', and -$(CH_2)_5NH_2$ modified in the 3' end was purchased from Eurogentec (London, UK). The aptamer was resuspended in MilliQ water and stored at -80°C. Quality control of the aptamer was carried out by MALDI-TOF analysis (Voyager-DE STR, Applied Biosystems, Carlsbad CA, USA) to ensure that the aptamer had not degraded before the biosensors were prepared.

The SWCNTs were purchased in bulk form from HeJi (Zengcheng, China) and had > 90 % purity, an average length of 150 μm and an average diameter of 1.4-1.5 nm. The SWCNTs were oxidized in a silica furnace chamber (365°C, synthetic air flow-rate of 100 cm^3 min^{-1} and 90 minutes) in order to selectively remove the amorphous carbon. Subsequently, SWCNTs were refluxed in 2.6 M nitric acid for 4 h to oxidize the metallic impurities remaining from the synthesis.[23] The carbon nanotubes became carboxylated after this latter oxidation step. The SWCNTs in nitric acid solution were filtered and thoroughly rinsed with water to remove the acid completely. The filtered SWCNTs were dried overnight at 80°C.

6.2.3.2. Instrumentation and materials

A FEI Quanta model 600 environmental scanning electron microscope (ESEM) (FEI Company, Inc., Hillsboro, USA) was used for the microscopic analysis. Potentiometric measurements were taken in all cases with a Keithley high-input impedance voltmeter M6514 (London, U.K.) using an Ag/AgCl/KCl (3 M) double junction reference electrode containing a 1 M LiAcO electrolyte bridge (type 6.0729.100, Metrohm AG, Herisau, Switzerland) and the SWCNT-based biosensor as the working electrode. EMF was automatically recorded to a Microsoft Excel sheet by means of an input/output add-in tool provided also by Keithley. Sterile cellulose acetate filters (13 mm diameter and 0.45 μm pore size) were purchased from GE (Brussels, Belgium).

6.2.3.3. Preparation of the aptasensor

The solid contact biosensor was made of a 50 mm-long 3 mm diameter glassy carbon cylindrical rod (HTW Hochtemperatur-Werkstoffe GmbH, Thierhaupten, Germany) covered by a Teflon jacket of 7 mm diameter. The surface of the glassy

carbon was successively polished using 25 and 1 µm grain size polishing alumina (Buehler, Lake Bluff, USA) before the SWCNT layer was deposited by spraying the SWCNT on the same surface. For the spraying process, we previously homogenized the SWCNT dispersion with a tip-sonicator (amplitude 60 %, 0.5 s^{-1}, Ultraschallprocessor UP200S, Dr. Hielscher, Teltow, Germany) for 30 minutes to prepare a solution of 25 mg of purified SWCNT dispersed in 10 mL of MilliQ water containing 100 mg of SDS. 10 mL of the SWCNT/SDS/H_2O solution was sprayed onto the exposed glassy carbon surface under a high temperature (200°C) air blow, and washed with MilliQ water to progressively remove the SDS. A 30 µm homogeneous layer of SWCNT (measured with ESEM) was deposited after the spraying process. The carboxylic groups on the sidewalls of the deposited SWCNTs were activated using a solution containing 100 nmol of EDC and 25 nmol of NHS in a 50 mM MES buffer pH 5 for 30 minutes[24]. Subsequently, the electrodes were soaked overnight in 500 µL of a 1 µM aptamer solution, which also consisted of PBS pH 7.4 (1 mM) and CTAB (0.2 mM). This well-known carbodiimide mediated chemistry was followed in order to form stable amide bonds between the carboxylic moieties on the sidewalls of the SWCNTs and the primary amine spacer on the 3' end of the aptamers.

6.2.3.4. Microorganism and culturing conditions

All the microbiological manipulations were performed using sterile material and in a microbiological safety cabinet, model BIO II A (Telstar Industrials, Terrassa, Spain). Lyophilized strains of *Escherichia coli* (CECT 675), *Salmonella enterica* (CECT 409) and *Lactobacillus casei* (CECT 4180) were purchased from Colección Española de Cultivos Tipo (Valencia, Spain), reactivated by resuspension in saline solution 0.85% and later selective enrichment in MacConkey broth (*E. coli*), XLD (*S. enterica*) and *Lactobacilli* MRS (*L. casei*) . *Escherichia coli* (CECT 4558) was kindly donated by the Biotechnology Department of the Universitat Rovira i Virgili (Tarragona, Spain). All bacteria strains were cultivated under the same incubation time and temperature conditions, but in different growth media: *E. coli* was cultivated in LB broth, *L. casei* in *Lactobacilli* MRS broth, and *S. enterica* in TSB. The bacteria samples were stored at -20 °C in glycerol / broth medium (10% v/v) and reactivated by incubating the bacteria in 10 mL of sterile broth medium at 37°C for 24 h. The bacteria samples were then centrifuged at 6000

rpm for 15 minutes and the supernatant was discarded. The precipitate was washed with PBS 1.7 mM, centrifuged again and the supernatant discarded. The pellet was then resuspended in 10 mL of sterile PBS 1.7 mM, and the resulting solution was eightfold 1:10 diluted to give a series of 10^{-1} to 10^{-8} stock solutions of bacteria. The stock solutions were quantified in quintuplicate using the standard plate count method[25] and in an appropriate culturing agar medium (TSA for *S. enterica*, LB for *E. coli* and MRS for *L. casei*), and the same procedure was also followed to standardize the variable aliquots of stock solutions that were used to inoculate the samples to be analyzed.

6.2.3.5. Analytical procedure

All the electromotive force (EMF) measurements were taken in low ionic strength buffer (1.7 mM PBS) at pH = 7.4, stirred at 300 rpm and contained in an isothermal vessel at 22±0.5 °C using 5 mL of sterile PBS before any bacteria were inoculated. The changes on the electromotive force were automatically measured at periods of 10 seconds by adding concentrations of bacteria in a stepwise mode and following changes on the recorded values. We used real samples contaminated with *E. coli* (CECT 675), control samples that did not contain any microorganism, and selectivity control samples which were contaminated with *E. coli* (CECT 4558), *L. casei* and *S. enterica* in either PBS or real-samples. The contaminated and control samples were stored at 4°C before use, and were previously inoculated with the appropriate microorganism as needed. The real samples used were semi-skimmed milk and apple juice purchased in a standard supermarket. Each analyzed sample (either stock solutions or real samples) was simultaneously evaluated following the standard plate count method in quintuplicate using the appropriate culturing agar in order to validate the method reported herein. For *E. coli*-containing samples, further confirmatory tests were carried out using the conventional method based on the MacConkey agar test.[11,25] The dilution was corrected for all the stepwise concentration experiments. Consecutive filtering of the matrix (the volume depended on the sample analyzed, but typically ranged from 1 mL to 2 mL) and washing with PBS (minimum 10 mL) was done with an on-line filtration system in order to remove the charged species that are usually present in real samples and which may interact with the carbon nanotubes, whilst also

keeping the total amount of microorganism cells on one side of the filter. Further elution of the retained cells was easily done by passing 6-8 mL of PBS in the opposite direction of the initial filtering, and the outcoming solution of eluted bacteria in PBS was injected directly into the measuring vessel in order to monitor the EMF response provided by the potentiometric system biosensor-reference electrode (see Figure 6.1). The total time of the filtration-washing-elution process remained in the order of less than one minute for PBS and juice samples to two minutes in the case of milk. After each set of inoculations and measurements, the biosensors were regenerated by dissociating the aptamers from the bacteria in 2 M NaCl for 30 min and then reconstituted by conditioning in PBS, thus leaving the aptasensor ready to record new measurements.

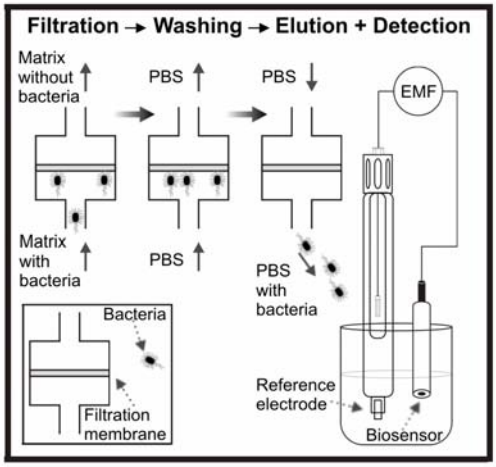

Figure 6.1. Experimental setup for the pre-treatment steps required to remove the matrix in real samples and to detect microorganisms contained therein using the potentiometric biosensor. Starting from left to right: first step, filtration of sample and matrix removal; second step, washing with PBS; third step, elution with PBS and potentiometric detection of bacteria recovered in eluate.

6.2.4. Results and discussion

Biosensors were exposed to stepwise increasing concentrations of *E. coli* CECT 675 in PBS and the EMF response was recorded as a function of time in order to assess the performance of each biosensor (sensitivity, precision, limit of detection, response time and stability) before the final deployment in real-samples (Figures 6.2 to 6.5). Under the experimental conditions, instrumental detection response (also known as critical value), measured as the average plus 3 standard deviations of the instrumental noise,[26] was 63.4 μV for all the sensors tested, so higher changes in the EMF response should be easily resolved. There was an immediate and evident change in the signal at all concentrations of the target bacteria when this was added. A quick increase in EMF was observed within the whole dynamic range as 50% of the potentiometric response was attained in the order of seconds when any concentration of *E. coli* CECT 675 was added, starting from as low as 4 CFU/mL (Figure 6.2a). Stabilization in EMF response strongly depended on the concentration. This is demonstrated by the fact that the EMF response could only be stabilized for the lowest concentration of bacteria detected (4 CFU/mL) after 120 seconds of the sample addition, whereas for higher values (e.g. 10^4 CFU/mL), the stabilization of the EMF response was rather slower and remained in the order of 10-20 minutes. Once the EMF response was reached, it was stable for at least one and a half hours at concentrations below 10^4 CFU/mL, which is enough time to perform any further analysis of bacteria in either PBS or real samples. Nonetheless, stability at concentrations above 10^4 CFU/mL dramatically decreased after inoculation because the response drifted once the maximum signal had been reached. This was possibly caused by stochastic charge transfer processes between the surface of the biosensor and the excessive amount of bacteria that is not tethered to the biosensor by means of the aptamers. This occurs when the available binding sites on the biosensor surface become over-saturated in high concentrations of the target microorganism. In any case, analysis of samples with concentrations of bacteria higher than 10^4 CFU/mL can be made but the exact amount of bacteria cannot be found. Figure 5.2 shows the calibration curve for the range of 4 to 10^4 CFU/mL. Electromotive force as a function of decade for the bacteria concentration can be approximated to a straight line model over the same calibration range and shows a dynamic range of 5

orders of magnitude. The average slope was 2.0 mV/Decade (Standard deviation = 0.8 mV/Decade) (the average value was obtained by testing three different biosensors), and the R^2 value was 0.96.

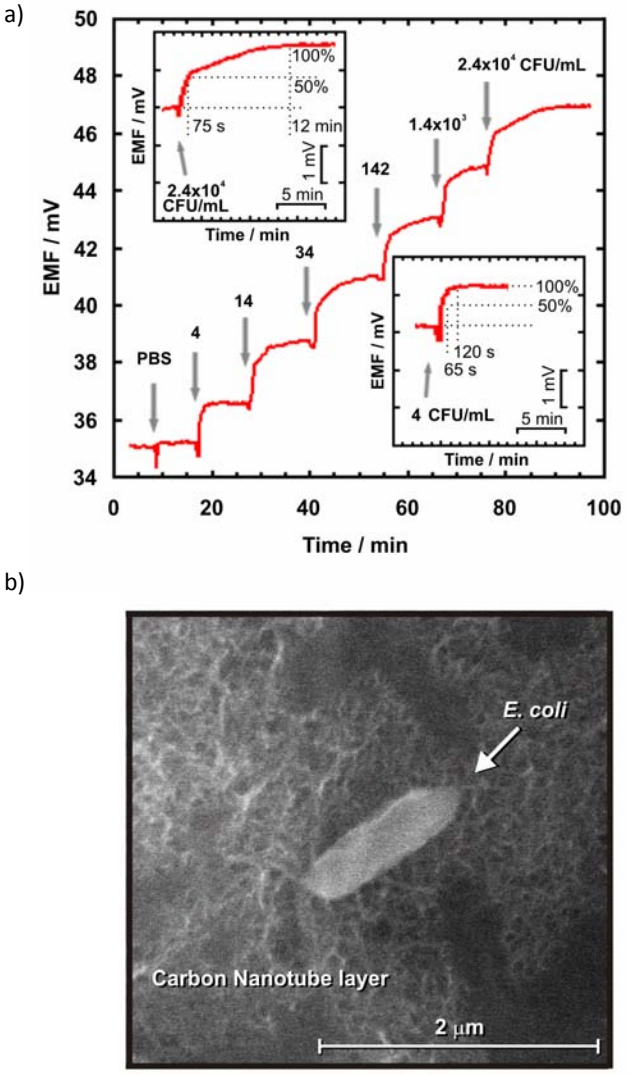

Figure 6.2. a) Performance of SWCNT biosensors functionalized with anti-*E. coli* CECT 675 RNA aptamer: EMF response exposed to stepwise increasing concentrations of *E. coli* CECT 675 as a function of time; insets show the time required to achieve 50% and 100% of the EMF response after inoculation with 4 CFU/mL (right-down) and $2.4x10^4$ CFU/mL (left-up). b) ESEM image of an *E. coli* CECT 675 cell captured on the SWCNT/aptamer.

It is interesting to note that at lower bacteria levels (see Figure 6.3 at the concentration range below $2.2x10^2$ CFU/mL) the biosensor offers a higher sensitivity and a slightly better coefficient of determination than at the whole concentration range indicated in the graph. This could be attributed to the fact that at low concentrations of bacteria there are evidently more available binding sites on the biosensor surface than at higher concentrations and thus, a higher efficiency on the binding event may be expected. However, both the linearity observed for the range 4 – $2.4x10^4$ CFU/mL and the standard deviation of the slope are still acceptable for the analytical purposes of the biosensor when the main concern is deciding whether the pathogen is present or absent in the sample analyzed, since the minimum amount of bacteria able to be detected remains unaffected.

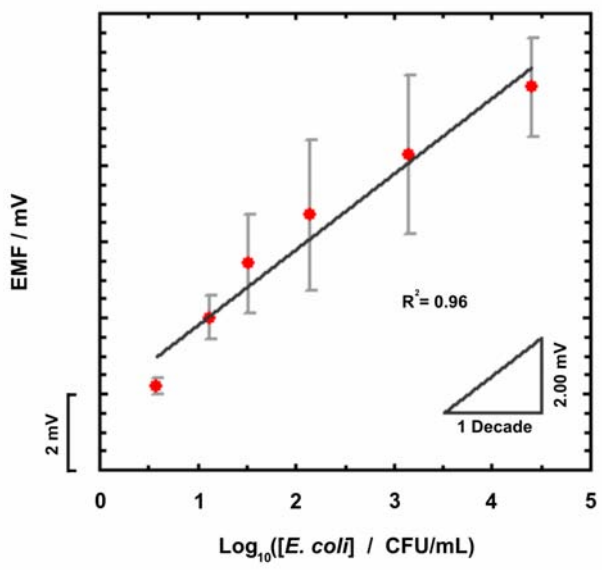

Figure 6.3. EMF response as a function of the logarithm of the *E. coli* CECT 675 concentration. The solid circles are the average potentiometric response of three different biosensors exposed to the same concentration values, the solid line is the linear regression fit, and the triangle inside represents the sensitivity of the method. Error bars indicate the minimum and maximum response values obtained with three different biosensors.

The sensor was regenerated after the assays by using an aqueous solution of 2 M NaCl to release the bacteria bound to the aptamers and by further washing with MilliQ water for 10 minutes. After the last step, the sensor was stored in PBS solution. Regenerated sensors remained practically unchanged in terms of sensitivity and limit of detection and we observed that they may be exposed to at least 5 regeneration cycles before the limit of detection and sensitivity are affected. The EMF noise of the regenerated sensors in all the cases remains, however, unaltered and does not depend on how many regeneration cycles the sensor has been exposed to.

Selectivity was tested by exposing the aptasensor to stepwise concentrations of *E. coli* CECT 4558, *L. casei* and *S. enterica*, in the same range of concentrations than the ones used for *E. coli* CECT 675 in PBS (Figure 6.4 curves 1-3). The results demonstrated that there is no cross-reactivity in either inter-species or inter-strain tests, which means that the biosensor is highly selective. Therefore, strain-specific tests for identifying bacteria could be created if the system is used to analyze real-samples. Control tests were also carried out to determine whether the potentiometric signal was due exclusively to the biosensor's bacterial recognition event and not to either unspecific interactions between the SWCNTs and the target bacteria or the leakage of adsorbed aptamers remaining from the functionalization step when the biosensors were prepared. To evaluate whether unspecific interactions led to a potentiometric response, a SWCNT electrode that had not been functionalized with the aptamer was exposed to stepwise increasing concentrations of target bacteria (*E. coli* CECT 675), starting from 0 CFU/mL up to 10^5 CFU/mL, but no response was observed (Figure 6.4 curve 4). In the same way, another control experiment assessed the possibility that the potentiometric response was generated by the release of those aptamer molecules that may be physically adsorbed onto the SWCNT walls. This test was carried out by preparing an SWCNT electrode that had previously been incubated directly in 500 µL of a 1 µM aptamer solution for 24 hours to allow the aptamer molecules to adsorb onto the SWCNT layer,[27] although the process did not include the chemical step of covalent bond formation between the carboxylic moieties of the SWCNT and the aptamer. This electrode was also exposed to increasing amounts of target bacteria and the potentiometric response was recorded in real time, but no EMF response was

obtained (Figure 6.4 curve 5). The comparison of the EMF response of the biosensor when the aptamers are covalently immobilized over the SWCNTs (Figure 6.2a) with the lack of EMF response when the aptamers are incubated overnight without linking to the SWCNTs (Figure 6.4 curve 5) clearly shows that the covalent immobilization of the aptamers on the SWCNTs assures the generation of the proper signal in our biosensor. Regeneration results presented previously in the manuscript also support this fact. According to Figure 6.4 (curves 4 and 5), both control experiments confirmed that the responses observed are caused exclusively by the binding event between the target bacteria and the aptasensor, because the EMF did not change when any of the control electrodes were exposed to target bacteria.

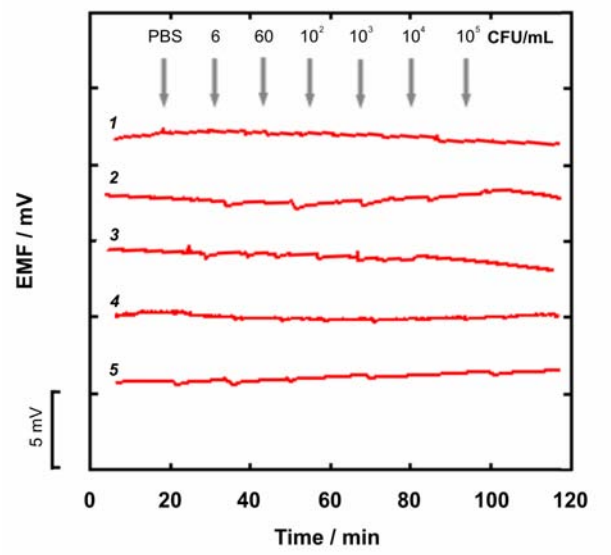

Figure 6.4. Selectivity assays and blanks: EMF response of the biosensor functionalized with aptamer exposed to *S. enterica* (***1***), *L. casei* (***2***), *E. coli* CECT 4558 (***3***); EMF response of the SWCNT electrodes exposed to *E. coli* CECT 675 (***4***) and SWCNT electrodes incubated with aptamer overnight (without functionalization) exposed to *E. coli* CECT 675 (***5***).

As in all potentiometric measurements, using the SWCNT/aptamer based biosensor to detect microorganisms in liquid samples requires control of the ionic strength of the sample, otherwise the different charged species contained in the samples may lead to a potentiometric response and false-positive results would be

produced. For example, the potentiometric response for milk and apple juice samples leads to a high jump in the potentiometric measurement if no pre-processing steps are carried out in a sample without target bacteria, as is demonstrated in Figure 6.5a and b (insets). For this purpose, we filtered the complex matrices that constitute the real samples containing microorganisms in order to separate the microorganisms from the real sample matrix. The microorganisms are further eluted in a controlled PBS medium prior to potentiometric measurement with the biosensor. The whole process of filtration, washing and elution each sample was completed within just a few minutes, as is explained in subsection ***6.2.3.5***. Control tests demonstrated that the pre-processing steps eliminate the possibilities of false-positives if applied to real samples (Figure 6.5a and 6.5b, see insets and curve 2 in both figures).

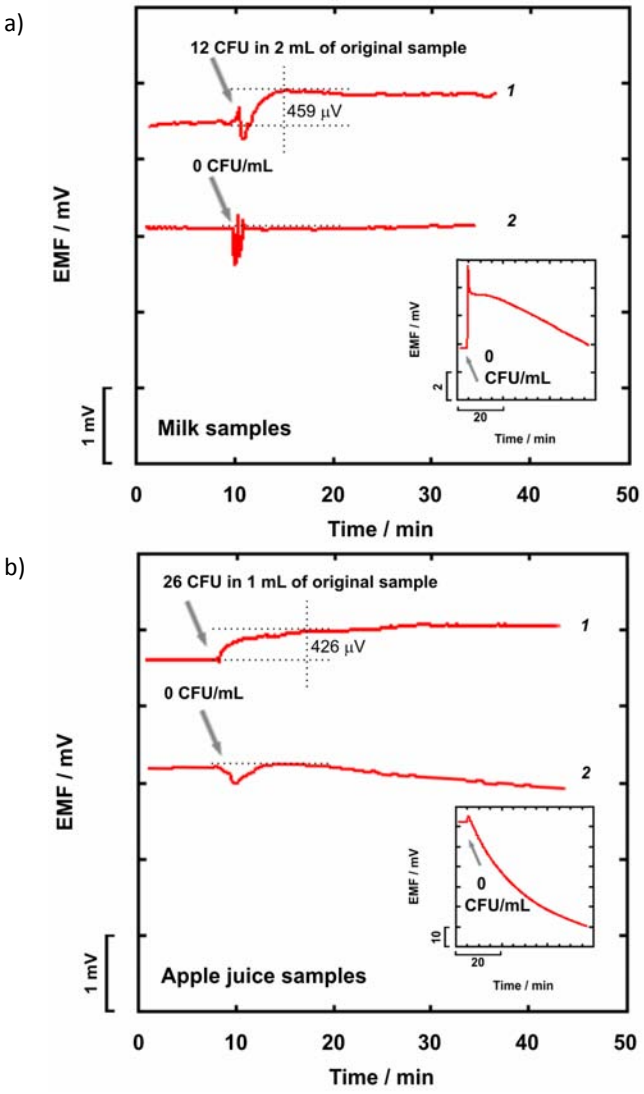

Figure 6.5. Potentiometric detection of microorganisms using aptasensors exposed to real samples (pre-treatment steps previously carried out to remove original matrix). a) Sample of milk: original matrix containing inoculated *E. coli* CECT 675 12 CFU in 2 mL of sample (***1***) and without inoculated bacteria (***2***). b) Sample of apple juice: original matrix containing inoculated *E. coli* CECT 675 26 CFU in 1 mL of sample (***1***) and without inoculated bacteria (***2***). Insets in a) and b) respectively show the potentiometric response for milk and apple juice samples if no pre-processing steps are carried out in a sample without target bacteria.

This procedure is also compatible with the selectivity of our biosensor. When this procedure is applied to real samples containing microorganisms, it is possible to differentiate between samples contaminated with *E. coli* CECT 675 and samples contaminated with other types of pathogen and, moreover, between different strains of the same pathogen type (see curve 1 in both Figures 6.5a and b, and compare with Figure 6.6). The lowest amount of bacteria detected in complex matrices was 12 CFU in 2 mL of milk (6 CFU/mL) and 26 CFU in 1 mL of apple juice, which means that the presence of target bacteria detected in real-samples can be assessed in almost zero-tolerance conditions and with close to real-time responses. According to the European Regulations 2073/2005 and 1441/2007, the concentration of *E. coli* allowed to be present in beverages must be below 1000 CFU/mL in the case of apple juice samples, and below 5 CFU/mL for milk samples.

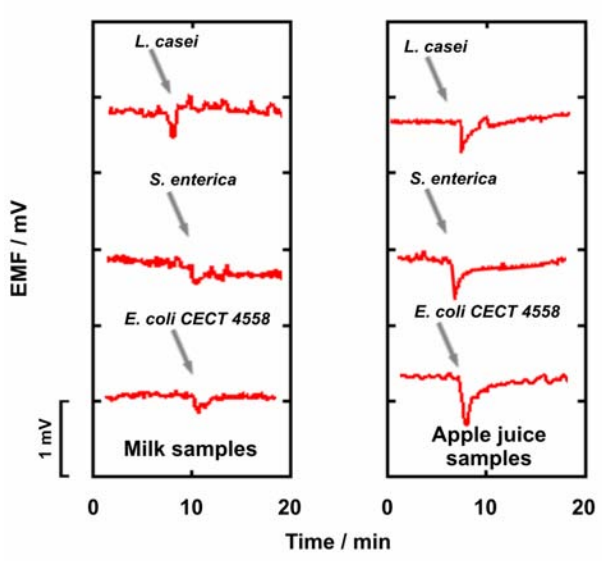

Figure 6.6. Selectivity assays in real samples (milk in left hand chart, and apple juice in right hand chart): original matrix containing 10^3 CFU/mL of the following bacteria: *L. casei* (up), *S. enterica* (center), *E. coli* CECT 4558 (down).

The previously estimated detection limit values show that our system could be successfully used to detect bacteria in complex samples at concentrations around the limit stated in the regulations. Even though the lowest amount of bacteria detected in

the case of milk is slightly above the limits established in the regulations, this limit could be lowered either by using aptamers with higher affinity towards the target bacteria or by improving the pre-processing protocols. In Chapter 4 we demonstrated that *Salmonella* could be potentiometrically detected in buffer solutions with an SWCNT/aptamer biosensor[16] based on anti-*Salmonella* Typhi Pili IVB aptamers[28] and that the corresponding limit of detection was 1 CFU/mL because of the high availability of pili on the bacteria's surface. Therefore, another approach that could increase performance at lower limits of detection would be to use aptamers synthesized against bacterial surface structures that are present in high numbers throughout the entire cell wall, for example, fimbriae, flagella or pili. It is interesting that the aptamer used in the development of our biosensor was initially isolated with the aim of detecting whole cells of *E. coli*, rather than a particular target situated on the external part of the cell wall (as in the case of anti-*Salmonella* Typhi pili aptamers, mentioned above); hence, the corresponding epitope in *E. coli* might be any surface structure that is present in low numbers or less exposed to tethering by aptamers (e.g. S-layer proteins),[29] which in turn might reduce the possibility of reaching ultra-low detection limits and be the reason why such a long stabilization time is required to achieve a 100% EMF signal (Figure 6.2a) for high concentrations of bacteria.

In order to evaluate whether the real sample-filtering/elution-of-microorganisms steps are appropriate to our purposes, we also assessed the recovery of the target microorganism. We used the standard plate count method to count the number of CFUs in equivalent filtered volumes of the same samples that we used in the potentiometric detection experiments. We observed that under these experimental conditions, the pre-processing procedure allows a recovery of 80-90% (Figure 6.7). We also observed that an eluent volume of 6 mL PBS enables a maximum recovery at low concentrations of bacteria (22 CFU/mL). Even though higher recovery rates can be obtained when the elution step is carried out with a higher volume of eluent PBS (8 mL) in samples containing higher concentrations of bacteria (240 CFU/mL), the procedure works better in real-samples when the elution volume is kept as low as possible so as not to dilute the possible low bacteria content of many unknown

samples. The same pre-treatment conditions were applied during both control and real samples.

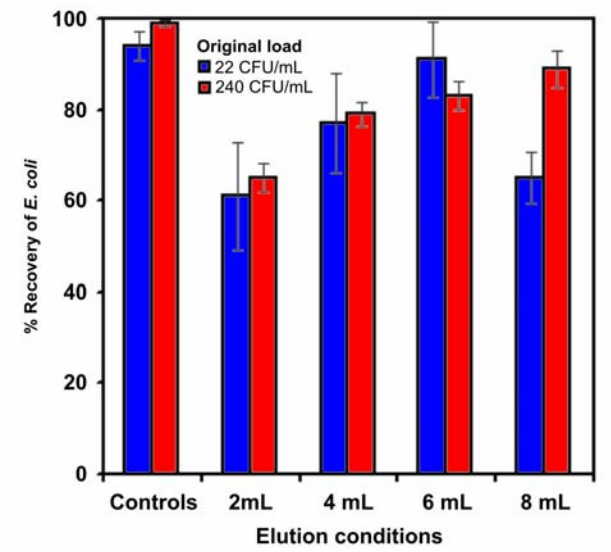

Figure 6.7. Recovery of *E. coli* CECT 675 loaded in PBS after pre-treatment steps with different elution conditions and in two different concentrations of bacteria (22 and 240 CFU/mL): Controls correspond to the bacteria detected after following the pre-treatment procedure when the filter membrane is removed from the system so as to assess the loss in recovery due to the irreversible attachment of bacteria onto the inner channels of the system. The different volumes (2, 4, 6 and 8 mL) indicated on the *x* axis represent the quantity of PBS used the in elution step of the pre-treatment process. The *y* axis represents the average % recovery performed in triplicate, compared to the initial amount of bacteria loaded. The error bars are the standard deviation (N=3). The bacteria were counted using the standard plate count method in triplicate.

The results obtained in the course of this chapter overcome many difficulties shown by other reported methods for the detection of pathogens. Available PCR-based detection methods have achieved detection limits as low as 5 CFU in a 20 minutes assay[4] and 6 CFU in 5 hours.[5] Other methods that are based on physical separation of pathogen cells using biofunctional magnetic nanoparticles and further optical counting[7] or traditional culturing[8] allow also similar limits of detection (1 to 10 CFU) in times of analysis of many hours. Electrochemical-based methods consisting of field-

effect transistors,[9] amperometric[10] and square wave voltammetric biosensors[11] have also reached low detection limits (10 to 10^3 CFU/mL) within analysis times in the order of half an hour to many hours. Even though the method reported in the present work allows limits of detection comparable to those mentioned above, our results have overcome some operational and performance parameters such as simplicity, time of analysis and selectivity. Thus, the main advantages of the method reported herein are: (i) A close to real-time analysis of real samples allowed by the fast electrochemical response observed when the bio-recognition event takes place and the very simple pre-processing steps involved in the sample pre-treatment; (ii) the ease of use and low cost of the potentiometric devices implicated in the electrochemical detection as well as the simplicity involved in the construction of the biosensor (iii) the inter-species and inter-strain selectivity observed so far are very important because they demonstrate that the identification of a particular pathogen strain could be carried out in a direct way and thus, the need of serological confirmatory tests that often require several hours or days to be accomplished might be eliminated or, in the worst case scenario, reduced.

6.2.5. Conclusions

In this chapter we have developed and deployed for the first time a potentiometric biosensor that uses carbon nanotubes chemically linked to aptamers as probes to selectively detect and identify a particular strain of *Escherichia coli* in real complex samples in a few minutes. A simple potentiometer, an on-line filtration system and a customizable aptasensor, which does not show both inter-species or inter-strain cross-reactivity, can be used in close to real-time conditions for the simple and rapid elimination of the matrix in real samples, to recover the microorganisms and to perform the on-site highly selective detection/quantitation of the target bacteria. The system displays a moderate sensitivity but the responses are clearly distinguishable from the noise. Our research demonstrates the feasibility of using potentiometry to identify microorganisms in complex matrices, because the whole system may be customized according to the pathogen to be detected, both the aptamer and the pre-treatment procedure can be selected depending on the type of

bacteria and the complexity of the matrix. This opens the door to using simple potentiometry for the immediate detection of bacteria in real samples thus simplifying the traditionally complex procedures for detecting and identifying pathogens and providing a detection technique that is easily available to almost every bio/chemical laboratory. It is necessary, however, to have the appropriate aptamer. It would be very interesting from the point of view of applying the technique to different samples to have aptamers with different selectivities in order to distinguish not only among serovars but also among different species or even families.

6.2.6. Acknowledgements

We thank Dr. Jeng-O Lee (Korea Research Institute of Chemical Technology) for helpful information provided. We also thank S. Moreno (Department of Biochemistry, URV) for providing essential equipment. This study has been supported by the Spanish Ministry of Education and Science, MEC, through the project grant CTQ2007-67570/BQU. G.A.Z.-G. thanks the Generalitat de Catalunya (Catalan Government) and European Social Fund for awarding the FI-DGR fellowship.

6.3. References

[1] P.S. Mead, L.Slutsker, V.Dietz, L.F. McCaig, J.S. Bresee, C. Shapiro, P.M. Griffin, R.V. Tauxe, *Emerg. Infect. Dis.* **1999**, *5*, 607-625.

[2] J. Durner, *Angew Chem Int. Ed.* **2010**, *49*, 1026-1051.

[3] C.A. Batt, *Science* **2007**, *316*, 1579-1580.

[4] P. Belgrader, W. Benett, D. Hadley, J. Richards, P. Stratton, R. Mariella, F. Milanovich, *Science* **1999**, *284*, 449-450.

[5] U. Dharmasiri, A.W. Małgorzata, A.A. Adams, J.K. Osiri, M.L. Hupert, T.S. Bianchi, D.L. Roelke, S.A. Soper, *Anal. Chem.* **2010**, *82*, 2844-2849.

[6] B. Ilic, D. Czaplewski, M. Zalalutdinov, H.G. Craighead, P. Neuzil, C. Campagnolo, C. Batt, *J. Vac. Sci. Technol. B* **2001**, *19*, 2825-2828.

[7] H. Gu, K. Xu, C. Xu, B. Xu, *Chem. Commun.* **2006**, 941-946.

[8] S. Liébana, A. Lermo, S. Campoy, M.P. Cortés, S. Alegret, M.I. Pividori, *Biosens. Bioelectron.* **2009**, *25*, 510-513.

[9] H.-M. So, D.-W. Park, E.-K. Jeon, Y.-H. Kim, B.S. Kim, C.-K. Lee, S.Y. Choi, S.C. Kim, H. Chang, J.-O Lee *Small* **2008**, *4*, 197-201.

[10] K. Abu-Rabeah, A. Ashkenazi, D. Atias, L. Amir, R.S. Marks, *Biosens. Bioelectron.* **2009**, *24*, 3461-3466.

[11] A.K. Deisingh, M. Thompson, *J. Appl. Microbiol.* **2004**, *96*, 419-429.

[12] T.H. Rider, M.S. Petrovick, F.E. Nargi, J.D. Harper, E.D. Schwoebel, R.H. Mathews, D.J. Blanchard, L.T. Bortolin, A.M. Young, J. Chen, M.A. Hollis, *Science* **2003**, *301*, 213-215.

[13] G.A. Crespo, S. Macho, F.X. Rius, *Anal. Chem.* **2008**, *80*, 1316-1322.

[14] G.A. Crespo, S. Macho, J. Bobacka, F.X. Rius, *Anal. Chem.* **2009**, *81*, 676-681.

[15] A. Düzgün, A. Maroto, T. Mairal, C. O'Sullivan, F.X. Rius, *Analyst* **2010**, *135*, 1037-1041.

[16] G.A. Zelada-Guillén, J. Riu, A. Düzgün, F.X. Rius, *Angew. Chem. Int. Ed.* **2009**, *48*, 7334-7337.

[17] H. Dai, *Acc. Chem. Res.* **2002**, *35*, 1035-1044.

[18] Y. Hong, D.G. Brown, *Langmuir* **2008**, *24*, 5003-5009.

[19] E. Bakker, E. Pretsch, *Angew. Chem. Int. Ed.* **2007**, *46*, 5660-5668.

[20] W. Yang, K.R. Ratinac, S.P. Ringer, P. Thordarson, J.J. Gooding, F. Braet, *Angew. Chem. Int. Ed.* **2010**, *49*, 2114-2138.

[21] B. Decludt, P. Bouvet, P. Mariani-Kurkdjian, F. Grimont, P.A. Grimont, B. Hubert, C. Loirat, *Epidemiol. Infect.* **2000**, *124*, 215-220.

[22] K.S. Venkitanarayanan, M.P. Doyle, Escherichia coli: Occurrence in: *Encyclopedia of Food Sciences and Nutrition*, Academic Press, New York, pp. 2149-2152 (**2003**).

[23] C.A. Furtado, U.J. Kim, H.R. Gutierrez, L. Pan, E.C. Dickey, P.C. Eklund, *J. Am. Chem. Soc.* **2004**, *126*, 6095-6105.

[24] D.-H. Jung, B.H. Kim, Y.K. Ko, M.S. Jung, S. Jung, S.Y. Lee, H.-T. Jung, *Langmuir* **2004**, *20*, 8886-8891.

[25] A.L. Koch, Growth measurement. In: P. Gerhardt et al. (eds.), *Manual of Methods for General Bacteriology*. American Society for Microbiology, Washington, D.C. pp. 179-207 (**1981**).

[26] L.A. Currie, *Pure Appl. Chem.* **1995**, *67*, 1699-1723.

[27] R.R. Johnson, A.T.C. Johnson, M.L. Klein, *Nano Lett.* **2008**, *8*, 69-75.

[28] Q. Pan, X.-L. Zhang, H.-Y. Wu, P.-W. He, F. Wang, M.-S. Zhang, J.-M. Hu, B. Xia, J. Wu, *Antimicrob. Agents Chemother.* **2005**, *49*, 4052-4060.

[29] D. White, Structure and function. In: *The Physiology and Biochemistry of Prokaryotes*. Oxford University Press, New York. pp. 1-36 (**2000**).

Chapter 7

Detection of parasite biomarkers in blood

7.1. Introduction

In the previous chapters, it has been demonstrated that the potentiometric biosensors based on carbon nanotubes as transducers and aptamers as biorecognition elements can be used in the detection of bacterial pathogens. Different species of bacteria, either gram-negative or gram-positive, have been targeted using RNA- and DNA-based aptamers. In the previous chapter, the biosensing platform was applied to the detection of *Escherichia coli* in complex foodstuff matrices such as fruit juice and milk. In this latter case, an online filtration system was designed. Such a system was applied for removing the sample matrix before bacteria detection in order to eliminate undesired electroactive species that may lead to inaccurate results. In this way, the target microorganisms were recovered in diluted buffer and consequently detected with the biosensor. However, sample pre-treatment steps such as matrix elimination, may not always represent a real solution. As an example, the detection of pathogen biomarkers at low concentrations may not be solved with filtration-based matrix elimination procedures because the matrix extraction may result on losses in target molecules. As a result, the direct use of the biosensing platform in the detection of smaller pathogen-related targets such as protein exoantigens in clinical samples has not been possible so far. In this chapter, we demonstrate that carbon nanotube based potentiometric aptasensors can be used in the real-time direct detection of small-sized targets, such as protein exoantigens. To address this issue, we show the application of the biosensing platform for the ultrasensitive detection of the Variable Surface Glycoprotein (VSG) from African trypanosomes as a model system for a pathogenic exoantigen protein in a clinical sample. The aptamer used in the development of the biosensor is a nuclease-resistant RNA aptamer able to recognize conserved epitopes between different VSG antigenic types. In general, we demonstrate that protein detection can be carried out in highly complex clinical samples such as in blood, without the need of a minimum sample pre-treatment. The aptasensors' insensitivity to undesired electroactive interferences is facilitated by the use of an appropriately tailored total ionic strength and potential buffer. Given the multidisciplinary nature of this part of the Thesis, as well as the biohazardous nature of the African trypanosomes,

interdisciplinary partners have been involved at different stages. The aptamer was synthesized at the research group of Prof. H. Ulrich Göringer from the Department of Genetics at Darmstadt University of Technology (Germany), based on a previous work published by his team. Prof. Göringer's team also performed the culturing of Trypanosomes as well as the extraction and purification of the VSG protein. The phlebotomy assays required for designing the ionic strength and potential buffer were performed in collaboration with Ms. Ailis Tweed-Kent from Harvard Medical School at Harvard University (USA). The content of this chapter has been submitted for publication in a peer-reviewed journal before the date of printing this Thesis, and it has been co-authored by Ailis Tweed-Kent, Moritz Niemann, H. Ulrich Göringer, Jordi Riu and F. Xavier Rius.

7.2. One-step, ultrasensitive and real-time detection of proteins in blood using potentiometric carbon-nanotube aptasensors

Detection of proteins is crucial in many areas such as clinical diagnostic, proteomic research and consumer diagnostic products as in home pregnancy tests.[1,2] The most commonly used methods rely on highly sensitive and specific label-based immunoassays.[1] However, these methods are unsuitable for high-throughput applications because they are labor-intensive, time-consuming and require highly trained staff and expensive equipment. Furthermore, an accurate quantification of the analyte is not possible and false negative results can be obtained if the target protein is not extracted from the matrix effectively.

Nanomaterials possess outstanding properties, which allow the design of simplified protein detection platforms at lower detection limits within shorter assay times than traditional techniques.[3] Biosensors that include nanostructured components as photoluminescent viral nanoparticles,[4] magnetic nanoparticle-based bio-barcodes[5] or optical resonators,[6] have demonstrated important advances in attomolar protein detection. However, electrochemical sensing techniques are preferred over others because they are fast, easy to use, cheap, small-sized and easily miniaturized. Recent work has shown that electrochemical techniques in combination with (bio)nanostructured materials as the transducer part, allow biomolecular sensing down to fM concentrations[7 – 11] and in the case of DNA detection, even down to the aM concentrations.[12] Potentiometry is one of the most common, cheapest, simplest and portable electrochemical techniques and it is widely used in the detection of ions for many decades. However, its use in label-free protein detection at concentration levels similar to those reached so far in DNA biosensing still remains a challenge.

Recently, our group demonstrated the detection of bacteria at zero-tolerance levels using single-walled carbon nanotubes (SWCNT) as ion-to-electron potentiometric transducers, and aptamers as biorecognition elements.[13] The excellent potentiometric transduction properties of SWCNT due to the extremely high

surface-to-volume ratio, the material's ability to support charge transfer between heterogeneous phases and its extraordinary double layer capacitance[14,15] combined with the quasi unlimited capability of aptamers (RNA and DNA molecules) to be tailored *in vitro* against ions, proteins, viruses and bacteria[16] convert such a platform into a tool with infinite possibilities in real-time biosensing. However, the use of aptamer-based biosensors (so-called aptasensors) has in the past been limited to non-clinical samples since the degradation of aptamers by nucleases in biofluids such as blood, severely affect their performance. Furthermore, SWCNT are highly sensitive to changes in the ionic environment at their interface as well as to redox conditions in the solution.[13,14] Therefore, it has remained unclear whether this technique could be directly used to detect traces of small-sized targets such as disease-related proteins, at clinically relevant conditions, without the need of preliminary matrix removal.[17] To address this crucial issue, here we demonstrate the real-time and ultrasensitive identification of a specific, medically relevant protein in a highly complex matrix, such as blood, using a new generation of nuclease-resistant potentiometric aptasensors without the need of any sample pretreatment facilitated by an appropriately tailored buffer. We elected the Variable Surface Glycoprotein (VSG) from African trypanosomes as a model system for a pathogenic exoantigen protein in a clinical sample. [†]

The aptasensors were prepared by covalently linking a VSG-specific nuclease-resistant aptamer to a uniform layer of carboxylated SWCNT via amide bonds formed between $–NH_2$ moieties previously introduced to the 3'-terminal of the aptamers and the –COOH groups at the SWCNT sidewalls, following standard carbodiimide-mediated chemistry. Once prepared, the aptasensors were exposed to increasing stepwise concentrations of a single antigenic VSG type in sterile buffer, while the electromotive force (EMF) between the aptasensors and a Ag/AgCl double junction reference electrode was recorded in real-time at 22±0.5 °C in stirring mode. This stage was performed to explore the aptasensor response towards the target analyte. After that, the sensor was exposed to blood samples (diluted 1:100 in buffer) containing VSG at

[†]Further information about the VSG protein can be found in subsection ***7.2.1***.

different concentrations to analyze the aptasensor response at clinically relevant conditions.[‡]

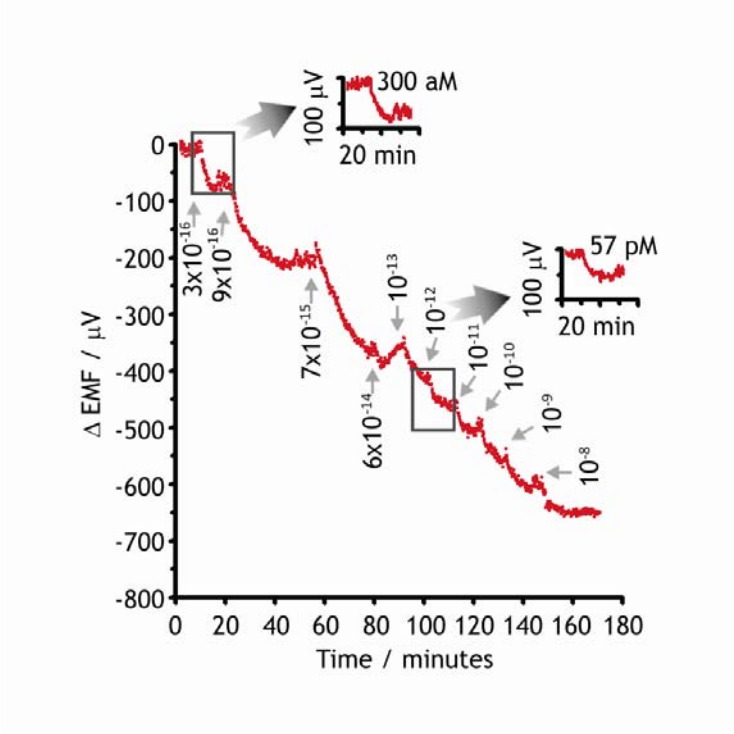

Figure 7.1. Performance of the aptasensor when exposed to increasing concentrations of VSG in buffer (ΔEMF indicates the difference between the measured EMF value and the average baseline recorded before VSG addition). Protein concentration values are in M units.

Potentiometric response in buffer was found to be distinguishable from the instrumental noise at a concentration of 300 aM (Figure 7.1). The biosensor response observed at higher concentrations showed two clearly differentiated regions termed region I and II. At VSG concentrations lower than 10 fM steep slope was measured (region I) likely the result of the high affinity interaction between the target protein and the aptamer. Above this value, the response was less pronounced (region II)

‡ Further information about the experimental procedures can be found in subsection ***7.2.1***.

presumably representing the saturation of available binding sites on the surface of the VSG protein (Figure 7.2).

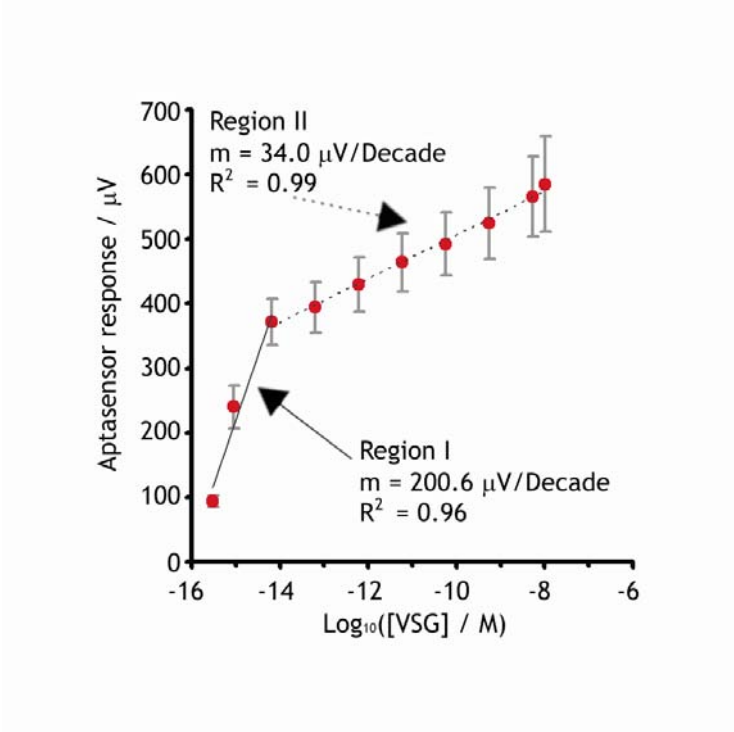

Figure 7. 2. Potentiometric response obtained for 6 different aptasensors. Solid circles are the average absolute value of ΔEMF; error bars are SD; the slope m and R^2 values for the linear approximation of regions I and II are indicated by arrows.

For simplicity, both regions can be fitted to a linear model. Importantly, both regions and their related linear approximations can be useful in either quantitative or semi quantitative assays. In any case, immediate changes in EMF were observed at all concentrations. Moreover, the aptasensors were able to distinguish between blood samples without target protein and those containing VSG at concentrations as low as 10 pM in blood (4 fM in the cell, Figure 7.3).[§]

[§] Further information about supporting results, controls, selectivity assays and assays with blood samples can be found in subsection ***7.2.1***.

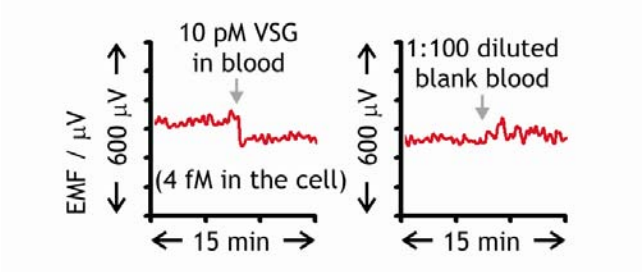

Figure 7. 3. Change in EMF for an aptasensor after addition of either 1:100 diluted blank blood or blood containing VSG.

Controls and selectivity assays demonstrated that the response is driven by the interaction between the aptasensor and the VSG.[§] Recent studies have demonstrated that the aptamers at similar conditions are ionically charged and self-assembled to SWCNT by π-π stacking interactions.[18,19] In the presence of a charged target analyte, aptamers adopt the conformational state needed to recognize the epitopes[20] and the target is consequently tethered to the nanotubes, thus, switching of the SWCNT surface charge takes place and this process results in a change of the EMF recorded.[13,14] In the case of the recognition of the negatively charged VSG protein[21] by the aptasensor, a similar behavior is therefore expected. However, further research is currently being carried out in order to unravel this trend in this type of sensors.

For many decades now, potentiometric ion-selective electrode sensing represents the preferred technique in many routine measurements of pH and ions not only in academic settings but in many production sectors. Unfortunately, the simplicity of the technique has not been exploited so far in high throughput biomolecular sensing. The technology described in this work represents a new step in protein detection due to the specific recognition capacity of the aptasensor at attomolar concentrations in real-time. The immediate identification of exoantigens in blood would open the door to real-time diagnostic assays for a wide range of diseases related to viruses, bacteria or parasite infections, but also to the rapid molecular detection of several other proteins and protein biomarkers in truly customizable protein biosensing platforms.

7.2.1. Supporting Information

7.2.1.1. The Variable Surface Glycoprotein of African Trypanosomes

American and African Trypanosomiasis are vector-borne lethal parasitic diseases that currently threaten more than 25 million people in 21 countries at the American continent and about 70 million people in 36 sub-Saharan African countries.[22] The American form, or Chagas disease, is caused by the parasite *Trypanosoma cruzi*, which is transmitted by a blood-sucking bug of the family *Reduviidae*. Human African Trypanosomiasis (HAT), also known as Sleeping sickness, is caused by the species *Trypanosoma brucei* (*T.b.*) and is transmitted by tsetse flies. HAT exists in two clinical manifestations depending on the infecting sub-species: one is chronic and latent while the other is acute and fatal. In both forms, the parasite infects blood first and at a later stage crosses the blood-brain-barrier to develop in the central nervous system.[23,24] Currently, HAT is diagnosed by microscopically examining blood, lymph node aspirate or cerebrospinal fluid either directly or after concentrating the parasites by capillary tube centrifugation, or mini-anion exchange chromatography techniques. Unfortunately, the amount of parasites in the blood can vary significantly from easily detectable 10,000 trypanosomes/mL to less than 100 trypanosomes/mL. As a result, the applied detection methods are inconvenient because they are labor-intensive, exhibit low sensitivities and depend on the individual skills of the examiner. PCR-based techniques have also been reported with promising results. However, they rely on expensive devices limiting their ample deployment, especially in low-resource settings. Other commonly used techniques are based on the detection of anti-*Trypanosoma* antibodies by ELISA, card or latex agglutination serological tests.[25,26] However, antibody-detection methods must be used with caution because antibodies persist for years after cure and as a consequence seropositive results are not necessarily related to a current infection. On the other hand, seronegativity can be due to the phenomenon of antigenic variation: *T. brucei* evades the host immune response by constantly changing its external surface composed of about 10^7 copies/parasite of a single Variable Surface Glycoprotein (VSG) type and by clearance of surface-bound antibodies through endocytosis.[27,28] VSG is a 60 kDa protein, it forms stable

homodimers that are linked to the cell membrane via a glycosylphosphatidylininositol (GPI) anchor at the C-terminal domain. VSG is slowly released into the bloodstream as an exoantigen.[29] *In vitro* it is released by shaking[30] or by detergent treatment.[31] In comparison to other cellular proteins, VSG represents a very stable protein.[32] In blood serum it has a half-life of about 189 h and thus can be used as a model polypeptide to perform biosensing experiments for the detection of exogenous proteins in blood matrices. Possibly, it may also be used as a biomarker for the diagnosis of HAT. Unfortunately, none of the above possibilities has been exploited to date because the highly polymorphic N-terminal domain at the external part of anchored VSG proteins displayed during antigenic variation, seriously limits the production of antibodies capable of recognizing different antigenic types.[33] Despite the previously mentioned structural variations between different VSG antigenic types, conserved structures remain largely inaccessible at the internal region due to the dense packing of VSGs on the parasite cell surface (Figure 7.4).

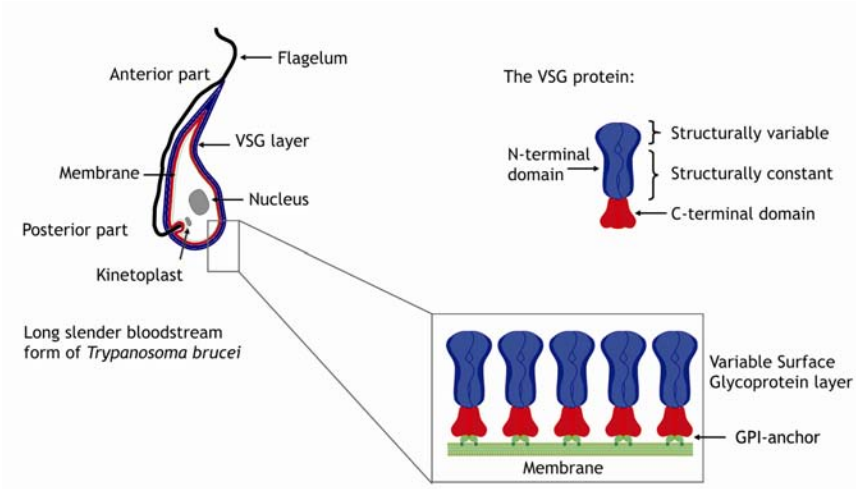

Figure 7.4. Schematic representation of the VSG protein (blue – N-terminal domain; red –C-terminal domain) attached to the *Trypanosoma brucei* membrane by means of a glycosylphosphatidylininositol (GPI) anchor.

Hence these conserved epitopes can not be reached by antibodies, but they can be reached by smaller molecules such as aptamers. We recently selected a family of RNA aptamers that bind to the structurally conserved domain of both, cell-anchored

and free (soluble) VSG with high affinity and specificity. In addition, the RNAs are highly nuclease-resistant due to the presence of 2' F-substituted C and U-nucleotides.[34] Here we demonstrate the creation of a new generation of nuclease-resistant aptasensors using the potentiometric transduction capabilities of SWCNTs in combination with the recognition capabilities of a protein-specific RNA aptamer (Figure 7.5).

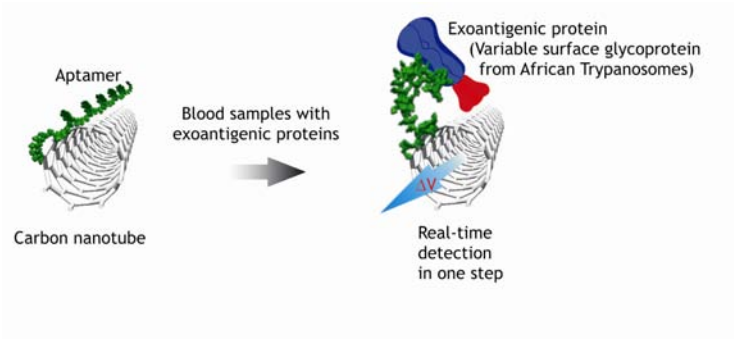

Figure 7.5. Schematic representation of the interaction between the SWCNT-aptamer hybrid material (one SWCNT included for graphic simplicity purposes), acting as recognition layer of the aptasensor, and the target VSG –the VSG variant used in the assessment of the biosensor was VSG117 from *T. b. brucei* MiTat 1.4–.

7.2.1.2. Additional results and discussion

To minimize the impact of the blood matrix, the working buffer was tailored by adjusting the osmotic pressure and the ionic strength (I) to near isotonic and physiological values with NaCl at 127 mM. The phosphate buffer (1.67 mM) was pH adjusted to the normal value of healthy human blood (pH 7.4). EDTA (ethylenediaminetetraacetic acid) was added as an anticoagulant and together with CDTA (trans-1,2-Cyclohexanediamine-N,N,N',N'-tetraacetic acid) as efficient chelating agents. In all solutions, both chelators were added to a final concentration of 2.6 mM in order to chelate normal amounts of free Ca^{2+} and other chelatable cations. Direct additions of non-diluted blood samples were performed to analyze the solutions' buffering capacity by recording EMF response profiles of different non-functionalized SWCNTs sensors when exposed to blood without VSG protein. The EMF signal

stabilized with a slow kinetic mainly driven by the redox reactive species present in blood, stochastic charge transfer between charged red blood cells and the biosensor surface as well as unspecific adsorption phenomena of charged free proteins.[35,36] $Fe(CN)_6^{4-/3-}$ was added at a low concentration of 2 mM (Total I=185 mM) to serve as an electron-transfer agent and as a redox-buffering agent. In this manner, the buffer in the electrochemical cell easily reaches the electrochemical equilibrium with the blood sample, and consequently, signal drift phenomena is substantially minimized (Figure 7.6a-b). Isotonic buffer conditions ensured that the destruction of red blood cells was minimized. Otherwise, when hypotonic buffers with low ionic strength are used, large quantities of redox-active hemoglobin can be released and undesired collateral redox reactions with $Fe(CN)_6^{4-/3-}$ could take place thereby changing the EMF and hindering any EMF response produced during the target recognition event. Higher ionic strengths (I>185 mM) were also tested, but despite the observed higher buffering capacity, the aptamer-VSG recognition was ionically screened and no response was observed when aptasensors were exposed to the VSG protein. Finally, unspecific changes in the EMF response were eliminated by diluting blank blood samples (1:100) in working buffer before the addition into the electrochemical cell (Figure 7.6a). From Figure 7.6a and 7.6b, it is evident that a low dilution of blood (1:10 to 1:1000) in buffer without $Fe(CN)_6^{4-/3-}$, prior to the addition to the electrochemical cell did not represent any real solution for the otherwise observed low stabilization time and undesired drift. Consequently, all the potentiometric measurements performed with the aim to assess the aptasensor performance in either real samples or only aqueous buffer solution where therefore carried out with $Fe(CN)_6^{4-/3-}$ at 2 mM.

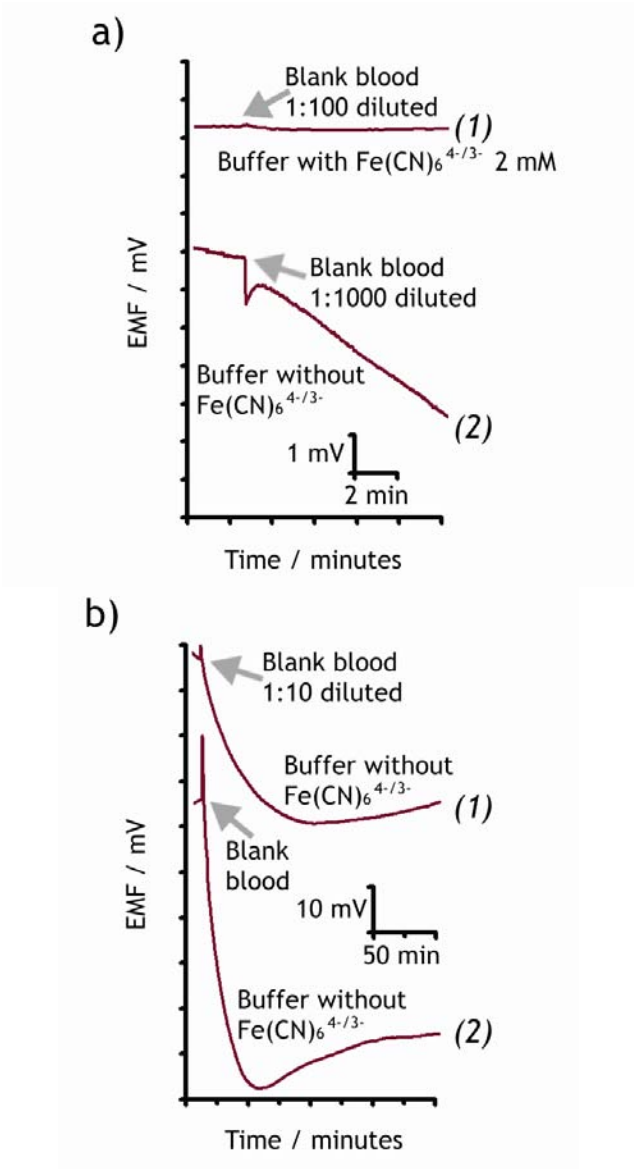

Figure 7.6. In a and b we observed the change in EMF originated in SWCNT-based sensors after the addition of blood (without VSG) at different buffer conditions (I=185 mM): (a *1*) blood 1:100 diluted in buffer with $Fe(CN)_6^{4-/3-}$ 2 mM; (a *2*) blood diluted 1:1000 in buffer solution without $Fe(CN)_6^{4-/3-}$; (b *1*) blood diluted 1:10 in buffer solution without $Fe(CN)_6^{4-/3-}$; (b *2*) non-diluted blood, added to buffer solution without $Fe(CN)_6^{4-/3-}$.

An instrumental noise (3 x standard deviation of the average noise[37]) equivalent to ±24.6 μV was observed during all experiments. This indicates that EMF changes larger than the previous value could be easily detected. At high VSG concentrations (VSG117 from *T. b. brucei* MiTat 1.4), a stable EMF response was reached after 2-5 minutes. At low VSG concentrations the response took about 10 minutes likely due to the low concentration of target molecules within the solution. Control assays were performed with non-functionalized SWCNT sensors by measuring EMF responses for increasing VSG concentrations in pure buffer. No response was observed in the concentration range 10^{-16} to 10^{-8} M (100 aM to 10 nM). Selectivity assays were carried out with different serum proteins such as thrombin, immunoglobulin G and albumin (Figure 7.7). No significant responses were measured in any case from 10^{-15} M to 10^{-9} M (fM to nM). In addition, we measured the aptasensor potentiometric response and sensitivity for several other VSG variants: *T. b. brucei* MiTat 1.2 and *T. b. brucei* AnTat 1.1 as well as *T. b. gambiense* LiTat 1.3, LiTat 1.1 and LiTat 1.6. The results were similar to those observed for the *T. b. brucei* MiTat 1.4 VSG (VSG117). The response profiles showed the characteristic separation into regions I and II, with slopes ranging between 150 to 243 μV/Log_{10}[VSG] (region I) and 18 to 54 μV/Log_{10}[VSG] in region II. Three VSG variant preparations did not produce any response: *T. b. rhodesiense* ETat 1.2, *T. b. gambiense* LiTat 1.5 and *T. evansi* RoTat 1.2. This indicates that the aptasensor is capable of recognizing isotypic VSG types and conserved epitopes between different VSG families, which is important considering the antigenic switching during the course of an infection. Variation in the EMF response slopes might be influenced by differences in the number of negative surface charges between the different VSG antigenic types or by small isomorphic differences between epitopes of different VSGs.[21,38] The inability of the aptasensor to recognize every VSG variant can be due to a variety of reasons. This includes protein denaturation phenomena during the extraction/purification of the protein as well as glycosylation differences of the different VSGs, which might mask the aptamer/protein interaction. Additional experiments are needed to unravel the origin of such a behavior at the molecular level.

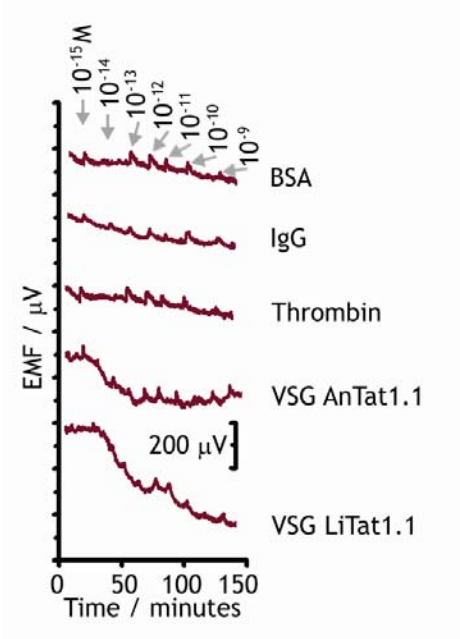

Figure 7.7. Performance of the aptasensors when exposed to stepwise increasing concentrations of different proteins in working buffer solutions: from above to below, EMF recorded when the aptasensors were exposed to increasing concentrations of bovine serum albumin (BSA), Immunoglobulin G (IgG), Thrombin, and to VSG antigenic types AnTat 1.1 and LiTat 1.3. Each small arrow in gray indicates the point of protein addition in M units.

Finally, the aptasensors were exposed to stepwise increasing concentrations of VSG in whole blood at concentrations between 1 pM to 1 nM. This corresponded to a range of VSG concentration between 10^{-16} and 10^{-12} M (aM to pM) in the electrochemical cell after addition of the previously diluted (1:100) blood samples. The sensors responded to the presence of VSG at concentration as low as 10 pM in blood (4 fM in the cell, Figure 7.8).

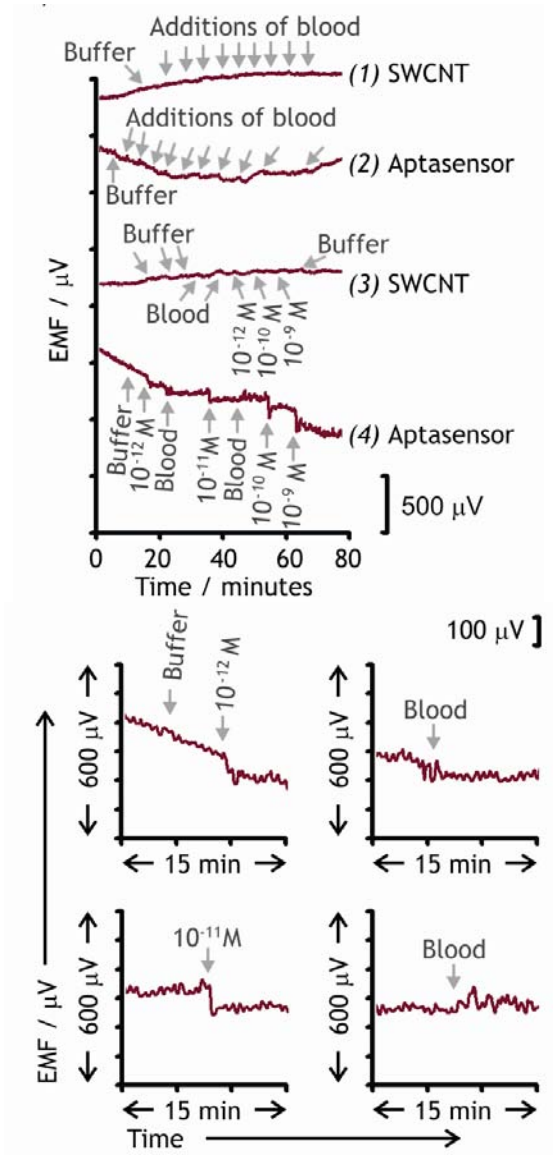

Figure 7.8. a) Change in EMF recorded for: *(1)* a SWCNT sensor without aptamer and *(2)* an aptasensor after consecutive additions of blank blood 1:100 diluted in buffer (first addition is only buffer); *(3)* a SWCNT sensor without aptamer and *(4)* an aptasensor after stepwise increasing concentrations of either 1:100 diluted blank blood or blood containing VSG at the concentrations indicated. b) Enlargement of certain segments of curve *4*. Gray arrows indicate the point of addition, the concentrations are in M units and represent the concentration of VSG in blood before diluted 1:100, blood additions are addition of blank blood 1:100 diluted.

In order to determine whether the aptasensors are capable of distinguishing between blood samples without target protein and those containing VSG, we performed consecutive additions of blood samples (diluted 1:100) either containing VSG or without target protein, into an electrochemical cell with the same aptasensor. The change in EMF observed after the addition of VSG-containing blood samples, the absence of response when samples without VSG were added (Figure 7.8a, curve *4* and Figure 7.8b) and the lack of signal in the controls (Figure 7.8a, curves *1* to *3*), confirmed that the signal was produced by the recognition of the target protein by the aptasensor. Moreover, during the same experiment, each aptasensor was able to undergo at least 10 consecutive blood sample inoculations into the electrochemical cell without loosing its capability to differentiate between those samples containing VSG from samples of blank blood (Figure 7.8). No difference was observed when different Rh blood groups were analyzed. Parallel control assays were carried out with aptasensors and SWCNT sensors exposed to successive additions of blank blood (diluted 1:100) in buffer, as well as SWCNT sensors exposed to VSG-containing blood 1:100 diluted in buffer at concentrations ranging from 1 pM to 1 nM (which corresponded to a concentration range between the aM and fM order in the electrochemical cell), but no response was recorded. The absence of EMF changes in the previous control experiments confirmed that the observed potentiometric response is driven by the interaction between the aptasensors and the target protein. The aptasensors were easily regenerated by a 1 h incubation in a 2M NaCl solution, followed by a washing step in deionized water (90 minutes). Preconditioning for the next round of usage was performed overnight in working buffer. No performance loss was observed during 5 months of use in buffer solutions. However, after the exposure with diluted blood samples, aptasensors needed to be washed thoroughly overnight after the 2M NaCl regeneration step and kept in phosphate buffer before the next round of usage in order to keep the aptasensors functional.

7.2.1.3. Experimental Section

All the solutions were prepared under sterile conditions using distilled and deionized water previously purified through a Mili-Q system (Millipore, Madrid, Spain) with a resistivity level of 18.2 MΩ cm and pH adjusted accordingly. Molecular biology

grade reagents (>99.5% purity) sodium sodium dodecyl sulfate (SDS), N-(3-dimethylaminopropyl)-N′-ethylcarbodiimide hydrochloride (EDC), N-hydroxysuccinimide (NHS), 2-(N-morpholino) ethanesulfonic acid (MES), and cetyltrimethylammonium bromide (CTAB), Bovine serum albumin (BSA), human serum Immunoglobulin G (IgG), KH_2PO_4, Na_2HPO_4, $K_3Fe(CN)_6$, $K_4Fe(CN)_6$, NaCl, ethylenediaminetetraacetic acid (EDTA) and trans-1,2-Cyclohexanediamine-N,N,N',N'-tetraacetic acid (CDTA) were purchased from Sigma-Aldrich (Tres Cantos, Spain) and used as received. Human α-thrombin was supplied by Haematologic Technologies (Vermont, U.S.A.). The working buffer solution used in the potentiometric sensing experiments (NaCl 127 mM, phosphates 1.67 mM, EDTA 2.6 mM, CDTA 2.6 mM, $K_3Fe(CN)_6$ 2mM and $K_4Fe(CN)_6$ 2mM, pH 7.4) was prepared starting from a 1:100 dilution of a 0.167 M sterile stock solution of corresponding amounts of KH_2PO_4 and Na_2HPO_4, while the appropriate amounts of NaCl, EDTA, CDTA, $K_3Fe(CN)_6$ and $K_4Fe(CN)_6$ were added under sterile conditions. Buffer solutions with different concentrations of the components previously mentioned were prepared in the same way.

The VSG-specific nuclease-resistant RNA aptamer (cl57) with the sequence 5'-GGGAGACGAUAUUCGUCCAUCAGCGCGCACCUACUGUGAUGUAGAAGUCACAGCAAGGC CCCGCUGUCCGACUGAAUU-3' was synthesized by run off *in vitro* transcription in the presence of 2'-F-uridine-5'-triphosphate and 2'-F-cytidine-5'-triphosphate (2 mM each) as previously described by Lorger et al.[34] Full length transcripts were purified in 8 M urea-containing polyacrylamide gels and subsequentially oxidized at the 3' end with $NaIO_4$ (38 mM) in 50 mM NaOAc pH 4.8, 100 mM NaCl, 10 mM $MgCl_2$. Oxidized RNA was purified by size exclusion chromatography (Sephadex G50), EtOH precipitated and resuspended in 100 mM $Na_xH_yPO_4$ pH 7.2, 150 mM NaCl. Reaction yields were ≥90% as determined by 3'end labeling using 5'-(^{32}P)-pCp and T4 RNA ligase. Oxidized aptamer preparations (approximately 10 μM) were further converted into a hydrazide derivative by overnight incubation at 4 °C in the dark with 22 mM freshly prepared adipic acid dihydrazide (ADH) in the presence of 110 mM $NaBH_3CN$ in 100 mM $Na_xH_yPO_4$ pH 7.2, 150 mM NaCl.[39] Hydrazide-derivatized RNA was purified by gel

filtration (Sephadex G50), EtOH precipitated and redissolved in 100 mM $Na_xH_yPO_4$ pH 7.4, 120 mM NaCl, 2.7 mM KCl before storage at -20 °C. Reaction yields were 73%.

The bloodstream life cycle stage of *Trypanosoma brucei brucei* was cultivated at 37 °C in HMI-9 medium[40] supplemented with 10% (v/v) heat inactivated bovine fetal calf serum. The following trypanosome strains were used: *T. brucei* Lister 427 – MiTat serodeme, variant clones 1.4 and 1.2.[41] Long slender bloodstream forms of *T. brucei* AnTat 1.1 were harvested from infected rats.[42] Soluble VSG protein was isolated essentially as described by Cross et al.[43] *T. b. gambiense* LiTat 1.1, LiTat 1.3, LiTat 1.5, LiTat 1.6, *T. b. rhodesiense* ETat 1.2 and *T. evansi* RoTat 1.2 were kindley provided by Philipp Bücher, Antwerp. All VSG isolates were purified by anion exchange chromatography and analyzed in discontinuous SDS-containing polyacrylamide gels. VSG homodimer formation was analyzed by circular dichroism (CD) spectroscopy. VSG stock solutions were stored at -80 °C before use and thawed adequately when needed. Aptamer cl57/VSG binding was tested by surface plasmon resonance[44] or alternatively by nitrocellulose (NC) filter binding using 5'-(^{32}P)-labelled cl57 preparations.

Single walled carbon nanotubes (SWCNTs) were purchased from HeJi (Zengcheng, China) with >90% purity, 150 µm average length and 1.4-1.5 nm diameter. The SWCNTs were oxidized in a silica furnace chamber (365 °C, synthetic air flow-rate of 100 cm^3 min^{-1}, and 90 min) to selectively remove the amorphous carbon. Afterwards, SWCNTs were refluxed in 2.6 M nitric acid for 4 h to both carboxylate them and oxidize the metallic impurities remaining from the synthesis.[45] The SWCNTs were then filtered and thoroughly rinsed with water to completely remove the acid and impurities. SWCNTs were finally were dried overnight at 80 °C.

The physical support and electric contact for the SWCNT electrodes consisted of a 50 mm long and 3 mm diameter glassy carbon cylindrical rod (HTW Hochtemperatur-Werkstoffe GmbH, Thierhaupten, Germany) covered by a Teflon jacket of 7 mm diameter. One of the exposed ends was successively polished with 25, 10 and 1 µm grain size polishing alumina (Buehler, Lake Bluff, U.S.A.) before the SWCNT layer was deposited on the same surface, while the other end served as a connector to the voltmeter. A 30 µm SWCNT layer (measured with a FEI Quanta 600 ESEM, from FEI Co.,

Hillsboro, U.S.A.) was deposited by spraying a dispersion of 25 mg of the purified SWCNTs with 25 mg SDS and 100 mL of Milli-Q water homogenized with a tip-sonicator for 30 minutes (amplitude 60%, 0.5 s^{-1}, Ultraschallprocessor UP200S, Dr. Hielscher, Teltow, Germany). Ten milliliters of the SWCNT prepared solution was sprayed onto the glassy carbon surface at high temperature (200 °C) and washed with sterile Milli-Q water intermittently. The residual SDS was removed by heating at 280 °C with air flow rate 100 cm^3 min^{-1} for 1 h (Teflon jacket was temporarily removed during this step).[46] Finally, the SWCNT electrodes were profusely washed with sterile Milli-Q water, dried overnight at 80 °C, sterilized with UV irradiation and stored at sterile conditions before use. The carboxylic groups on the sidewalls of the deposited SWCNTs were activated with a solution of 100 nmol of EDC and 25 nmol of NHS in 50 mM MES buffer pH 5 for 30 minutes.[47,48] The SWCNT electrodes were then incubated overnight at room temperature in 500 µL of a 1 µM RNA aptamer solution, which also included phosphate buffer solution (PBS) 1mM (pH 7.4) and CTAB 0.2 mM. This well-known carbodiimide mediated chemistry was performed in order to form stable amide bonds between the carboxylic groups on the SWCNT sidewalls and the free $–NH_2$ moieties on the 3' end of the aptamers. Aptasensors where then washed with sterile deionized water and stored at sterile conditions in PBS 1.67mM pH 7.4 until needed.

Electromotive force (EMF) measurements were automatically taken at periods of 10 s in all cases with a high-input impedance voltmeter model EMF-16 (Lawson Laboratories, Inc., Malvern, PA, U.S.A.) using a Ag/AgCl/KCl (3 M) double junction reference electrode containing a 1 M LiAcO electrolyte bridge (type 6.0729.100, Metrohm AG, Herisau, Switzerland) and the SWCNT-based electrode or aptasensor as the working electrode. Constant stirring at 300 rpm was applied during all the potentiometric measurements in an isothermal vessel at 22 ±0.5 °C containing 5 mL of sterile working buffer solution before sample addition. Analyzed protein solutions were prepared from standardized 8.33 µM stock solutions and serially diluted 1:10 in working buffer before testing the aptasensor potentiometric response towards each protein tested. Stepwise increasing concentrations of the proteins were introduced into the electrochemical cell by addition of the previously prepared serial dilution and dilution factor correction was applied accordingly. Aptasensors and SWCNT electrodes

were always preconditioned in working buffer before every electrochemical measurement. After each round of use with protein-containing aqueous solutions, aptasensors were regenerated in 2 M NaCl for 1 hour, further washed in deionized water for 90 minutes and kept in working buffer until the next use. Aptasensors exposed to blood-containing samples were regenerated in 2 M NaCl overnight under stirring mode, washed generously in deionized water and kept in PBS 1.67 mM pH 7.4 until needed again, and then, aptasensors were again preconditioned in working buffer solution before use.

Venous blood was drawn from healthy donors in blood collection tubes (Beckton, Dickinson and Company, Sparks, U.S.A.) following standard phlebotomy techniques. Blood was used as soon as collected, within the following two hours after extraction. Blood samples containing different VSG concentrations were prepared by inoculating the protein accordingly in a sterile manner and used within the same time frame previously mentioned. Ethical review board approval and donor's informed, signed consent was obtained for this study. Blank blood and blood containing VSG were diluted (1:100) in working buffer before inoculating the electrochemical cell during experiments for aptasensor performance measurements.

7.2.2. Acknowledgements

We thank S. Moreno (Department of Biochemistry, URV), S. Macho and T. Codera (Department of Analytical and Organic Chemistry, URV) and P. Bücher (Antwerp) for their unconditional support. We also thank R. Peeling (London School of Hygiene & Tropical Medicine) for kind suggestions. This study has been supported by the Spanish Ministry of Science and Innovation (MICINN) through project grant CTQ2010-18717. G.A.Z.-G. thanks the Generalitat de Catalunya (Catalan Government) and the European Social Fund for awarding the FI-DGR fellowship.

7.3. References

[1] J.M. Walker (ed.), *The protein protocols handbook*. Humana Press, Totowa NJ. 1146 p. **2002**.

[2] M. Zourob, S. Elwary, A. Turner (eds.), *Principles of bacterial detection: Biosensors, recognition receptors and Microsystems*. Springer, New York, NY. 970 p. **2008**.

[3] J. Durner, *Angew. Chem. Int. Ed.* **2010**, *49*, 1026-1051.

[4] J.-S. Park, M.K. Cho, E.J. Lee, K.-Y. Ahn, K.E. Lee, J.H. Jung, Y. Cho, S.-S. Han, Y.K. Kim, J. Lee, *Nat. Nanotechnol.* **2009**, *4*, 259-264.

[5] J.-M. Nam, C.S. Thaxton, C.A. Mirkin, *Science* **2003**, *301*, 1884-1886.

[6] A.M. Armani, R.P. Kulkarni, S.E. Fraser, R.C. Flagan, K.J. Vahala, *Science* **2007**, *317*, 783-787.

[7] C.J. Moreau, J.P. Dupuis, J. Revilloud, K. Arumugam, M. Vivaudou, *Nat. Nanotechnol.* **2008**, *3*, 620-625.

[8] A. Star, E. Tu, J. Niemann, J.-C.P. Gabriel, C.S. Joiner, C. Valcke, *Proc. Natl. Acad. Sci.* **2006**, *103*, 921-926.

[9] H.R. Byon, H.C. Choi, *J. Am. Chem. Soc.* **2006**, *128*, 2188-2189.

[10] H.-M. So, K. Won, Y.H. Kim, B.-K. Kim, B.H. Ryu, P.S. Na, H. Kim, J.-O Lee, *J. Am. Chem. Soc.* **2005**, *127*, 11906-11907.

[11] S.-J. Park, T.A. Taton, C.A. Mirkin, *Science* **2002**, *295*, 1503-1506.

[12] T. Kurkina, A. Vlandas, A. Ahmand, K. Kern, K. Balasubramanian, *Angew. Chem. Int. Ed.* **2011**, *50*, 3710-3714.

[13] G.A. Zelada-Guillén, J. Riu, A. Düzgün, F.X. Rius, *Angew. Chem. Int. Ed.* **2009**, *48*, 7334-7337.

[14] P. Yañez-Sedeño, J.M. Pingarrón, J. Riu, F.X. Rius, *Trends Anal. Chem.* **2010**, *29*, 939-953.

[15] A. Düzgün, G.A. Zelada-Guillén, G.A. Crespo, S. Macho, J. Riu, F.X. Rius *Anal. Bioanal. Chem.* **2011**, *399*, 171-181.

[16] S. Tombelli, M. Minunni, M. Mascini, *Biosens. Bioelectron.* **2005**, *20*, 2424-2434.

[17] G.A. Zelada-Guillén, S.V. Bhosale, J. Riu, F.X. Rius, *Anal. Chem.* **2010**, *82*, 9254-9260.

[18] W. Yang, K.R. Ratinac, S.P. Ringer, P. Thordarson, J.J. Gooding, F. Braet, *Angew. Chem. Int. Ed.* **2010**, *49*, 2114-2138.

[19] R.R. Johnson, A.T.C. Johnson, M.L. Klein, *Nano Lett.* **2008**, *8*, 69-75.

[20] B. Bouvier, K. Zakrzewska, R. Lavery, *Angew Chem. Int Ed.* **2011**, DOI: 10.1002/anie.201101417.

[21] P. Rautenberg, E. Reinwald, H.-J. Risse, *Mol. Biochem. Parasitol.* **1981**, *4*, 129-138.

[22] World Health Organization, WHO, **2010**:
a) http://www.who.int/mediacentre/factsheets/fs259/en/
b) http://www.who.int/mediacentre/factsheets/fs340/en/

[23] K. Vickerman, *Br. Med. Bull.* **1985**, *41*, 105-114.

[24] D. Kruel, *Trypanosomiasis*. Infobase Publishing, New York NY. 134 p. **2007**.

[25] F. Chappuis, L. Loutan, P. Simarro, V. Lejon, P. Büscher, *Clin. Microbiol. Rev.* **2005**, *18*, 133-146.

[26] J.E. Rosenblatt, *Clin. Infect. Dis.* **2009**, *49*, 1103-1109.

[27] M. Engstler, T. Pfohl, S. Herminghaus, M. Boshart, G. Wiegertjes, N. Heddergott, P. Overath, *Cell* **2007**, *131*, 505-515.

[28] M.C. Field, M. Carrington, *Nat. Rev. Microbiol.* **2009**, *7*, 775-786.

[29] B.G.F. Weitz, *Nature* **1960**, *185*, 788-789.

[30] E. Reinwald, P. Rautenberg, H.J. Risse, *Exp. Parasitol.* **1979**, 48, 384-397.

[31] M.L. Cardoso de Almeida, M.J. Turner, *Nature* **1983**, *302*, 349-352.

[32] R. Bülow, C. Nonnengässer, P. Overath, *Mol. Biochem. Parasitol.* **1989**, *32*, 85-92.

[33] A. Schwede, N. Jones, M. Engstler, M. Carrington, *Mol. Biochem. Parasitol.* **2011**, *175*, 201-204.

[34] M. Lorger, M. Engstler, M. Homann, H.U. Göringer, *Eukaryot. Cell* **2003**, *2*, 84-94.

[35] W. Simon, D. Ammann, P. Anker, U. Oesch, D.M. Band, *Ann. NY Acad. Sci.* **1984**, *428*, 279-285.

[36] M.Sh. Khubutiya, A.K. Evseev, V.A. Kolesnikov, M.M. Goldin, A.D. Davydov, A.G. Volkov, A.A. Stepanov, *Russ. J. Electrochem.* **2010**, *46*, 537-541.

[37] L.A. Currie, *Pure Appl. Chem.* **1995**, *67*, 1699-1723.

[38] T. Souto-Padrón, *An. Acad. Bras. Cienc.* **2002**, *74*, 649-675.

[39] G.T. Hermanson, *Bioconjugate techniques*. Academic Press, Oxford, UK. 1323 p. **2008**.

[40] H. Hirumi, K. Hirumi, *Parasitol. Today* **1994**, *10*, 80-84.

[41] G.A.M. Cross, *Parasitology* **1975**, *71*, 393-417.

[42] F. Michiels, G. Matthyssens, P. Kronenberger, E. Pays, B. Dero, S. Van Assel, M. Darville, A. Cravador, M. Steinert, R. Hamers, *EMBO J.* **1983**, *2*, 1185-1192.

[43] G.A.M. Cross, *J. Cell. Biochem.* **1984**, *24*, 79-90.

[44] M. Brecht, M. Niemann, E. Schlüter, U.F. Müller, K. Stuart, H.U. Göringer, *Mol. Cell.* **2005**, *17*, 621-630.

[45] C.A. Furtado, U.J. Kim, H.R. Gutierrez, L. Pan, E.C. Dickey, P.C.J. Eklund, *J. Am. Chem. Soc.* **2004**, *126*, 6095-6105.

[46] A.P. Washe, S. Macho, G.A. Crespo, F.X. Rius, *Anal. Chem.* **2010**, *82*, 8106-8112.

[47] D.H. Jung, B.H. Kim, Y.K. Ko, M.S. Jung, S. Jung, S.Y. Lee, H.T. Jung, *Langmuir* **2004**, *20*, 8886-8891.

[48] S.S. Wong, E. Joselevich, A.T. Woolley, C.L. Cheung, C.M. Lieber, *Nature* **1998**, *394*, 52-55.

Chapter 8

Conclusions (English)

Conclusions (Català)

8.1. Conclusions

The aim of this Thesis was to demonstrate for the first time that potentiometric biosensors based on carbon nanotubes as ion-to-electron transducers and aptamers as biorecognition elements could be used in the real-time detection of pathogens and related biomolecules. In order to demonstrate that this new generation of aptamer based biosensors could be customized for the detection of different pathogens and related biomolecules, four different biosensors were prepared using different aptamers, addressed against their corresponding specific pathogenic targets: *Salmonella* Typhi and *Escherichia coli* as gram-negative bacteria models, *Staphylococcus aureus* as a gram-positive bacteria example and trypanosomal variable surface glycoprotein as a model for the detection of pathogenic exoantigen proteins. Detection of the corresponding targets was successful in all the cases studied and their performance parameters were estimated.

The proof of concept of the sensing capabilities of the hybrid material carbon nanotubes-aptamers was demonstrated by the real-time detection of *Salmonella* Typhi in phosphate buffer solutions. It was also demonstrated that this hybrid material is a powerful tool with outstanding capabilities in the direct and selective detection of microorganisms in real-time at very low concentrations. In this case, the biosensor was addressed towards the type IV B pili, a protein externally anchored to the surface of the microorganism. The biosensors prepared with the selected aptamer provided excellent analytical performance parameters. In *Chapter 4*, the door to simpler microbiological analysis methods without the need of highly skilled staff was also opened.

Different functionalization methods were compared in terms of biosensor performance parameters with the selective detection of *Staphylococcus aureus* in phosphate buffer solutions (*Chapter 5*). Carbon nanotubes were functionalized with aptamers following two different approaches: 1) non-covalent linkage of drop-casted pyrenil-modified aptamers onto the external walls of the nanotubes and 2) covalent bond formation between amine-modified aptamers and carboxylic groups previously

introduced by oxidation at the ends of the nanotubes. Very important differences were observed in the performance of the biosensors depending on the functionalization approach followed. Biosensors prepared using the covalent linkage method exhibited lower detectable bacteria concentrations, lower sensitivities and higher mid-term stabilities than those values achieved when biosensors were prepared by the non-covalent approach. Therefore, **aptamer/carbon nanotube based potentiometric biosensors display more advantages in terms of performance parameters when are prepared by the covalent method, while those prepared following the non-covalent approach lead to biosensors with important performance limitations**. Finally, the analysis of freshly excised pig skin contaminated with the pathogen opened the possibility for aptamer/carbon nanotube based potentiometric biosensors to be used as a tool for the real-time detection of *Staphylococcus aureus* in human skin.

A rapid and simple protocol for the recovery of pathogens from foodstuff samples was developed in *Chapter 6*. The protocol was validated and tested with real complex food matrices such as fruit juice and milk. Additionally, **its compatibility with aptamer/carbon nanotube based potentiometric biosensors was demonstrated by the detection of a nonpathogenic strain of *Escherichia coli* as a surrogate for pathogenic *Escherichia coli* O157:H7**. The detection was achieved with excellent intra and inter strain selectivity. The whole analytical procedure could be carried out in close to real-time conditions due to the simple and rapid elimination of the matrix in real samples and the subsequent on-site highly selective detection/quantitation of the target bacteria. This chapter opened the possibility for high throughput real-time microbiological analysis of complex matrices with a special focus on foodstuff.

The real-time identification of ultra low concentrations of a particular protein in highly complex matrix conditions such as blood was demonstrated in a one-step process without observing cross-reactivity with other proteins (*Chapter 7*). A carbon nanotube potentiometric biosensor based on aptamers targeted against trypanosomal Variable Surface Glycoprotein (VSG) was designed, developed and validated with the detection of VSG as a model for pathogenic exoantigens in clinical samples. A total ionic strength and potential adjustment buffer (TISPAB) was adequately designed, tailored and used to eliminate undesired blood matrix effects with the purpose of

demonstrating that the aptamer/carbon nanotube biosensing platform can also be used in protein identification within highly complex matrices in a straightforward way and without the need of complicated sample pre-treatment procedures. Moreover, in this chapter, the possibility to use VSG as a potential biomarker in Human African Trypanosomiasis and the potential use of this aptamer/carbon nanotube based biosensing platform as a powerful tool in proteomic research and disease diagnostics was shown.

This new generation of solid-state potentiometric aptasensors based on the hybrid material aptamer/carbon nanotubes exhibits many advantages. The possibility to customize the biosensing platform for the detection of different targets by an adequate incorporation of the suitable aptamer sequence is a clear advantage over currently available protein and pathogen biosensing platforms. Moreover, the high sensitivity of the biosensors originated by the extraordinary transducing properties of carbon nanotubes as well as the real-time detection of the aptamer-target binding event are in combination, the most important added value that this platform can provide to the current repertoire of available biosensing techniques. Furthermore, the requirement of a minimum sample pretreatment simplifies both the bacteria and protein detection processes. However, the most important strength of this biosensing platform is that simple positive/negative tests can be carried out at very low concentrations of either protein or bacteria and without cross reaction with other targets. The ease with which measurements are taken in potentiometric analysis opens the door to the detection of bacteria and protein in real time as easy as measuring the pH value.

However, this potentiometric biosensing platform exhibited some limitations and drawbacks. The sensing capability for each individual biosensor depended on the success of several critical steps. As an example, an appropriate deposition of the carbon nanotube transducing layer on the surface of the supporting electrode was a challenging step that depended on individual skills. In the case that the nanotube layer was not adequately deposited, leaching of carbon nanotubes present on the more external layers would represent a serious limitation for aptamer-functionalized sensors since the recognition layer may be lost after the functionalization step. Additionally,

the functionalization procedure depended on technical skills, such as the adequate preparation of the solutions involved during the functionalization steps or the adequate management of materials. Therefore, the rate of functional biosensors has remained variable so far and depended on the technical skills exhibited during the preparation of the sensors.

The instrumental response of the biosensors is high enough to be differentiated from the noise level; however, the sensitivity of the devices is very low when compared to the Nernstian response of the 'classical' potentiometric ion-selective electrodes. This is due to the completely different sensing mechanism that applies to each type of sensor. While an equilibrium system is established between the two immiscible layers (polymeric membrane/water sample) in ISEs, a change of the electrical charges at the surface of the carbon nanotubes during the target recognition event is the origin of the EMF in our sensors. The fact that the EMF signal is driven by the charges at the target's surface forces to maintain the ionic strength of the test solution under strict control, otherwise, false positive results may occur.

The sensors are basically designed to be of a single use. They are regenerable but they are not reversible (i.e. they cannot be used successively to test different samples containing decreasing target concentrations). As a consequence, the individual sensors cannot be calibrated. The calibration should be achieved at the batch level as long as the reproducibility in the performance characteristics of the sensors developed is high enough.

The aptamers have been demonstrated to be very selective recognition elements. Depending of the purpose of the analysis, this can be an enormous benefit or a disadvantage. For instance, it is a benefit when testing a single serovar of a bacterial species but can be a drawback when we are interested in detecting the presence of microorganisms at the species or even genus level. In this latter case, the simultaneous use of several aptamers, isolated considering the different species –and serovars- should be considered.

The cost of the aptamer synthesis was additionally, a serious limitation. As an example, 1 µmol of a RNA oligomer of about 50-100 bases may cost between 500-1600

euro according to the year 2011 market prices. This factor is critical, especially when the functionalization of nanotubes with aptamers yields to a low rate of functional biosensors. However, the exponential increase on the number of patents and published scientific articles related to aptamers observed since the year 2002 (Scheme 8.1) may be translated into a decrease on market prices in a future. This same phenomenon was observed in recent years with carbon nanotubes, which can be nowadays acquired at reasonable prices.

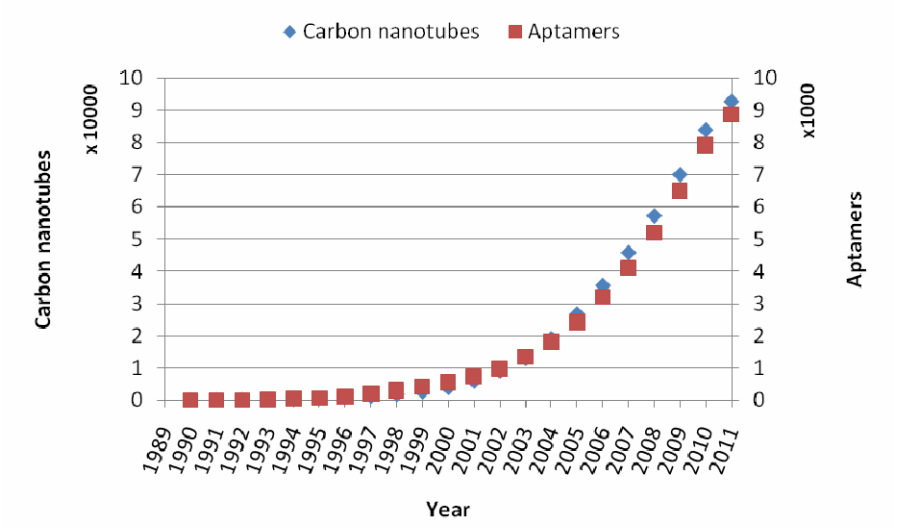

Scheme 8.1. Patents and scientific articles published on the topics aptamer and carbon nanotubes between the years 1990 and 2011.[1]

Biosensor miniaturization would represent an opportunity area for improving this new generation of aptamer-based potentiometric biosensors in a near future. The advantages of miniaturization are evident in terms of cost, since a less amount of

[1] Search performed with Scifinder Scholar (R) on the research topics indicated in Scheme 8.1 as of August 2011.

aptamers and nanotubes would be therefore needed. As an example, our group is currently developing the first examples of single-use potentiometric sensors in a miniaturized planar format. The combination between the aptasensor technology and the reduced planar format of potentiometric sensors may be translated into single-use potentiometric aptasensors in a future, thus eliminating the need of aptamer regeneration steps in pathogen and protein detection. However, the possible repercussions on biosensor performance when the sensor surface is dramatically reduced have not been explored so far.

Finally, the possibility to expand the biosensing platform for the detection of other targets than bacteria or proteins is a very interesting research area for the future. As an example, the real-time detection of whole infectious agents such as viruses or parasites would represent a very important advance in pathogen biosensing.

8.2. Conclusions

L'objectiu d'aquesta Tesi ha estat demostrar per la primera vegada que els biosensors potenciomètrics basats en nanotubs de carboni com a transductors ió-electró i aptàmers com a elements de reconeixement biomolecular poden ser utilitzats per a la detecció immediata de patògens i biomolècules relacionades. Per tal de demostrar la versatilitat d'aquesta nova generació de biosensors, es van preparar quatre biosensors diferents utilitzant distints aptàmers capaços de reconèixer de forma específica diferents objectius patogènics: Com a models de bacteris gramnegatius es van detectar la *Salmonella* Typhi i l'*Escherichia coli*, mentre que el *Staphylococcus aureus* va ser utilitzat com a exemple de bacteri grampositiu i les glicoproteïnes variables de superfície provinents de tripanosomes africans van ser usats com a model en la detecció de exoantígens patogènics. La detecció de aquests quatre objectius va ser duta a terme exitosament mitjançant els biosensors desenvolupats i els corresponents paràmetres de qualitat van ser estimats.

La prova del concepte de les capacitats sensores del material híbrid aptàmer/nanotubs de carboni va ser duta a terme amb la detecció en temps real del bacteri *Salmonella* Typhi en solucions tamponades. També es va demostrar que el material híbrid és una eina prometedora en la detecció selectiva de microorganismes en temps real a concentracions molt baixes. En aquest cas el biosensor es va emprar pel reconeixement del pili tipus IV B, una proteïna ancorada a la part externa de la superfície del microorganisme. En el *Capítol 4*, es va obrir la porta a mètodes d'anàlisi microbiològic més simples, reduint la necessitat de personal altament qualificat.

Diferents mètodes de funcionalització de la capa transductora de nanotubs de carboni van ser explorats mitjançant la detecció selectiva de *Staphylococcus aureus* en solucions tamponades (*Capítol 5*). Els nanotubs de carboni van ser funcionalitzats amb aptàmers seguint dos mètodes diferents: 1) Mitjançant enllaç no covalent dels aptàmers prèviament modificats amb un grup pirenil sobre la capa de nanotubs i 2) Mitjançant enllaç covalent dels aptamers als nanotubs de carboni mitjançant els grups carboxílics dels nanotubs i grups amina introduïts prèviament als aptàmers. Es va observar diferències molt importants en els paràmetres de qualitat analítica dels

biosensors segons el tipus de funcionalització emprada. Els biosensors funcionalitzats de manera covalent van detectat concentracions mesurables de bacteri més baixes, sensibilitats més baixes i estabilitats més altes que els corresponents valors observats a l'emprar biosensors funcionalitzats de manera no covalent. Per tant, **els biosensors basats en nanotubs de carboni i aptàmers presenten molt més avantatges respecte als paràmetres de qualitat si el mètode de funcionalització elegit és el covalent. Per l'altra banda, els biosensors funcionalitzats de manera no covalent presenten serioses limitacions analítiques**. Finalment, els biosensors van ser provats amb mostres contaminades de pell de porc amb la qual cosa es va poder obrir la possibilitat de fer l'ús d'aquest biosensor com a una eina de detecció en temps real de el *Staphylococcus aureus* en pell humana.

Al *Capítol 6* **es va desenvolupar un protocol molt simple i ràpid per a la recuperació i detecció de patògens en mostres alimentàries**. Aquest protocol va ser validat i provat amb mostres d'aliment complexes com a suc de fruita i llet. Addicionalment, **la compatibilitat del mètode amb els biosensors potenciomètrics basats en aptamers i nanotubs de carboni va ser demostrada mitjançant la detecció de una variant no patògena de l'*Escherichia coli* usada com a substitut del bacteri altament tòxic *Escherichia coli* O157:H7**. La detecció del bacteri objectiu va ser duta a terme amb un excel·lent grau de selectivitat intra i inter espècie. Aquest procediment analític pot ser dut a terme quasi en temps real a causa de la ràpida eliminació de la matriu de les mostres reals i la conseqüent detecció selectiva del bacteri. Aquest capítol va obrir la possibilitat d'analitzar mostres alimentàries complexes amb un alt rendiment i de manera immediata.

La identificació en temps real de una proteïna que es troba en molt baixes concentracions en mostres que tenen una matriu altament complexa com la sang va ser demostrada amb un procés de detecció d'un sol pas i sense reactivitat creuada amb altres proteïnes (*Capítol 7*). Es va dissenyar i desenvolupar un biosensor potenciomètric basat en nanotubs de carboni i aptàmers seleccionats per al reconeixement de la glicoproteïna variable de superfície de tripanosomes africans. El biosensor es va validar amb la detecció de la proteïna com a model d'exoantígen en mostres clíniques. Es va dissenyar i ajustar una solució tampó de força iònica i

potencial determinats amb el propòsit de demostrar que la plataforma de detecció basada en nanotubs de carboni i aptàmers pot ser utilitzada per a la detecció de proteïnes contingudes dins de matrius molt complexes de una manera molt simple i sense la necessitat de processos complicats per al tractament previ de la mostra. Així mateix, en aquest capítol, es va obrir la possibilitat per a l'ús de la glicoproteïna variable de superfície com a un marcador biològic de la tripanosomiasis humana africana i a més, es va obrir també l'ús potencial d'aquesta plataforma de detecció basada en nanotubs de carboni i aptàmers dins de la recerca proteòmica i el diagnòstic de malalties.

Aquesta nova generació de sensors potenciomètrics en estat sòlid basats en el material híbrid aptàmer/nanotubs de carboni presenta molts avantatges. Un clar avantatge sobre altres plataformes de detecció de patògens i proteïnes actualment disponibles és la possibilitat d'adaptar aquesta plataforma a la detecció de diferents analits mitjançant la incorporació de aptàmers amb la seqüència adequada. A més, l'alta sensibilitat dels biosensors originada per les extraordinàries propietats dels nanotubs de carboni com a transductors en combinació amb la detecció dels esdeveniments de reconeixement aptàmer/analit en temps real són el màxim valor afegit que aquesta plataforma ha contribuït al repertori actual de tècniques de biodetecció. Addicionalment, els mínims requeriments de pretractament de mostra simplifica enormement tant la detecció de bacteris com la detecció de proteïnes. No obstant això, la major fortalesa d'aquesta plataforma de biodetecció radica en que es poden dur a terme assajos simples de presència/absència de l'analit a concentracions molt baixes per a la detecció de bacteris i proteïnes sense que s'observi cap reacció creuada amb interferents. La facilitat amb la qual es fan les mesures en l'anàlisi potenciomètric obre la porta a la detecció de bacteris i proteïnes en temps real i d'una forma tan fàcil com mesurar el pH.

No obstant això, aquesta plataforma de biodetecció ha presentat limitacions i desavantatges. La capacitat sensora individual de cada biosensor va dependre de l'èxit de diverses etapes. Com a exemple, una apropiada deposició de la capa transductora de nanotubs de carboni sobre l'elèctrode suport va ser un pas crític que va dependre de habilitats individuals. En el cas que la capa de nanotubs no estigués dipositada

adequadament, els nanotubs presents en la part exterior de la capa transductora podrien passar a la solució problema després de l'etapa de funcionalització, creant així forats dins de la capa de transducció, i per tant representar una seriosa limitació d'aquest tipus de biosensors. Addicionalment, el procés de funcionalització va dependre de las habilitats tècniques, com la preparació de solucions involucrades en la funcionalització ó un maneig adequat dels materials. Per tant, la taxa de biosensors funcionals va romandre fins ara variable i dependent de las habilitats tècniques mostrades durant la preparació dels sensors.

La resposta instrumental dels biosensors és considerable com per a ser diferenciada del soroll intrínsec; no obstant això, la sensibilitat dels mateixos és molt baixa si es compara amb la resposta potenciomètrica Nernstiana dels elèctrodes selectius d'ions 'clàssics'. Aquest fenomen és originat pels diferents mecanismes de detecció que governen cada tipus de sensor. En el cas dels elèctrodes selectius d'ions, s'estableix un sistema d'equilibri entre dues capes no miscibles (membrana polimèrica/mostra aquosa), mentre que en els nostres sensors es dóna un canvi en les càrregues elèctriques sobre la superfície dels nanotubs de carboni durant el procés de reconeixement molecular amb la qual cosa s'origina un canvi de força electromotriu. El fet que la senyal potenciomètrica sigui deguda a les càrregues superficials de l'analit obliga a mantenir sota un estricte control la força iònica de la solució analitzada, o en cas contrari es podrien originar falsos positius en els resultats.

Els sensors estan bàsicament dissenyats per a un sol ús. Són regenerables però no són reversibles (per exemple, no poden ser usats successivament per analitzar diferents mostres que continguin concentracions decreixents de l'analit). Com a conseqüència, els sensors no poden ser calibrats individualment. El calibratge haurà de dur-se a terme en tot cas, a nivell de lot, sempre que la reproductibilitat dels paràmetres de qualitat analítics sigui prou alta.

S'ha demostrat que els aptàmers són altament selectius com a elements de reconeixement molecular. Depenent del propòsit de l'anàlisi, això pot ser un enorme benefici o un desavantatge. Per exemple, és un benefici quan es detecta una sola varietat d'una espècie de bacteri, però pot ser un desavantatge quan estem interessats

a detectar la presència de microorganismes al nivell d'espècie o fins i tot de gènere. En aquest últim cas, es podria considerar l'ús simultani de diversos aptàmers, aïllats cadascun d'ells per a les diferents espècies -i varietats-.

El cost de la síntesis de l'aptàmer va ser una altre limitació. Com a exemple, 1 µmol d'un oligòmer de RNA de 50-100 bases pot costar entre 500 i 1600 euros, d'acord als preus del any 2011. Aquest factor és crític, especialment en el cas d'un baix rendiment de funcionalització de biosensors. No obstant això, el creixement exponencial en el nombre de patents i articles científics publicats relacionats amb els aptàmers (Esquema 8.2) pot veure's traduït en un decreixement dels preus de mercat en un futur. Això mateix va ser observat amb els nanotubs de carboni, els quals poden ser adquirits actualment a preus raonables.

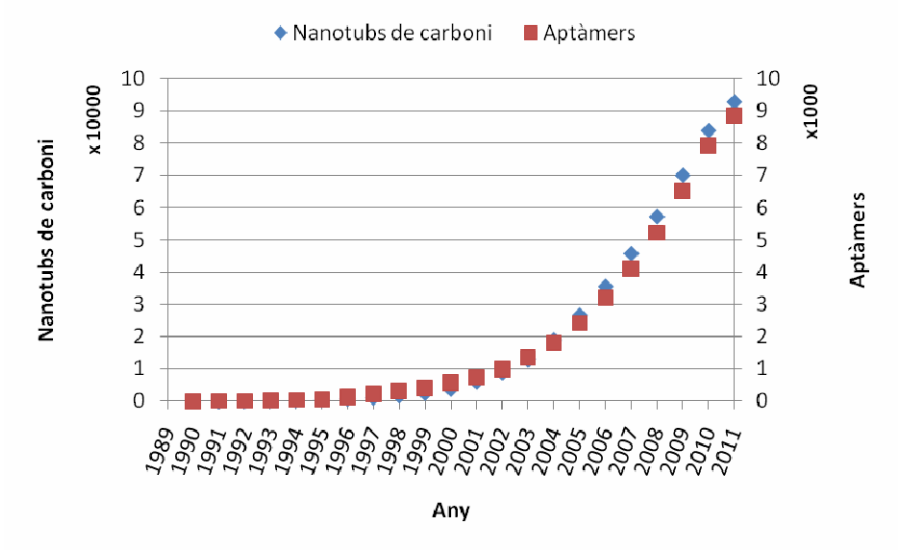

Esquema 8.2. Patents i articles científics publicats sobre els tòpics d'aptàmer i nanotubs de carboni entre els anys 1990 i 2011.[2]

La miniaturització del biosensor podria representar en el futur una àrea d'oportunitat per a millorar aquesta nova generació de biosensors basats en nanotubs de carboni i aptàmers. Els avantatges de miniaturitzar els biosensors són evidents en

[2] Cerca realitzada amb el Scifinder Scholar (R) sobre els tòpics de recerca indicats en l'Esquema 8.2 fins a l'Agost de 2011.

termes de cost, per que es redueix la quantitat d'aptàmer i nanotubs necessaris. Com a exemple, el nostre grup està actualment desenvolupant els primers exemples de sensors potenciomètrics plans en format miniaturitzat d'un únic ús. La combinació de la tecnologia de biosensors basats en aptàmers i el format pla de mida reduït dels sensors potenciomètrics pot veure's traduït en un futur en biosensors potenciomètrics d'un únic ús, i per tant, s'eliminaria la necessitat de les etapes de regeneració dels aptàmers en la detecció de patògens i proteïnes. No obstant això, las possibles repercussions de reduir la superfície del sensor sobre el rendiment analític no han estat explorades fins al moment.

Finalment, la possibilitat de expandir las aplicacions de aquesta plataforma biosensora per a la detecció d'altres objectius diferents dels bacteris o de les proteïnes, és un area molt interessant per a la recerca en el futur. Com a exemple, la detecció en temps real d'agents infecciosos com els virus o els paràsits podria representar un avanç molt important en la biodetecció de patògens.

Summary

Summary
(English)

Resum
(Català)

Summary

The control of diseases has been one of the most important public health concerns of our society for decades. Typical standard methods that are used to assess the presence of microbiological threats consist of specific enrichment media to multiply, separate, identify and count bacterial cells. The process duration depends on the target pathogen, but in most of the cases a confirmatory result can take from a few days to even weeks after the test sample has been obtained.

Additionally, disease control and more specifically, clinical diagnostic, is also carried out by means of the detection of pathogen-related proteins, protein biomarkers and exoantigens. The most commonly used methods rely on highly sensitive and specific label-based immunoassays. However, these methods are unsuitable for high-throughput applications because they are labor-intensive, time-consuming and require highly trained staff and expensive equipment. Furthermore, an accurate quantification of the analyte is not always possible and false negative results can be obtained if the target protein is not extracted from the matrix effectively.

Numerous biosensing platforms have incorporated nanostructured materials as a strategy for improving several performance and operational parameters such as reducing the limits of detection or the assay times in both pathogen and protein detection. Electrochemical sensing techniques are preferred over other detection methods because they present a series of advantages such as rapid response, ease of use, low-cost and small sized commercial detectors. Among the electrochemical techniques, the simplest, most widespread and field-portable methodologies are based on potentiometry. The new wave of potentiometric solid-state electrodes represents an attractive tool for real-time bioanalysis in liquid samples. However, to date, it has been difficult to carry out the specific and direct electrochemical detection

of whole living bacterial cells or disease-related proteins without chemical labelling because the interaction receptor-bacteria/receptor-protein does not provide a measurable electrochemical signal.

In this Thesis, the real-time potentiometric detection of bacteria and disease-related proteins is demonstrated for the first time. To accomplish such a challenging task, a novel and universal biosensing platform is designed using single-walled carbon nanotubes as potentiometric transducers, and aptamers as biorecognition elements. The excellent potentiometric transduction properties of carbon nanotubes combined with the quasi-unlimited capability of aptamers (RNA and DNA synthetic oligonucleotide segments) to be tailored *in vitro* against ions, proteins, viruses and bacteria converts such a platform into a tool with unrestricted possibilities in real-time biosensing.

This PhD Thesis is divided in eight chapters:

Chapter 1 includes a chronological overview of the current state of the art in biosensing platforms for pathogen and disease-related protein detection.

In ***Chapter 2***, the objectives of the Thesis are presented.

Chapter 3 includes a description of all the chemicals, microorganisms, materials and instruments used. This chapter also describes the basic procedures followed in the experimental part of the Thesis.

In ***Chapter 4***, the proof of concept is demonstrated by the real-time detection of *Salmonella enterica* serovar Typhi (*Salmonella* Typhi) in phosphate buffer solutions, in which the biosensor is addressed towards a specific protein anchored to the surface of the microorganism.

Chapter 5 focuses on the functionalization of carbon nanotubes with aptamers following two different approaches. The biosensor performance parameters are compared in terms of the functionalization approach with the detection of *Staphylococcus aureus* in phosphate buffer solutions. The biosensors are also used in

the detection of the target bacteria in freshly excised pig skin as a human skin surrogate.

In ***Chapter 6***, a nonpathogenic strain of *Escherichia coli* (*E. coli*) is used as a surrogate for pathogenic *E. coli* O157:H7 in foodstuff samples such as fruit juice and milk. The bacteria detection process is facilitated by the rapid elimination of the matrix and further recovery of the target bacteria using a new on-line sample pre-processing protocol.

Chapter 7 describes the detection of pathogenic exoantigen proteins in highly complex clinical samples, such as blood, with biosensors developed against trypanosomal variable surface glycoprotein (VSG). A total ionic strength and potential adjustment buffer (TISPAB) is adequately designed, tailored and used to eliminate undesired blood matrix effects. Such a buffer was developed and used with the purpose of demonstrating that the biosensing platform can be also used in protein identification within highly complex matrices in a straightforward way and without the need of complicated sample pre-treatment procedures.

Finally, ***Chapter 8*** includes the conclusions of the Thesis. This chapter also includes the description of some limitations of the biosensing platform developed as well as the opportunity areas for improvement of this new generation of potentiometric biosensors.

Resum

El control de malalties ha estat durant dècades una de las preocupacions més importants de la nostra societat. Els mètodes tradicionals més comuns utilitzats per a la detecció de microbis depenen principalment de medis d'enriquiment específic amb la qual cosa, las cèl·lules del patogen objectiu poden ser multiplicades, separades, identificades i quantificades. La duració del procés depèn del tipus de patogen, però en la majoria dels casos, es pot requerir d'uns dies fins a diverses setmanes per aconseguir un resultat final.

Addicionalment, el control de malalties i més específicament, el diagnòstic clínic, també es porta a terme mitjançant la detecció de proteïnes relacionades amb patògens, marcadors biològics i exoantígens. Els mètodes més comuns consisteixen en l'ús d'assaigs immunològics específics que empren molècules traçadores. No obstant això, aquests mètodes no són adequats per a les aplicacions que requereixen d'un alt rendiment, ja que són mètodes bastant laboriosos, lents i necessiten personal qualificat per al seu maneig. Més encara, aquests mètodes no permeten una quantificació precisa de l'analit i en alguns casos, és fins i tot possible obtenir falsos negatius en els resultats finals si la proteïna objectiu no és apropiadament extreta de la matriu.

Un gran nombre de plataformes de detecció biològica han incorporat materials nanoestructurats com una estratègia per a millorar diversos paràmetres operacionals i de qualitat tals com reduir els temps d'anàlisis i els límits de detecció. Les tècniques electroquímiques de detecció es prefereixen sobre altres tècniques ja que presenten una sèrie d'avantatges com a rapidesa, facilitat de maneig, cost reduït i la reduïda mida dels detectors comercials. Entre les tècniques electroquímiques, les metodologies més simples, comunes i més fàcils de transportar són aquelles basades en la potenciometria. La nova tendència seguida amb els elèctrodes potenciomètrics d'estat

sòlid representa una eina atractiva en l'anàlisi de mostres líquides en temps real. No obstant això, fins avui ha estat difícil dur a terme la detecció electroquímica directa de bacteris i proteïnes, sense utilitzar marcadors químics, donat que les interaccions receptor-bacteri i receptor-proteïna no produeixen un senyal elèctric mesurable.

En aquesta tesi, es demostra per primera vegada la detecció potenciomètrica en temps real de bacteris i proteïnes relacionades amb diverses malalties. Aquesta tasca va ser duta a terme mitjançant el disseny d'una plataforma universal de detecció utilitzant nanotubs de carboni com a transductors potenciomètrics i aptàmers com a elements de reconeixement molecular. Les excel·lents propietats de transducció ofertes pels nanotubs de carboni combinades amb la gairebé il·limitada possibilitat dels aptàmers de ser dissenyats in vitro per reconèixer ions, proteïnes, virus i bacteris converteix aquesta plataforma en una eina amb possibilitats inesgotables de detecció biològica en temps real.

Aquesta Tesi doctoral és divideixi en vuit capítols:

El ***Capítol 1*** inclou una revisió cronològica de la bibliografia més recent en plataformes de detecció de patogens i proteïnes relacionades amb malalties.

En el ***Capítol 2*** s'esmenten els objectius de la Tesi.

El ***Capítol 3*** inclou una descripció de totes les substàncies químiques, microorganismes, materials i instruments utilitzats. Aquest capítol també descriu els procediments bàsics que van seguir-se en el desenvolupament experimental de la Tesi.

En el ***Capítol 4***, es demostra la prova del concepte mitjançant la detecció en temps real de la *Salmonella enterica* serovar Typhi (*Salmonella* Typhi) continguda en solucions tamponades del pH i força iònica. En aquest cas, el biosensor és dirigit cap a la identificació d'una proteïna en particular que es troba incorporada a la superfície del microorganisme.

El ***Capítol 5*** s'enfoca en la funcionalització dels nanotubs de carboni amb aptàmers seguint dues vies diferents. El rendiment analític dels biosensors preparats per diferents vies es compara en funció del tipus de funcionalització mitjançant la detecció

del bacteri *Staphylococcus aureus* en solucions tamponades. Els biosensors s'empren així mateix en la detecció del bacteri en mostres fresques de pell de porc utilitzades com a substitut de la pell humana.

En el ***Capítol 6***, es detecta una variant no patògena de l'*Escherichia coli* (*E. coli*) com a substitut de la variant tòxica *E. coli* O157:H7. El bacteri es detecta en mostres alimentàries com a suc de fruita i llet. El procés de detecció del microorganisme es facilita gràcies a la ràpida eliminació de la matriu i la subseqüent recuperació dels microorganismes utilitzant un nou protocol de pretractament de mostres dissenyat exclusivament per a aquesta fi.

El ***Capítol 7*** descriu la detecció de proteïnes exoantigèniques en mostres clíniques d'alta complexitat tals com la sang, mitjançant la detecció de glicoproteïnes variables de superfície de tripanosomes africans. Per a aquesta finalitat es va dissenyar, desenvolupar, adaptar i utilitzar una solució tampó de força iònica i potencial per tal d'eliminar l'efecte matriu de la sang. Aquest tampó va ser desenvolupat i usat per tal de demostrar que la plataforma de detecció pot ser utilitzada també en la identificació de proteïnes dins de matrius altament complexes d'una forma fàcil i directa, i sense la necessitat de complicats procediments de pretractament de mostra.

Finalment, el ***Capítol 8*** inclou les conclusions de la Tesi. Aquest capítol inclou també la descripció d'algunes limitacions que presenta la plataforma de detecció desenvolupada així com també s'identifiquen les àrees d'oportunitat de millora d'aquesta nova generació de biosensors potenciomètrics.

Scientific contributions

Publications

- G.A. Zelada-Guillén, J. Riu, A. Düzgün, F.X. Rius. "Immediate detection of living bacteria at ultralow concentrations using a carbon nanotube based potentiometric aptasensor". *Angewandte Chemie International Edition*. **2009**, *48*, 7334-7337.

- G.A. Zelada-Guillén, S.V. Bhosale, J. Riu, F.X. Rius. "Real-time potentiometric detection of bacteria in complex samples". *Analytical Chemistry*. **2010**, *82*, 9254-9260.

- G.A. Zelada-Guillén, J.L. Sebastián-Avila, P. Blondeau, J. Riu, F.X. Rius. "Label-free detection of *Staphylococcus aureus* in skin using real-time potentiometric biosensors based on carbon nanotubes and aptamers". *Submitted*.

- G.A. Zelada-Guillén, A. Tweed-Kent, M. Niemann, H.U. Göringer, J. Riu, F.X. Rius. "One-step, ultrasensitive and real-time detection of proteins in blood using potentiometric carbon-nanotube aptasensors". *Submitted*.

Conferences, invited lectures and scientific meetings

- *"Potentiometric solid-state electrode based on aptamer functionalized single-walled carbon nanotubes for real-time detection of living Salmonella enterica at ultra low concentrations"*. **Oral presentation at the II Workshop on Nanosciences and Analytical Nanotechnologies**. Tarragona, Spain. September, 2008.

- *"Direct, label-free and real-time potentiometric detection of living bacteria using carbon nanotube-based biosensors"*. **Oral presentation at the International Conference on Nanotechnology, Nanotech Insight**. Barcelona, Spain. March-April, 2009.

- *"Detección en tiempo real de bacterias vivas mediante biosensores potenciométricos basados en nanotubos de carbono"*. **Lecture at the Faculty of Chemistry, National Autonomous University of Mexico, UNAM**. Mexico City. April, 2009.

- *"Rapid detection of bacteria using nanostructured surfaces"*. **Oral presentation at the NANOJASP 2010 Workshop SPAIN-JAPAN, Nanomaterials based biosensors and biosystems**. Barcelona, Spain. November, 2010.

- *"Real-time potentiometric detection of bacteria in complex samples"*. **Poster presentation at the IV Workshop on Nanosciences and Analytical Nanotechnologies**. Zaragoza, Spain. September, 2010.

- *"On the detection of living bacteria in real samples by potentiometry: a new generation of label-free and real-time biosensors"*. **Graduate research seminar at the Gordon Research Conference on Bioanalytical Sensors**. New London NH, USA. June, 2010.

- *"On the detection of living bacteria in real samples by potentiometry: a new generation of label-free and real-time biosensors"*. **Poster presentation at the Gordon Research Conference on Bioanalytical Sensors**. New London NH, USA. June, 2010.

- *"A new generation of carbon nanotubes-based biosensors for the real-time detection of living bacteria"*. **Oral presentation at the IV Annual Global Infectious Disease Scientific Symposium of the Harvard Institute for Global Health**. Boston, USA. March, 2011.

- *"Biosensores basados en nanotubos de carbono: Una nueva generación de plataformas de detección de patógenos en tiempo real"*. **Oral presentation at the V Interuniversity Conference on Biotechnology**. Tarragona, Spain. July, 2011.